LATE PLEISTOCENE AND HOLOCENE VEGETATION, FIRE AND CLIMATE DYNAMICS IN THE LAKE VICTORIA AREA

INAUGURAL DISSERTATION

OF THE FACULTY OF SCIENCE,

UNIVERSITY OF BERN

PRESENTED BY

YUNUÉN TEMOLTZIN LORANCA

FROM PUEBLA, MEXICO

SUPERVISORS OF THE DOCTORAL THESIS:

PROF. DR. WILLY TINNER

INSTITUTE OF PLANT SCIENCES AND OESCHGER CENTRE FOR CLIMATE CHANGE RESEARCH, UNIVERSITY OF BERN

PROF. DR MARTIN GROSJEAN

INSTITUTE OF GEOGRAPHY AND OESCHGER CENTRE FOR CLIMATE CHANGE RESEARCH, UNIVERSITY OF BERN

LATE PLEISTOCENE AND HOLOCENE VEGETATION, FIRE AND CLIMATE DYNAMICS IN THE LAKE VICTORIA AREA

INAUGURAL DISSERTATION

OF THE FACULTY OF SCIENCE,

UNIVERSITY OF BERN

PRESENTED BY

YUNUÉN TEMOLTZIN LORANCA

FROM PUEBLA, MEXICO

SUPERVISORS OF THE DOCTORAL THESIS:

PROF. DR. WILLY TINNER

INSTITUTE OF PLANT SCIENCES AND OESCHGER CENTRE FOR CLIMATE CHANGE RESEARCH, UNIVERSITY OF BERN

PROF. DR MARTIN GROSJEAN

INSTITUTE OF GEOGRAPHY AND OESCHGER CENTRE FOR CLIMATE CHANGE RESEARCH, UNIVERSITY OF BERN

ACCEPTED BY THE FACULTY OF SCIENCES

BERN, AUGUST 8TH 2023

THE DEAN

PROF. DR. MARCO HERWEGH

TABLE OF CONTENTS

Chapter I: Introduction, Study Site and Methods

1.1 PALAEOECOLOGICAL STUDIES IN EAST AFRICA

Palaeorecords have contributed to our understanding of vegetation dynamics, fire regimes, climatic changes, and on the effect of anthropogenic impact on local ecosystems and landscapes (Gillson, 2006; Githumbi et al., 2020; Willis et al., 2013; Wooller et al., 2003). These studies have shed light on the long-term sustainability of human-environment systems and provide important information for elaborating conservation and management strategies in the face of ongoing environmental changes (Brown et al., 2018; Gillson & Ekblom, 2020; Gillson & Marchant, 2014; Spencer et al., 2017). Even though lake sediment palaeorecords have revealed important findings, such as shifts in precipitation patterns, changes in lake levels, fluctuations in vegetation cover, as well as impacts of human activities on local ecosystems and the fire regime, these studies have been concentrated in higher latitudes, leaving behind the number of studies conducted in the tropics, where logistical and funding challenges are still present (Escobar et al., 2020).

Palaeoecological studies in East African lakes started in the 1960's, with a primary focus on examining environmental changes between 16,000 cal yr BP and today. However, pioneering studies, including those conducted in the Rukiga highlands and Mt. Kenya (Coetzee, 1967, 1987; Olago et al., 2000), extended back to ca. 42,000 cal yr BP. Contemporary research has unveiled insights into the spatial variability of palaeoclimates and palaeovegetation, demonstrating significant contrasts within proximate locations (Colombaroli et al., 2014; Githumbi, 2017; Johnson et al., 1998; Schüler et al., 2012; Sinninghe Damsté et al., 2011; Ssemmanda & Vincens, 1993; Temoltzin-Loranca et al., 2023; Tierney et al., 2011; Vincens et al., 2005; Vincens et al. 2007). Nonetheless, reconstructions of palaeoenvironments in tropical Africa are often restricted by the nature of the sediments, their preservation under arid conditions and discontinuities present in the sediment (Lézine, 2007).

The study of past climate change impacts in East Africa has evidenced the sensitivity of ecosystems. Vegetational belts were displaced altitudinally and latitudinally over millennia, with biome reorganizations, for instance, the savanna replacement in the Lake Victoria area at ca. 10,700 cal yr BP. Kendall (1969) elaborated the first comprehensive study which included 15,000 years of the chemical history of the lake, the fossil record (diatoms, green algae and pollen) and vertebrate evolution. And it was not until 30 years later, that Beuning (1999)

published the second pollen record using a new sediment core with the aim of checking if the signal from Kendall's core was representing more regional or only local environmental changes. In general, Beuning (1999) found a similar pollen signal, reporting chronological differences in the major transitions (e.g. the beginning of the forest expansion), however, in this study a sediment discontinuity was found and a good chronological control was missing. Therefore, besides a robust chronological model, more high-resolution pollen studies in the area, are needed to better understand the vegetation dynamics.

In eastern Africa, the long-term linkages between vegetation and fire regimes have been barely explored during the Pleistocene-Holocene transition (e.g. Garcin et al., 2007; Githumbi, 2017). In this region, past fire occurrence is likely to have been primarily driven by two factors: First, climatic conditions, which determine temperature, rainfall, the length of the dry and wet seasons and thus moisture availability (Nelson et al., 2012); and second, biomass availability, which depends on the climatically controlled biome type (e.g. Schüler et al., 2012), as well as the vegetation type within the Afromontane regions (Courtney Mustaphi et al., 2021; Hemp, 2005; Hemp & Beck, 2001). Several studies (e.g. Colombaroli et al., 2014; Nelson et al., 2012; Power et al., 2008; Thevenon et al., 2003) have emphasized the substantial influence of climatic and vegetation shifts on biomass burning regimes, which are dependent on biomass as fuel, and moisture acting either as fire inhibitor or facilitator. However, high-resolution fire reconstructions for the Lake Victoria basin are lacking, and the extent to which fires were controlled by climate and biomass change remains unknown. This gap reduces our ability to understand the processes and mechanisms which controlled past fire regimes in the Lake Victoria basin. Such information remains as an opportunity to explore for many regions of equatorial eastern Africa (Githumbi, 2017).

1.2 RESEARCH GAPS AND AIMS OF THE THESIS

This PhD thesis work emerged as part of the large Swiss National Science Foundation project – 20,000 years of evolution and ecosystem dynamics in the world's largest tropical lake reconstructed from sediment cores, fossils and ancient DNA– with grant number 183566, devoted to understand fish evolution under strongly changing environmental conditions. The project explores the evolution and ecosystem dynamics in Lake Victoria, as reconstructed from sediment cores, fossils and ancient DNA. In particular, this PhD project explores

palaeoecological proxies and establishes high precision ^{14}C chronologies with the aim of characterizing and assigning an accurate timing to the environmental changes in the Lake Victoria ecosystem before significant human disturbance. At the same time, this research is also dedicated to address the current palaeoecological research gaps in the Lake Victoria area. For instance, the lack of a comprehensive analysis of macrocharcoal. Although previous studies have examined aspects of fire history, there is a need for a continuous record spanning the latest Pleistocene and the Holocene, which would enable us to identify shifts in fire regimes and identify the primary sources of fire and their impacts on terrestrial vegetation under strongly varying climates. Another gap in current research, pertains to the understanding of ecosystem responses to climate during the savanna–rainforest transition. While previous studies have provided valuable insights, there is a lack of detailed and high–resolution pollen records in this critical period. Therefore, this thesis contains two main chapters dedicated to tackle these gaps, Chapter II: A chronologically reliable record of 17,000 years of biomass burning in the Lake Victoria Area, and Chapter III: Ecological long-term successions around Lake Victoria from the latest Pleistocene to the onset of the African Humid Period.

Chapter II (Temoltzin-Loranca, et al. 2023) strives to achieve two primary aims. First, to provide a novel chronology for three new sediment cores from the deepest part of Lake Victoria, based predominantly on macroscopic charcoal (>200 µm). This chronology has been validated by the biostratigraphy (pollen), over a three-core transect. Second, to provide the first continuous macroscopic charcoal analysis reconstructing the Late Glacial and Holocene fire history. Such novel (e.g. charcoal, pollen) and established palaeoclimate data are used to discuss the long-term linkages between climate, fire, and vegetation at a biome level in the Lake Victoria area.

Given that vegetational changes happen in relatively short time spans, high-resolution studies are needed to understand major ecosystem transitions. In the Lake Victoria basin, major biome reorganizations occurred during the late Pleistocene and the early Holocene (Beuning, 1999; Kendall, 1969; Temoltzin-Loranca et al., 2023). Therefore, in Chapter III (Temoltzin-Loranca, et al. in prep), the first high-resolution pollen record from Lake Victoria, covering the late-glacial and early Holocene, is used to assess the major vegetation and ecosystem transformations and elucidate their corresponding responses to climatic fluctuations and disturbance.

Our hope is that this PhD thesis serves as a valuable reference for those interested in exploring the fascinating niche of East African palaeolimnology and palaeoecology, and to contribute to the advancement of tropical research as a whole. In addition to bridging the gaps in knowledge, our study also attests to the importance of innovation and method adaptations in the pursuit of scientific understanding.

1.3 STUDY SITE

Located in East Africa and bordered by Kenya, Uganda and Tanzania, Lake Victoria (LV), is the world's second–largest freshwater lake by surface area, covering approximately 68,800 km^2. The lake lays between latitudes 0.5° N and 2.5° S, and longitudes 32° E and 34° E, at an average elevation of approximately 1135 m above sea level (Bootsma & Hecky, 2003), having a mean water depth of 40 m, with maximum depth of 68 m (Johnson et al., 2000). Geologically, Lake Victoria is part of the East African Rift System (EARS), on the northern section of the Tanzanian craton between the western and eastern rift valleys (Johnson et al., 2000; Odada et al., 2003). The Lake Victoria basin formed as a result of faulting and downfaulting, and its geology is dominated by Precambrian rocks, including granite, gneiss, and schist, which form the basement rock.

The climate is regulated by the movement of the Intertropical Convergence Zone (ITCZ) and the Indian Monsoon, therefore creating two rainy seasons, one as the ITCZ moves northwards from March to May, known as the long “Masika” rains; and another from October to November as the ITCZ moves southwards known as the short "Vuli” rains, (Gamoyo et al., 2015; Kijazi & Reason, 2009; Palmer et al., 2023). The difference in precipitation between the dry and rainy seasons can amount up to 8 mm/day. In modern times, from 2003–2007 a mean annual precipitation of 1506 mm/yr was recorded over the lake, slightly varying depending on local topography and other factors (Vanderkelen et al., 2018). The lake's large surface area and relatively warm waters can contribute to the formation of local microclimates, with rainfall patterns influenced by the lake's presence. Specifically, the lake's evaporation rates affect local humidity and cloud formation, which can in turn influence rainfall patterns in the surrounding areas (Palmer et al., 2023). The lake also has a significant impact on local temperature and wind patterns. Its large surface area acts as a heat sink, moderating temperatures and creating local breezes that can influence weather patterns.

1.3.1 VEGETATION IN THE SURROUNDINGS OF LAKE VICTORIA

In order to understand and examine the vegetation within a geographical area, it is crucial to consider the floristic, physiognomic, and functional aspects, thus facilitating the categorization of plant communities (Pfadenhauer & Klötzli, 2020). When interpreting vegetation in relation to its dependence on macroclimate features, we designate a vegetation unit as having zonal character, while formations influenced by specific soil or water properties are identified as azonal vegetation (Mucina et al., 2006; Pfadenhauer & Klötzli, 2020). The habitats characterized by zonal vegetation are referred to as biomes, and in the vicinity of Lake Victoria, three primary terrestrial biomes shape the landscape, the savanna, the rainforest and the Afromontane forest (Mafuta & Westerveld, 2017).

- **Savanna**

Today's African savannas are integrated by grasses, forbs, shrubs and trees, which have adaptations to seasonal drought and browsing (IUCN, 2020), and therefore a different physiognomy during the rainy or the dry season (Blösch, 2002). Contrary to other biomes, where herbaceous plants, are the 'antagonists' of arboreal plants, in the savannas their co-existence is common. In seasonally flooded areas with clay soils, an azonal vegetation type develop – the thicket clumps –, being little hotspots of nutrient (carbon, phosphate, mineral nitrogen, potassium and calcium) accumulation, having therefore a denser cover of woody plants (Pfadenhauer & Klötzli, 2020). In Northern Tanzania the mean annual rainfall is reported from 400 to 1200 mm while in the Kenyan highlands it descends to 300-600 mm (Belsky, 1990).

- **Rainforest**

The Lake Victoria semi-evergreen Guineo-Congolian rainforests occur between 1000 and 1750 m asl under a mean annual precipitation of 1200–1400 mm. This vegetation type dominates today's landscape in the western lake shore of Lake Victoria. Moreover, Lake Victoria transitional rainforests occur between 1600 and 1900 m asl according to White (1983), with similar mean annual precipitation as the Guineo-Congolian rainforests. Often, the rainforest penetrates the savanna as gallery forests either as forests islands on the plateau or along the riverbanks (Hopkins, 1992) acting then as azonal vegetation.

- Afromontane forest

The Afromontane forests are located in areas of moderate rainfall (700–1230 mm/yr, subject to orographic influences) and are usually growing at higher elevations than the rainforest, generally between 1200 and 2500 m asl under cooler conditions (Gadow et al., 2016). In tropical East Africa, the lower and central slopes of the mountains and volcanoes are surrounded by this kind of vegetation which comprises arboreal taxa such as *Podocarpus, Olea* and *Juniperus* (Scoon, 2018). The lower parts of this peculiar ecosystem merge most of the time with the savanna woodlands, however, in modern times they have been heavily impacted by humans due to land–use change.

The vegetation of east Africa has followed a series of modifications. Initially, White (1983) described the vegetation of the African continent using phytocoria, and in order to describe azonal vegetation, he used additional categories such as mangroves, herbaceous swamps, aquatic vegetation and saline and brackish swamps. To describe the flora of the Lake Victoria area, this unit was denominated as "The Lake Victoria Regional Mosaic" which is surrounded by mainly five distinct phytocoria: Guineo–Congolian, Sudanian, Zambezian, Somalia–Masai, and the Afromontane. These phytocoria were originally defined under a 1:5,000,000 scale, causing heterogenicity within the same floristic units. Later, the VECEA –Vegetation and Climate Change in Eastern Africa – project, proposed higher resolution vegetation maps such as the Potential Natural Vegetation (PNV) map for Eastern Africa (Lillesø et al., 2011), which show the vegetation structure becoming established in accordance with the present climate and edaphic conditions without anthropogenic influence. Offering more well-defined units and a resolution that can be directly transferred to the landscapes. According to the PNV map, considering the growth form, height, ground cover, and type of leaves, the area in the surroundings of Lake Victoria (Fig. 1) can be grouped into physiognomic categories and contains the vegetation types mentioned below.

- Bushland and thicket clumps

Afromontane bamboo (B), Somalia-Masai *Acacia-Commiphora* deciduous bushland and thicket (Bd), *Acacia-Commiphora* stunted bushland (Bds), Evergreen and semi-evergreen bushland and thicket (Be), Montane Ericaceous Belt (E).

- **Forest**

Afromontane rainforest (Fa), Afromontane undifferentiated forest (Fb), Afromontane single-dominant *Hagenia abyssinica* forest (Fd), Afromontane moist transitional forest (Fe), Lake Victoria transitional rainforest (Ff), Afromontane dry transitional forest (Fh), Lake Victoria drier peripheral semi-evergreen Guineo-Congolian rainforest (Fi). Having the latter rainforest vegetation type largely widespread in the western and northern areas around the lake (Fig. 1).

- **Grassland**

Grassland (g), edaphic grassland on volcanic soils (gv).

- **Woodland and wooded grassland**

Dry *Combretum* wooded grassland (Wcd), moist *Combretum* wooded grassland (Wcm), *Acacia-Commiphora* deciduous wooded grassland (Wd), Upland *Acacia* wooded grassland (We), Drier miombo woodland (Wmd), Wetter Miombo woodland (Wmw). Having these generally dry woodland and wooded grassland vegetation types largely widespread in the southern areas around the lake (Fig. 1).

- **Swamp**

Freshwater swamp (X).

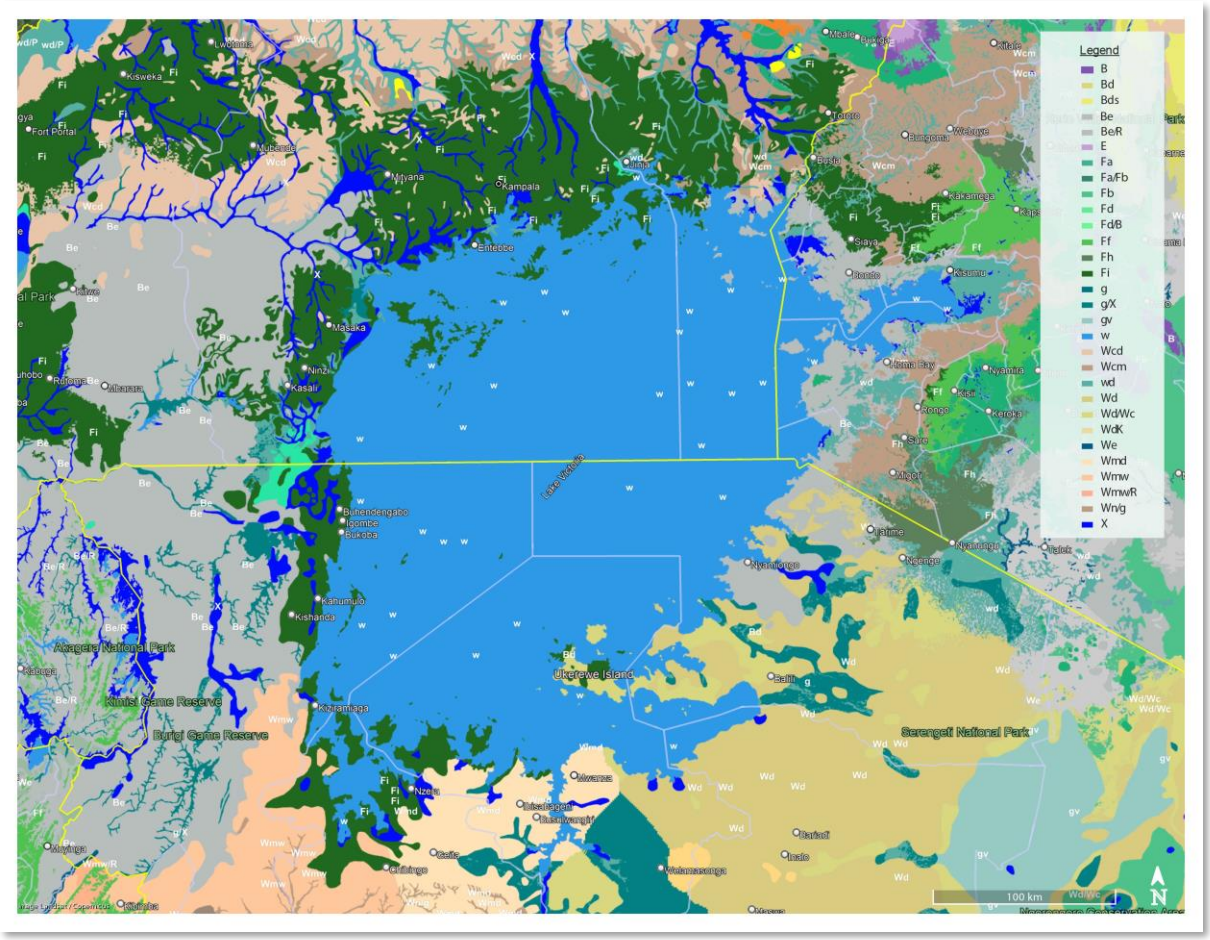

Figure 1. Potential Natural Vegetation (PNV) map for Eastern Africa extracted and adapted from Lillesø et al. (2011). The letters in the legend indicate the vegetation type. Afromontane bamboo (B), Somalia-Masai Acacia-Commiphora deciduous bushland and thicket (Bd), Acacia-Commiphora stunted bushland (Bds), Evergreen and semi-evergreen bushland and thicket (Be), Montane Ericaceous Belt (E), Afromontane rainforest (Fa), Fa/Fb, Afromontane undifferentiated forest (Fb), Afromontane single-dominant Hagenia abyssinica forest (Fd), Fd/B,Afromontane, Lake Victoria transitional rainforest (Ff), Afromontane dry transitional forest (Fh), Lake Victoria drier peripheral semi-evergreen Guineo-Congolian rainforest (Fi). Grassland (g), Edaphic grassland on volcanic soils (gv), Dry Combretum wooded grassland (Wcd), moist Combretum wooded grassland (Wcm), Acacia-Commiphora deciduous wooded grassland (Wd), Upland Acacia wooded grassland (We), Drier miombo woodland (Wmd), Wetter Miombo woodland (Wmw), and Freshwater swamp (X).

1.4 METHODS

In order to achieve our research objectives, we applied standard palaeoecological methods, making certain modifications when needed. In **Section 1.4.1** we describe the coring campaign. Then, **Sections 1.4.2** and **1.4.3** provide more comprehensive information about the adapted procedures, and explored methods, offering possibilities for further refinement. Finally, in **Section 1.4.4** the standard methods are briefly enlisted and further described in detail in **Chapters II** and **III**.

1.4.1 CORING CAMPAIGN

During October 2018, a joint field campaign between the University of Bern and the Tanzanian Fisheries Research Institute (TAFIRI) took place, aiming to retrieve sediment cores from four locations along a transect in the Shirati Bay of Lake Victoria (Table 1). The coring operation was carried out using the UWITEC Niederreiter coring system from the Institute of Plant Sciences at the University of Bern. In order to ensure the coring system's stability for seaworthy conditions at the lake, eight aluminum pontoons (instead of rubber) were adapted to the platform (Fig. 2), and specialized sea anchors were utilized.

Table 1. Details of the sediment cores retrieved in the coring expedition of 2018. Including coordinates and water depth.

Core	Referred to as	Coordinates	Water depth (m)	Coring date
LVC18_S1	LV1	01°06.914' S, 33°55.146' E	37.0	16.10.2018
LVC18_S2	LV2	01°07.850' S, 33°56.780' E	22.6	18.10.2018
LVC18_S3	LV3	01°08.343' S, 33°58.599' E	13.4	19.10.2018
LVC18_S4	LV4	01°02.966' S, 33°47.768' E	63.0	21.10.2018

Figure 2. Coring platform in Lake Victoria. October 2018.

1.4.2 SUBSAMPLING AND SIEVING

Given the interdisciplinary nature of this project, we utilized the sediment for multiple analyses. As such, we designed a strategic sediment-splitting approach at the beginning of the study, allowing us to cut 2 cm slices from a 6 cm diameter sediment core (Fig. 3). Only ¼ of the core was set aside for the purpose of producing a macrofossil record and obtaining ^{14}C datable materials (B1.1). Additionally, 1 cm^3 subsamples of sediment were reserved for pollen analysis (B1.2). To ensure the retrieval of fish bones and teeth, charcoal and palynomorphs, we employed a sieve tower with four distinct mesh sizes – 200 µm, 100 µm, 50 µm and 20 µm – to process subsamples of approximately 7 cm^3 (see **Chapter 2.3.2**).

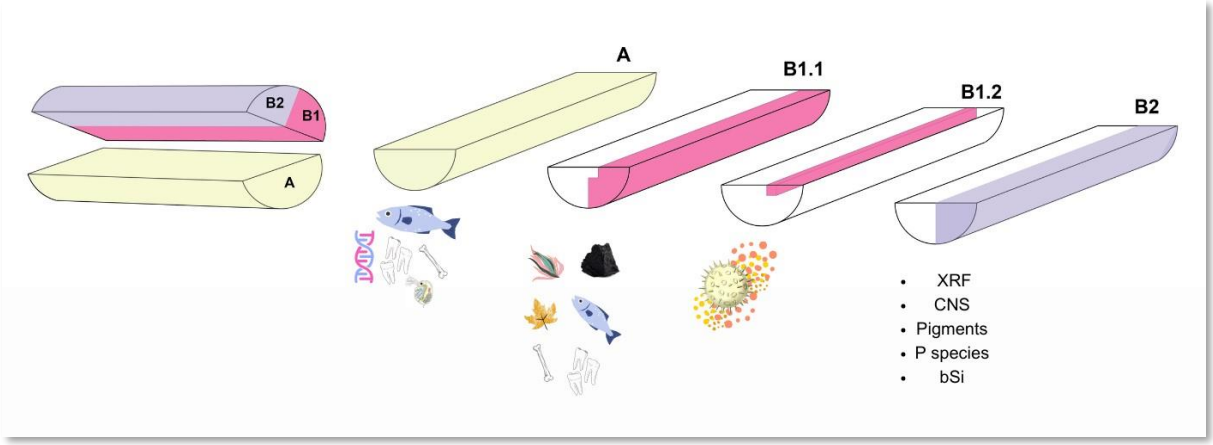

*Figure 3. Sediment splitting for sediment analysis. **A** represents the fraction for recovering DNA, fish teeth and bones and zooplankton. **B1.1** represents the fraction to sieve for retrieving terrestrial macrofossils. **B1.2** represents the sediment reserved for pollen analysis. And **B2** represents the fraction for XRF, CNS, Pigments, P species and bSi analyses.*

1.4.3 EXPLORING THE CELL SORTING APPROACH FOR RADIOCARBON DATING

As our cores were retrieved from a considerable distance offshore (ca. 6, 10 and 30 km) within the vast waters of Lake Victoria, it was anticipated that the presence of terrestrial macrofossils would be scarce. Therefore, we decided to explore an alternative technique that would allow us to get material for radiocarbon dating. Research has shown that pollen is a good resource for radiocarbon dating when macrofossils are sparse or absent (e.g. Fletcher et al., 2017; Tennant et al., 2013; Tunno et al., 2021). And, in order to extract these pollen grains from the sediment, physical and chemical techniques are required.

Flow cytometry (FCM), is known to be a technique which analyzes cells suspended in a solution, making them pass through multiple lasers (Radbruch, 2000). There are several types

of flow cytometers, a specific type is the cell sorter which allows to select a population of particles or cells which matches or not the indicated parameters, and then can re-direct them to a collection tube (McKinnon, 2018). In the initial phase of this technique, a liquid moves through a light beam produced by multiple lasers; this fluid contains droplets which carry distinct suspended particles, each one of them known as an "event." The particles scatter the laser light in various ways, and an array of detectors captures the resulting optical characteristics (Yamada et al., 2021). These characteristics are then presented in a series of dot plots, with each dot representing a single particle for the corresponding detector. A specific subset of particles can be chosen and separated by placing gates on certain areas of the data, which are known as areas of interest. This gated subset can be reanalyzed on a separate plot to further isolate "events" or to be utilized as the parameter for sorting (McKinnon, 2018).

Before the application of FCM to our sediment samples, a first step was considered to remove larger particles and to avoid clogging the nozzles of the sorter. The sediment was then pre-treated with a modified version of the protocol for extracting pollen for AMS radiocarbon dating (Brown, 1994), substituting the mesh size to 100 µm in the first sieving step (Fig. 4). Once the humic acids, carbonates, silicates, organic detritus, and cellulose were removed by using KOH 1.6N, HCl 1N, HF 40%, NaOCl 2-3% and H_2SO_4 1.2M respectively (Fig. 4).Three different CsCl (Cesium chloride) solutions were prepared taking into account the theoretical densities of charcoal (ca. 1.30-1.506 g/cm^3) and pollen (ca. 1.2-1.4 g/cm^3, Fletcher et al., 2017) with the aim of separating them, each one of these having a density of 1.51, 1.45 and 1.34 g/cm^3. Then, by adding the CsCl 45% concentration the sample was separated into two different layers, the top containing Pollen, *Botryococcus*, and *Pediastrum* and the bottom containing charcoal and lignin. Later, by using CsCl 35% ρ=1.34, we would in theory separate *Pediastrum* and *Botryococcus* from the pollen (Fig. 4). Despite multiple attempts at the separation of the terrestrial pollen grains from the algae (*Pediastrum* and *Botryococcus*) in our sediment samples, we did not observe any significant improvement in the results.

We decided to use FCM as a separation technique to achieve better results. Our sediment samples had an average pollen concentration of 62,700 grains/cm^3, which was in theory sufficient for extracting pure pollen concentrates. However, this concentration varied along the sequence between 8200 and 214,000 grains/cm^3, requiring different amounts of sediment at the time of starting the extraction.

Figure 4. *Lab methodology for extracting pollen concentrates. Adapted from Brown (1994).*

For the test runs, we used 2 cm^3 of sediment treated with the procedure mentioned above. Later, before injecting the sediment concentrate to the sorter, we filtered the sample through a 50 µm *CellTrics* filter (Sysmex) to avoid nozzle clogging. Once the concentrate was being analysed inside the sorter, we needed to define the gate region for pollen grains by visually inspecting one of our samples via a Side Scatter (SSC) vs Forward Scatter (FCS) plot identifying clearly defined areas of 'events' with similar characteristics. However, the scatter was too complex to segregate (all events were sparse and did not form clusters in the graph). Therefore, we analysed a blank of *Corylus* pollen to determine the gate region for pollen grains using the SSC vs FCS plot. After identifying the region in which pollen grains were grouped, we designated this area as a gate region of interest (R10; Fig. 5 a).

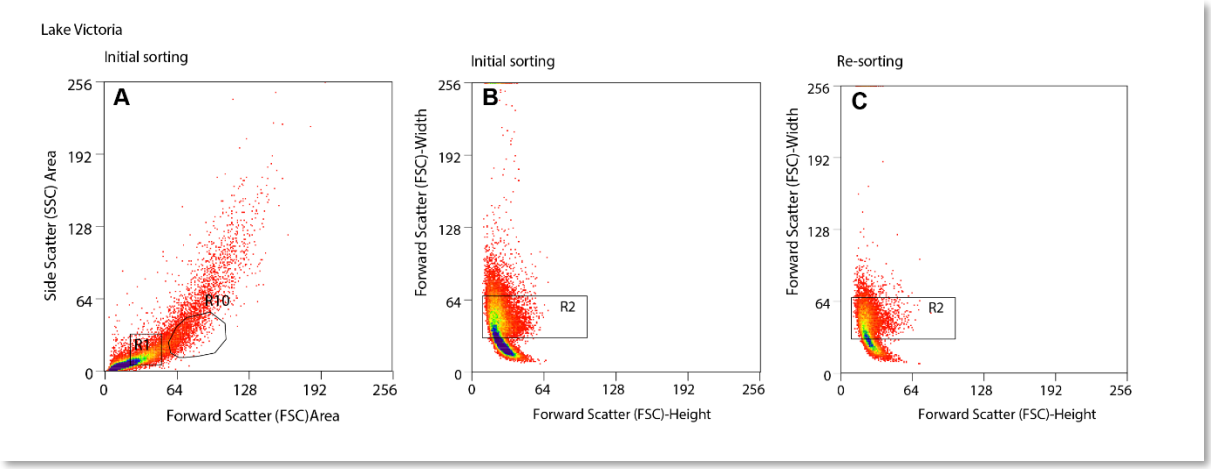

*Figure 5. Scatter plots obtained from the Flow cytometer at 488nm, the coloured dots represent each "event". **A)** Illustrates a FSC Area plot vs SSC Area. R1 indicates the gating for debris and R10 represents the gating for events of interest. **B)** Represents a FSC-Height vs FSC-Width plot. R2 is the gate for events of interest. **C)** Represents a FSC-Height vs FSC-Width plot. R2 is the gate for events of interest. **A** and **B** are the initial sorting step, while **C** represents a resorting step.*

Then, we performed the first separation run on our test sample, in which we detected > 50,000 events (Fig. 5 a). Then, through an SSC vs FCS plot, and using our previously defined gate region of interest we excluded the debris (R1; Fig. 5 a). Subsequently, we commenced gating individual events (R2; Fig. 5 b). Nevertheless, the event count was considerably lower than expected, with only 13,280 obtained. Additional sorting was performed to eliminate extraneous debris (Fig. 5 c), which led to a further reduction in event count, leaving only 7204 events (possible pollen grains). After analyzing the sorted liquid under the microscope, a few algae were still present, leading to a further reduction in the potential number of pollen grains for radiocarbon dating. To ensure an adequate amount of carbon for AMS analysis, a minimum

threshold of 10,000 grains was set, with the optimal range being between 20,000 and 30,000 (Zimmerman et al., 2019). This threshold was established to guarantee enough carbon for accurate analysis. However, our sorted sample contained only 7204 events, which were still a combination of pollen and algae. Additionally, the purification process was more time–consuming than the alternative method of using miniature radiocarbon measurements obtained from macrofossils (Zander et al., 2020). Taking these factors into consideration, we decided to proceed with the miniature radiocarbon measurement method as it would provide a more efficient and practical approach, allowing us to obtain enough carbon content for analysis in less time.

To sum up, it is crucial to acknowledge the trade-off between sample purity and the potential loss of pollen grains during the sorting process (Tunno et al., 2021). While resorting may improve the purity, it can result in the exclusion of a large number of pollen grains. To address this, a thorough evaluation of the filtering step using the *CellTrics* filter is necessary. Starting experiments with a higher volume of sediment is recommended whenever feasible so that the chances of obtaining a more representative and comprehensive sample for analysis are enhanced. However, it is important to consider time constraints when refining or deciding on a method. In situations like this one, where the purification process proves to be more time-consuming than alternative approaches, such as systematic sieving, it may be necessary to opt for the more efficient method. It can be inferred that this method requires adaptations for each lake and needs to be adjusted to the pollen density within the core.

1.4.4 ESTABLISHED PALAEOECOLOGICAL METHODS

In order to recover datable material for providing a novel chronology for three newly recovered sediment cores from Lake Victoria (LV1, LV2 and LV4), we decided to cease the cell sorting method because of time constraints. Instead, we proceeded with the conventional approach of macrofossil dating and subsequently conducted dating analyses on supplementary samples of a palynomorph-bulk concentrate as outlined in **Chapter II**. For making combined (palynomorph concentrate-charcoal) age-depth models we needed to assess chronological biases caused by the ^{14}C reservoir effect. Therefore, we constructed two age-depth models for each site: the first one, exclusively with dates originating from the palynomorph-bulk concentrate (Fig. 6), which also contained algae cells such as *Pediastrum* and *Botryococcus*;

and the second one, with dates originating solely from macrocharcoal (Fig. 6). Then, we measured paired samples, and we calculated (i) the difference in ages of same depths between the 20–50 µm palynomorph concentrate and the macrocharcoal and (ii) the mean and standard deviation of the differences of all three sites. The corrected ages of the 20–50 µm palynomorph concentrate and the terrestrial macrofossil ages were used to construct a combined model with its 95% (2σ) probabilities using *rbacon* (Blaauw et al., 2021; Blaauw & Christen, 2011) in R software and the IntCal20 calibration curve (Reimer et al., 2020).

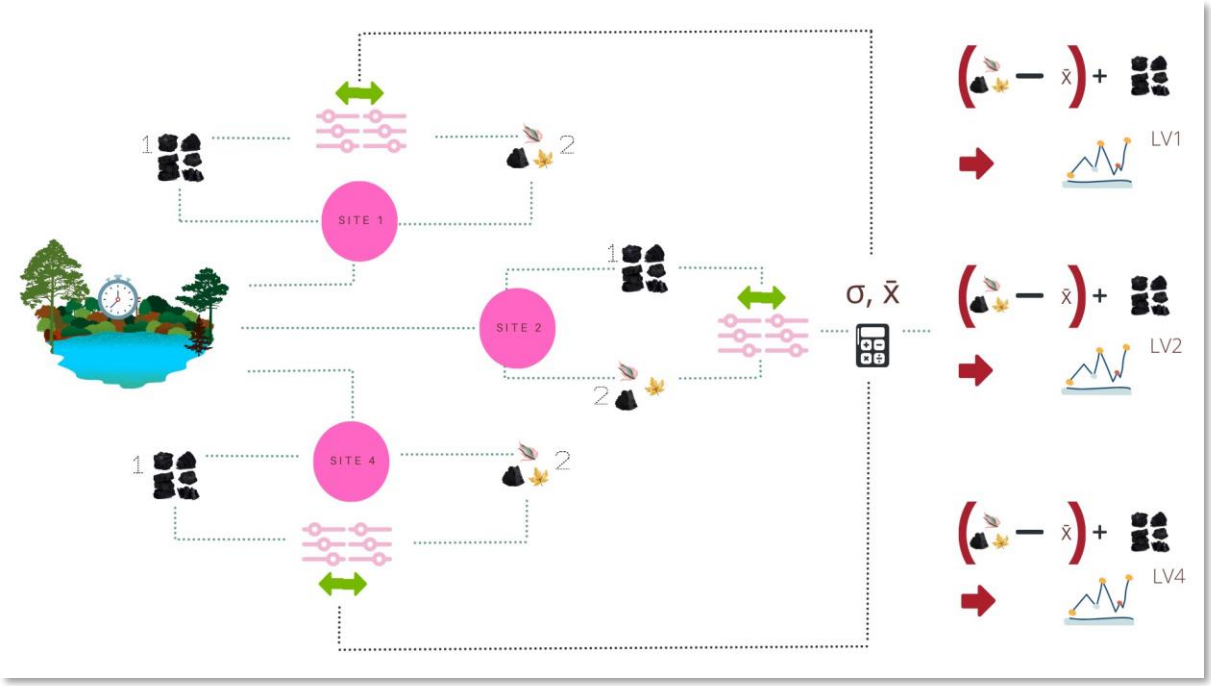

Figure 6. Illustrated procedure for obtaining the age-depth models of LV1, LV2 and LV4. Number 1 represents the age-depth models elaborated with only charcoal dates. Number 2 represents the age-depth models elaborated with the palynomorph-bulk concentrate. The green arrows represent the calculated difference in paired samples. The calculator icon represents the calculation of the mean and standard deviation. The red arrows point to the final age-depth model for each site.

For reconstructing the vegetation dynamics, samples were prepared for pollen analyses following standard procedures using HCl, KOH, HF and acetolysis (Moore et al., 1991). Tablets containing *Lycopodium clavatum* (Batch number 3862 with 9666 spores per tablet ± 671 Std dev.) were added to the samples prior to chemical treatment in order to calculate microfossil concentrations and influx (Stockmarr, 1971). All samples were stained with fuchsine and diluted with glycerine for mounting. The slides were analyzed under a light microscope (Leica 2500) at 400× magnification. We used palynological keys, atlases (Gosling et al., 2013; Reille, 1992; Roubik & Moreno P., 1991; Schüler & Hemp, 2016), and the pollen reference collection

of Kilimanjaro region located at the palynological laboratory of the University of Göttingen, Germany. For more details about the pollen analyses please see **Chapters II** and **III**.

For biomass burning assessment, we analysed macrocharcoal samples obtained from ca. 9 cm^3 of lake sediment taken continuously at 2 cm intervals and sieved through a mesh size of 200 µm (see **Chapter II**). The samples were analysed under a stereomicroscope (Leica M125) at 40× magnification, and the charcoal was picked. Additionally, charcoal morphotypes (wood vs grass) were determined following Colombaroli et al.'s (2014) approach (see **Chapter III**). Charcoal particles with a length–width ratio ≥ 3:1 and stomata within the rows of epidermal cells (Colombaroli et al., 2014; Jensen et al., 2007) were considered to originate from grass, whereas particles with thicker structure and a length–width ratio of ≤3:1 were identified as wood charcoal pieces (Umbanhowar & McGrath, 1998). For more details about the charcoal analyses please see Chapters II and III.

By applying the methodologies mentioned in this section as well as various numeric approaches (see **Chapters II** and **III**), we could accomplish the aims proposed in this PhD thesis. Enough quantity of pollen and spores were found, facilitating the reconstruction of vegetation dynamics. Even though macrofossils were challenging to find, we could gather and classify an abundant supply of macroscopic charcoal (<200 µm), allowing us to provide robust chronologies and elucidate the fire regimes and its impacts on vegetation. Comprehensive documentation about the methodologies, analyses and results is presented in the following chapters.

References

Belsky, A. J. (1990). Tree/Grass Ratios in East African Savannas: A Comparison of Existing Models. Journal of Biogeography, 17(4/5), 483. https://doi.org/10.2307/2845380

Beuning, K. R. M. (1999). A re-evaluation of the Late Glacial and Early Holocene vegetation history of the Lake Victoria region, East Africa. In E. M. van Zinderen Bakker & K. Heine (Eds.), Palaeoecology of Africa and the Surrounding Islands (First, pp. 115–136). Routledge.

Blaauw, M., & Christen, J. A. (2011). Flexible paleoclimate age-depth models using an autoregressive gamma process. Bayesian Analysis, 6(3). https://doi.org/10.1214/11-BA618

Blaauw, M., Christen, J. A., & Aquino Lopez, M. A. (2021). Age-depth modelling using Bayesian Statistics, Package "rbacon."

Blösch, U. (2002). The dynamics of thicket clumps in the Kagera savanna landscape, East Africa. ETH Zürich.

Bootsma, H. A., & Hecky, R. E. (2003). A Comparative Introduction to the Biology and Limnology of the African Great Lakes. Journal of Great Lakes Research, 29, 3–18. https://doi.org/10.1016/S0380-1330(03)70535-8

Brown, K. J., Power, M. J., & Hebda, N. J. R. (2018). Integrating paleoecology into landscape management. In D. X. Viegas (Ed.), Advances in forest fire research (pp. 1137–1145). Imprensa da Universidade de Coimbra. https://doi.org/10.14195/978-989-26-16-506_127

Coetzee, J. A. (1967). Pollen analytical studies in East and Southern Africa. Palaeoecology of Africa, 3, 1–46.

Coetzee, J. A. (1987). Palynological intimations on the East African mountains. Palaeoecology of Africa, 18, 231–244.

Colombaroli, D., Ssemmanda, I., Gelorini, V., & Verschuren, D. (2014). Contrasting long-term records of biomass burning in wet and dry savannas of equatorial East Africa. Global Change Biology, 20(9), 2903–2914. https://doi.org/10.1111/GCB.12583

Courtney Mustaphi, C. J., Kinyanjui, R., Shoemaker, A., Mumbi, C., Muiruri, V., Marchant, L., Rucina, S. M., & Marchant, R. (2021). A 3000-year record of vegetation changes and fire at a high-elevation wetland on Kilimanjaro, Tanzania. Quaternary Research, 99, 34–62. https://doi.org/10.1017/qua.2020.76

Escobar, J., Serna, Y., Hoyos, N., Velez, M. I., & Correa-Metrio, A. (2020). Why we need more paleolimnology studies in the tropics. Journal of Paleolimnology, 64(1), 47–53. https://doi.org/10.1007/s10933-020-00120-6

Fletcher, W. J., Zielhofer, C., Mischke, S., Bryant, C., Xu, X., & Fink, D. (2017). AMS radiocarbon dating of pollen concentrates in a karstic lake system. Quaternary Geochronology, 39, 112–123. https://doi.org/10.1016/j.quageo.2017.02.006

Gadow, K. v., Zhang, G., Durrheim, G., Drew, D., & Seydack, A. (2016). Diversity and production in an Afromontane Forest. Forest Ecosystems, 3(1), 15. https://doi.org/10.1186/s40663-016-0074-7

Gamoyo, M., Reason, C., & Obura, D. (2015). Rainfall variability over the East African coast. Theoretical and Applied Climatology, 120(1–2), 311–322. https://doi.org/10.1007/s00704-014-1171-6

Garcin, Y., Vincens, A., Williamson, D., Buchet, G., & Guiot, J. (2007). Abrupt resumption of the African Monsoon at the Younger Dryas—Holocene climatic transition. Quaternary Science Reviews, 26(5–6), 690–704. https://doi.org/10.1016/j.quascirev.2006.10.014

Gillson, L. (2006). A “large infrequent disturbance” in an East African savanna. African Journal of Ecology, 44(4), 458–467. https://doi.org/10.1111/j.1365-2028.2006.00662.x

Gillson, L., & Ekblom, A. (2020). Using palaeoecology to explore the resilience of southern African savannas. KOEDOE - African Protected Area Conservation and Science, 62(1). https://doi.org/10.4102/koedoe.v62i1.1576

Gillson, L., & Marchant, R. (2014). From myopia to clarity: sharpening the focus of ecosystem management through the lens of palaeoecology. Trends in Ecology & Evolution, 29(6), 317–325. https://doi.org/10.1016/j.tree.2014.03.010

Githumbi, E., Marchant, R., & Olago, D. (2020). Using the Past to Inform a Sustainable Future: Palaeoecological Insights from East Africa. In M. Ramutsindela & D. Mickler (Eds.), Africa and the Sustainable Development Goals. Sustainable Development Goals Series (pp. 187–195). Springer. https://doi.org/10.1007/978-3-030-14857-7_18

Githumbi, E. N. (2017). Holocene environmental and human interactions in East Africa. (Doctoral dissertation, University of York).

Gosling, W. D., Miller, C. S., & Livingstone, D. A. (2013). Atlas of the tropical West African pollen flora. Review of Palaeobotany and Palynology, 199, 1–135. https://doi.org/10.1016/J.REVPALBO.2013.01.003

Hemp, A. (2005). Climate change-driven forest fires marginalize the impact of ice cap wasting on Kilimanjaro. Global Change Biology, 11(7), 1013–1023. https://doi.org/10.1111/j.1365-2486.2005.00968.x

Hemp, A., & Beck, E. (2001). Erica excelsa as a fire-tolerating component of Mt. Kilimanjaro’s forests. Phytocoenologia, 31(4), 449–475. https://doi.org/10.1127/phyto/31/2001/449

Hopkins, B. (1992). Ecological processes at the forest-savanna boundary. In P. A. Furley, J. Proctor, & J. A. Ratter (Eds.), Tropical savannas. Ecosystems of the world (Vol. 13). Elsevier.

IUCN. (2020). IUCN Global Ecosystem Typology 2.0: descriptive profiles for biomes and ecosystem functional groups (D. A. Keith, J. R. Ferrer-Paris, E. Nicholson, & R. T. Kingsford, Eds.). IUCN, International Union for Conservation of Nature. https://doi.org/10.2305/IUCN.CH.2020.13.en

Jensen, K., Lynch, E. A., Calcote, R., & Hotchkiss, S. C. (2007). Interpretation of charcoal morphotypes in sediments from Ferry Lake, Wisconsin, USA: Do different plant fuel sources produce distinctive charcoal morphotypes? Holocene, 17(7). https://doi.org/10.1177/0959683607082405

Johnson, T. C., Chan, Y., Beuning, K. R. M., Kelts, K., Ngobi, G., & Verschuren, D. (1998). Biogenic Silica Profiles in Holocene Cores from Lake Victoria: Implications for Lake Level History and Initiation of the Victoria Nile. 75–88. https://doi.org/10.1007/978-94-017-1437-2_6

Johnson, T. C., Kelts, K., & Odada, E. (2000). The Holocene history of Lake Victoria. Ambio, 29(1), 2–11. https://doi.org/10.1579/0044-7447-29.1.2

Kendall, R. L. (1969). An Ecological History of the Lake Victoria Basin. Ecological Monographs, 39(2), 121–176.

Kijazi, A. L., & Reason, C. J. C. (2009). Analysis of the 2006 floods over northern Tanzania. International Journal of Climatology, 29(7), 955–970. https://doi.org/10.1002/joc.1846

Lézine, A.-M. (2007). Postglacial pollen records of Africa. In S. C. Elias (Ed.), Encyclopaedia of Quaternary Sciences (Vol. 4, pp. 2682–2698). Elsevier.

Lillesø, J.-P. B., van Breugel, P., Kindt, R., Bingham, M., Demissew, S., Dudley, C., Friis, I., Gachathi, F., Kalema, J., Mbago, F., Minani, V., Moshi, H. N., Mulumba, J., Namaganda, M., Ndangalasi, H. J., Ruffo, C., Jamnadass, R., & Graudal, L. O. V. (2011). Potential Natural Vegetation of Eastern Africa (Ethiopia, Kenya, Malawi, Rwanda, Tanzania, Uganda and Zambia).: Vol. Volume 1: The Atlas. Forest & Landscape, University of Copenhagen.

Mafuta, C., & Westerveld, L. (2017). Lake Victoria Basin: Atlas of our Changing Environment.

McKinnon, K. M. (2018). Flow Cytometry: An Overview. Current Protocols in Immunology, 120(1). https://doi.org/10.1002/cpim.40

Mucina, L., Rutherford, M. C., Powrie, L. W., Gerber, H., Bezuidenhout, H., Sieben, E. J., Cilliers, S. S., du Preez, P. J., Manning, J. C., Hoare, D. B., & Boucher, C. (2006). Inland azonal vegetation. In The Vegetation of South Africa, Lesotho and Swaziland (Vol. 19, pp. 630–631).

Nelson, D. M., Verschuren, D., Urban, M. A., & Hu, F. S. (2012). Long-term variability and rainfall control of savanna fire regimes in equatorial East Africa. Global Change Biology, 18(10), 3160–3170. https://doi.org/10.1111/j.1365-2486.2012.02766.x

Odada, E. O., Olago, D. O., Bugenyi, F., Kulindwa, K., Karimumuryango, J., West, K., Ntiba, M., Wandiga, S., Aloo-Obudho, P., & Achola, P. (2003). Environmental assessment of the East African Rift Valley lakes. Aquatic Sciences - Research Across Boundaries, 65(3), 254–271. https://doi.org/10.1007/s00027-003-0638-9

Olago, D. O., Street-Perrott, F. A., Perrott, R. A., Ivanovich, M., & Harkness, D. D. (2000). Late Quaternary primary tephras in Sacred Lake sediments, northeast Mount Kenya, Kenya. Journal of African Earth Sciences, 30(4), 957–969. https://doi.org/10.1016/S0899-5362(00)00063-4

Palmer, P. I., Wainwright, C. M., Dong, B., Maidment, R. I., Wheeler, K. G., Gedney, N., Hickman, J. E., Madani, N., Folwell, S. S., Abdo, G., Allan, R. P., Black, E. C. L., Feng, L., Gudoshava, M., Haines, K., Huntingford, C., Kilavi, M., Lunt, M. F., Shaaban, A., & Turner, A. G. (2023). Drivers and impacts of Eastern African rainfall variability. Nature Reviews Earth & Environment, 4(4), 254–270. https://doi.org/10.1038/s43017-023-00397-x

Pfadenhauer, J. S., & Klötzli, F. A. (2020). Fundamentals towards Understanding Global Vegetation. In Global Vegetation (pp. 1–120). Springer International Publishing. https://doi.org/10.1007/978-3-030-49860-3_1

Power, M. J., Marlon, J., Ortiz, N., Bartlein, P. J., Harrison, S. P., Mayle, F. E., Ballouche, A., Bradshaw, R. H. W., Carcaillet, C., Cordova, C., Mooney, S., Moreno, P. I., Prentice, I. C., Thonicke, K., Tinner, W., Whitlock, C., Zhang, Y., Zhao, Y., Ali, A. A., … Zhang, J. H. (2008). Changes in fire regimes since the Last Glacial Maximum: an assessment based on a global synthesis and analysis of charcoal data. Climate Dynamics, 30(7–8), 887–907. https://doi.org/10.1007/s00382-007-0334-x

Radbruch, A. (2000). Flow cytometry and cell sorting (2nd ed.). Springer.

Reille, M. (1992). Pollen et spores d'Europe et d'Afrique du nord. Laboratoire de Botanique Historique et Palynologie.

Reimer, P., Austin, W., Bard, E., Bayliss, A., Blackwell, P., Bronk Ramsey, C., . . . Talamo, S. (2020). The IntCal20 Northern Hemisphere Radiocarbon Age Calibration Curve (0–55 cal kBP). Radiocarbon, 62(4), 725-757. doi:10.1017/RDC.2020.41

Roubik, D. W., & Moreno P., J. E. (1991). Pollen and spores of Barro Colorado Island [Panama].

Schüler, L., & Hemp, A. (2016). Atlas of pollen and spores and their parent taxa of Mt Kilimanjaro and tropical East Africa. Quaternary International, 425, 301–386. https://doi.org/10.1016/J.QUAINT.2016.07.038

Schüler, L., Hemp, A., Zech, W., & Behling, H. (2012). Vegetation, climate and fire-dynamics in East Africa inferred from the Maundi crater pollen record from Mt Kilimanjaro during the last glacial-interglacial cycle. Quaternary Science Reviews, 39, 1–13. https://doi.org/10.1016/j.quascirev.2012.02.003

Scoon, R. N. (2018). Geology of National Parks of Central/ Southern Kenya and Northern Tanzania. Cham:Springer.

Sinninghe Damsté, J. S., Verschuren, D., Ossebaar, J., Blokker, J., van Houten, R., van der Meer, M. T. J., Plessen, B., & Schouten, S. (2011). A 25,000-year record of climate-induced changes in lowland vegetation of eastern equatorial Africa revealed by the stable carbon-isotopic composition of fossil plant leaf waxes. Earth and Planetary Science Letters, 302(1–2), 236–246. https://doi.org/10.1016/j.epsl.2010.12.025

Spencer, J. D., Brunelle, A., & Hepola, T. (2017). Using Paleoecology to Inform Land Management as Climates Change: An Example from an Oak Savanna Ecosystem. Environmental Management, 60(6), 1090–1100. https://doi.org/10.1007/s00267-017-0936-y

Ssemmanda, I., & Vincens, A. (1993). Végétation et climat dans le bassin du lac Albert (Ouganda, Zaïre) depuis 13000 ans BP: Apport de la palynologie. Comptes Rendus de l'Académie Des Sciences. Série 2, Mécanique, Physique, Chimie, Sciences de l'univers, Sciences de La Terre, 4(316), 561–567.

Stockmarr, J. (1971). Tablets with spores used in absolute pollen analysis. Pollen Spores, 13, 615–621.

Temoltzin-Loranca, Y., Gobet, E., Vannière, B., van Leeuwen, J. F. N., Wienhues, G., Szidat, S., Courtney-Mustaphi, C., Kishe, M., Muschick, M., Seehausen, O., Grosjean, M., & Tinner, W. (2023). A chronologically reliable record of 17,000 years of biomass burning in the Lake Victoria area. Quaternary Science Reviews, 301. https://doi.org/10.1016/j.quascirev.2022.107915

Temoltzin-Loranca, Y., Gobet, E., Vannière, B., van Leeuwen, J. F. N., Wienhues, G., Courtney-Mustaphi, C., Kishe, M., Muschick, M., King, L., Misra, P., Ngoepe, N., Matthews., Vogel, H., Heiri, O., Seehausen, O., Grosjean, M., & Tinner, W. (2023). Ecological long-term successions around Lake Victoria in response to the latest Pleistocene and Early Holocene climatic changes. [Manuscript in preparation]

Tennant, R. K., Jones, R. T., Brock, F., Cook, C., Turney, C. S. M., Love, J., & Lee, R. (2013). A new flow cytometry method enabling rapid purification of fossil pollen from terrestrial sediments for AMS radiocarbon dating. Journal of Quaternary Science, 28(3), 229–236. https://doi.org/10.1002/jqs.2606

Thevenon, F., Williamson, D., Vincens, A., Taieb, M., Merdaci, O., Decobert, M., & Buchet, G. (2003). A late-Holocene charcoal record from Lake Masoko, SW Tanzania: climatic and anthropologic implications. The Holocene, 13(5), 785–792. https://doi.org/10.1191/0959683603hl665rr

Tierney, J. E., Russell, J. M., Sinninghe Damsté, J. S., Huang, Y., & Verschuren, D. (2011). Late Quaternary behavior of the East African monsoon and the importance of the Congo Air Boundary. Quaternary Science Reviews, 30(7–8), 798–807. https://doi.org/10.1016/j.quascirev.2011.01.017

Tunno, I., Zimmerman, S. R. H., Brown, T. A., & Hassel, C. A. (2021). An Improved Method for Extracting, Sorting, and AMS Dating of Pollen Concentrates From Lake Sediment. Frontiers in Ecology and Evolution, 9. https://doi.org/10.3389/fevo.2021.668676

Umbanhowar, C. E., & McGrath, M. J. (1998). Experimental production and analysis of microscopic charcoal from wood, leaves and grasses. Holocene, 8(3). https://doi.org/10.1191/095968398666496051

Vanderkelen, I., van Lipzig, N. P. M., & Thiery, W. (2018). Modelling the water balance of Lake Victoria (East Africa) - Part 1: Observational analysis. Hydrology and Earth System Sciences , 22(10). https://doi.org/10.5194/hess-22-5509-2018

Vincens, A., Buchet, G., Williamson, D., & Taieb, M. (2005). A 23,000 yr pollen record from Lake Rukwa (8°S, SW Tanzania): New data on vegetation dynamics and climate in Central Eastern Africa. Review of Palaeobotany and Palynology, 137(3–4), 147–162. https://doi.org/10.1016/j.revpalbo.2005.06.001

Vincens, A., Garcin, Y., & Buchet, G. (2007). Influence of rainfall seasonality on African lowland vegetation during the Late Quaternary: pollen evidence from Lake Masoko, Tanzania. Journal of Biogeography, 34(7), 1274–1288. https://doi.org/10.1111/j.1365-2699.2007.01698.x

White. (1983). The Vegetation of Africa. A Descriptive Memoir to Accompany the Unesco/AETFAT/UNSO Vegetation Map of Africa. UNESCO.

Willis, K. J., Bennett, K. D., Burrough, S. L., Macias-Fauria, M., & Tovar, C. (2013). Determining the response of African biota to climate change: using the past to model the future. Philosophical Transactions of the Royal Society B: Biological Sciences, 368(1625), 20120491. https://doi.org/10.1098/rstb.2012.0491

Wooller, M. J., Swain, D. L., Ficken, K. J., Agnew, A. D. Q., Street-Perrott, F. A., & Eglinton, G. (2003). Late Quaternary vegetation changes around Lake Rutundu, Mount Kenya, East Africa: evidence from grass cuticles, pollen and stable carbon isotopes. Journal of Quaternary Science, 18(1), 3–15. https://doi.org/10.1002/jqs.725

Yamada, K., Omori, T., Kitaba, I., Hori, T., & Nakagawa, T. (2021). Extraction method for fossil pollen grains using a cell sorter suitable for routine 14C dating. Quaternary Science Reviews, 272, 107236. https://doi.org/10.1016/j.quascirev.2021.107236

Zander, P. D., Szidat, S., Kaufman, D. S., Żarczyński, M., Poraj-Górska, A. I., Boltshauser-Kaltenrieder, P., & Grosjean, M. (2020). Miniature radiocarbon measurements (150 µg C) from sediments of Lake Żabińskie, Poland: effect of precision and dating density on age–depth models. Geochronology, 2(1), 63–79. https://doi.org/10.5194/gchron-2-63-2020

Zimmerman, S. R. H., Brown, T. A., Hassel, C., & Heck, J. (2019). Testing Pollen Sorted by Flow Cytometry as the Basis for High-Resolution Lacustrine Chronologies. Radiocarbon, 61(1), 359–374. https://doi.org/10.1017/RDC.2018.89

Chapter II: A Chronologically Reliable Record of 17,000 years of Biomass Burning in the Lake Victoria Area

Declaration of contribution

The following study was published in Quaternary Science Reviews (Volume 301, 1st of February 2023, p. 107915). Yunuén Temoltzin Loranca, Willy Tinner and Erika Gobet conceptualized the study, Boris Vannière assessed the fire reconstructions. Jacqueline van Leeuwen and Yunuén Temoltzin Loranca conducted the palynological investigations. Yunuén Temoltzin Loranca did the numerical investigations, the data visualization and wrote the draft of the manuscript. Erika Gobet, Boris Vannière, Jacqueline van Leeuwen, Giulia Wienhues, Sönke Szidat, Colin Courtney-Mustaphi, Mary Kishe, Moritz Muschik, Ole Seehausen, Martin Grosjean and Willy Tinner discussed the results and commented on the manuscript. Ole Seehausen and Martin Grosjean acquired the funding. All authors agree on the science and the style of the manuscript.

A chronologically reliable record of 17,000 years of biomass burning in the Lake Victoria area

Yunuen Temoltzin-Loranca*[a,b], Erika Gobet[b], Boris Vannière[b,c], Jacqueline F.N. van Leeuwen[b], Giulia Wienhues[a], Sönke Szidat[d], Colin Courtney-Mustaphi[e], Mary Kishe[f], Moritz Muschick[g,h], Ole Seehausen[g,h], Martin Grosjean[a], Willy Tinner[b]

[a] Institute of Geography and Oeschger Center for Climate Change Research, University of Bern, Bern, Switzerland
[b] Institute of Plant Sciences and Oeschger Center for Climate Change Research, University of Bern, Bern, Switzerland
[c] Chrono-environement, MSHE, CNRS, Université Bourgogne Franche Comté, Besançon, France
[d] Department of Chemistry, Biochemistry and Pharmaceutical Sciences and Oeschger Center for Climate Change Research, University of Bern, Bern, Switzerland
[e] Department of Environmental Sciences, Geoecology, University of Basel, Basel, Switzerland
[f] Tanzania Fisheries Research Institute, Dar es Salaam, Tanzania
[g] Department of Fish Ecology and Evolution, Center for Ecology, Evolution, and Biogeochemistry, Swiss Federal Institute for Aquatic Science and Technology (EAWAG), Kastanienbaum, Switzerland
[h] Aquatic Ecology and Evolution, Institute of Ecology and Evolution, University of Bern, Bern, Switzerland

*Correspondence to: Yunuén Temoltzin Loranca (yunuen.temoltzin@unibe.ch)

Keywords:
Fire, Charcoal, Chronology, Radiocarbon, Late Pleistocene, Holocene, Pollen, Lake Victoria

2.1 ABSTRACT

Fire regimes differ across tropical and subtropical biomes depending on multiple parameters whose interactions and levels of importance are poorly understood, particularly at multidecadal and longer time scales. In the catchment of Lake Victoria, savanna, rainforest, and Afromontane vegetation have interspersed over the last 17,000 years, which may have influenced the fire regime and vice versa. However, climate and humans are most often the primary drivers of fire regime changes, and analyzing their respective roles is critical for understanding current and future fire regimes. Besides a handful of radiocarbon dates on grassy charcoal, the timescales of published studies of Lake Victoria sediment chronologies rely mostly on dates of bulk sediment, and chronological disagreements persist, mainly due to variation between estimations of the ^{14}C reservoir effect. Here, we provide independent ^{14}C chronologies for three Late Glacial and Holocene lacustrine sediment cores from various water depths and compare them with the biostratigraphy to establish a new chronological framework. We present the first continuous sedimentary charcoal records from Lake Victoria; these suggest that fire activity varied substantially during the past 17,000 years. Our new pollen

records reveal the long-term vegetation dynamics. The available evidence suggests that before human impact increased during the Iron Age (ca. 2400 yr BP), biomass burning was linked to climate and vegetation reorganizations, such as warming, drying, and the expansion of rainforests and savannas. Our results imply that climate can trigger substantial fire regime changes and that vegetation responses to climate change can co-determine the fire regime. For instance, biomass burning decreased significantly when the rainforest expanded in response to increasing temperatures and moisture availability. Such insights into the long-term linkages between climate, vegetation, and the fire regime may help to refine ecosystem management and conservation strategies in a changing global climate.

2.2 INTRODUCTION

The Late Pleistocene and Holocene chronology of Lake Victoria's palaeoenvironmental history has been widely discussed but remains uncertain (Kendall, 1969; Beuning, 1999; Stager and Johnson, 2000; Talbot and Lærdal, 2000; Beuning et al., 2002). The timescales of published studies of Lake Victoria since the lake refilled with water during the Late Pleistocene rely on sediment cores that were predominantly bulk dated with only a couple of radiocarbon dates. The age–depth relationship has been modelled with a range of ^{14}C reservoir effect estimates (e.g. Beuning et al., 1997; Kendall, 1969; Stager et al., 1997). Although early studies extended to the Late Glacial period, more recent studies have not gone beyond the Holocene (Nakintu and Lejju, 2016; Andama, 2012). However, substantial chronological uncertainty and disparity exists between these records, which makes it difficult to compare the available palaeo time series both across East Africa and within the lake. This chronological issue represents a challenge when seeking to compare the signals of different proxies, for instance fire and vegetation responses to large-scale events such as Heinrich Event 1 and the African Humid Period and to local processes such as the desiccation of Lake Victoria (Stager et al., 2011; Garcin et al., 2007).

The long-term linkages between climate, fire regimes, and vegetation have been explored in eastern Africa for the Younger Dryas period (e.g. Garcin et al., 2007; Githumbi, 2017). Some studies emphasized how biomass burning regimes were strongly influenced by climatic and vegetation changes, largely depending on biomass acting as fuel and moisture availability as fire inhibitor or facilitator (Colombaroli et al., 2014; Nelson et al., 2012; Thevenon

et al., 2003). Similar linkages have been observed in other regions of the world such as the Americas and Asia (e.g. Behling, 2002; Burbridge et al., 2004; Whitlock et al., 2010; Zhao and Yu, 2012).

Assessing the causes of fire regime shifts is important because burning modulates the structure, composition, productivity, and diversity of vegetation. It may also create positive or negative feedbacks via fuel availability and flammability, for instance if more or less flammable species are promoted by disturbance (e.g. Henne et al., 2015; Pedrotta et al., 2021). Moreover, the diverse properties of the three major vegetation types around Lake Victoria, the savanna, the rain forest and the Afromontane, may have significantly affected the fire regimes (e.g. Beuning, 1999; Kendall, 1969).

Due to the lack of continuous Holocene fire reconstructions for the Lake Victoria basin, the extent to which fires were controlled by climate, biomass change, and human impact remains unknown. This gap in information reduces our ability to understand the processes and mechanisms which controlled past fire regimes in the Lake Victoria basin. Such information is lacking for many regions of equatorial eastern Africa (Githumbi, 2017). However, the few studies which are available suggest that biomass burning increased in response to regional drought phases at Lake Albert, Mount Kenya, and Mount Kilimanjaro during Heinrich Event 1 (Beuning et al., 1997; Rucina et al., 2009; Schüler et al., 2012).

This study has three aims. The first is to provide a novel chronology for three new sediment cores from Lake Victoria based predominantly on macroscopic charcoal (>200 µm). The established chronology is validated for internal coherence by the biostratigraphy of our three cores. The second is to present the first continuous macroscopic charcoal analysis to reconstruct Late Glacial and Holocene fire history. The third is to discuss the long-term linkages between climate, fire, and vegetation in the Lake Victoria area.

2.3 Material and Methods

2.3.1 Study Site

Lake Victoria is located in East Africa at an altitude of 1135 m above sea level (m a.s.l). Overall, the rainfall regime in the catchment has two rainy and two dry seasons per year. Mean present-day annual precipitation ranges from 1000 to 1500 mm. It is mainly controlled by the

migration of the Intertropical Convergence Zone and of the African monsoons and the variability in the eastward-westward position of the Congo Air Boundary (CAB), and it is locally modified by orography and local albedos (Beverly et al., 2020; Colombaroli et al., 2018; Marchant et al., 2007; Nicholson, 2018; Okungu et al., 2005). At the lake's elevation, the mean annual temperature varies between 24 and 25 °C, while in the highlands at 1950 m a.s.l, it ranges around 14.3 °C and at 3250 m a.s.l. around 7.1 °C. Thus, the mean lapse rate is ca. 0.5 °C/100 m, but this varies across the altitudinal gradient and through geological time (Loomis et al., 2017). Monthly temperatures vary slightly throughout the year, resulting in a tropical climate (Duane et al., 2008).

In the Lake Victoria basin, the strong moisture gradient results in various tropical climates, that span from equatorial climate (Af) to monsoon climate (Am) and savanna climate (Aw) according to Köppen's classification (Köppen, 1936). Along this moisture gradient, the associated biomes develop: the rain forests and the wooded savannas with Af climate and the grassy savannas with Aw climate. Under cooler and more humid conditions and higher elevations, the area hosts Afromontane vegetation: subtropical and temperate climates (Cwb) according to Köppen. The lake extends into Tanzania, Kenya, and Uganda, and the lake basin gathers distinct vegetation types: Guineo–Congolian rainforest, transitional rainforest, swamp forest, scrub forest, riverine forest, Afromontane rainforest, Afromontane undifferentiated forest, evergreen and semi–evergreen bushland, and thicket and derived communities (White, 1983).

2.3.2 SEDIMENT CORES, CHRONOLOGY, AND MACROCHARCOAL

In October 2018, a field campaign organized by the University of Bern in collaboration with the Tanzania Fisheries Research Institute (TAFIRI) recovered sediment cores from four locations along a transect near the Shirati Bay (Fig. 1). The coring was performed with the UWITEC Niederreiter coring system of the Institute of Plant Sciences at University of Bern, which was adapted to reach seaworthy conditions with the aid of eight pontoons made of aluminium instead of rubber and special sea anchors. This paper relies on data from three cores (Fig. 1 a, b): Core LVC18_S1 (hereafter LV1) located at 01°06,914′ S, 33°55,146′ E at a water column depth of 37 m; core LVC18_S2 (LV2) located at 01°07,850′ S, 33°56,780′ E at a

water column depth of 22.6 m; and core LVC18_S4 (LV4) located at 01°02,966′ S, 33°47,768′ E at a water column depth of 63 m.

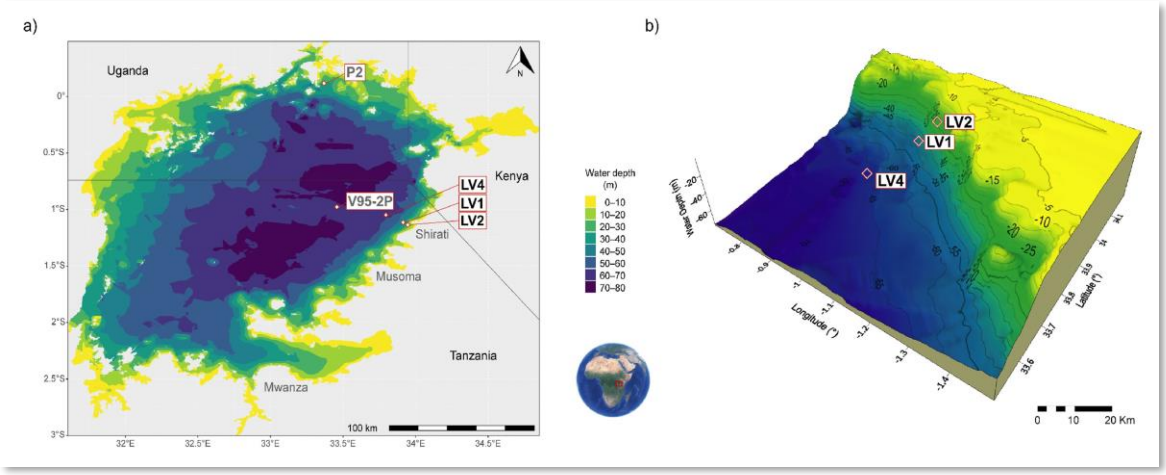

Figure 1. (a) Bathymetry of Lake Victoria indicating the location of the new cores LV1, LV2, and LV4, and previously published cores: P2 (Kendall, 1969) and V95–2P (Beuning, 1999). Colour chart shows the water depth as of 2017. (b) Relief map of the lake floor according to water depth of 2017. Datapoints for elaborating both maps were extracted from Hamilton et al. (2016).

The amount of sediment was limited, and its use had to be optimized for as many analyses as possible, leading us to modify the charcoal extraction (see Appendix A), and avoid the usage of chemical products as proposed in some standard methods (Millspaugh and Whitlock, 1995; Mooney and Tinner, 2011). For the sieved charcoal analysis, a total of 1151 sediment samples (361 from LV1, 401 from LV2, and 389 from LV4) of ca. 9 cm^3 were taken continuously at 2 cm intervals and passed through a graded series of screens of mesh size 200, 100, 50, and 20 µm. Samples containing particles >200 µm were analysed under a stereoscopic microscope LEICA M125 at 50 × magnification to separate, measure, and count the charcoal particles and to screen for plant and animal macrofossils.

Charcoal particles were standardized as number of particles per cm−3, and the sedimentation rate (cm/yr) was extracted from the age–depth model with Long et al.'s (1998) technique. These were then multiplied to calculate the charcoal influx or charcoal accumulation rate (CHAR; number of particles cm−2 yr−1). Given that in large water bodies charcoal particles can reach similar distances to those of pollen grains (Genet et al., 2021), and due to the lack of >0.6 mm particles, the fire signal was taken as regional (Adolf et al., 2018). The charred plant macroremains were separated, dried in the oven at 80 °C, and weighed.

Subsequently, samples >0.10 mg were selected for AMS radiocarbon dating, which corresponded to 8% of the total samples.

In all three cores, the top of the composite was taken as the surface, and a total of 93 samples were radiocarbon dated. This was done with the MICADAS accelerator mass spectrometry (AMS) system at the Laboratory for the Analysis of Radiocarbon with AMS (LARA) at the University of Bern (Szidat et al., 2014) using two different approaches (Table 1). First, 31 samples of the 20–50 µm sieved fraction (containing all organic structures resistant to decay; from now on referred to as '20–50 µm palynomorph concentrate') representing all sites were treated for 3 h with 0.5 mol/L hydrochloric acid (HCl) at 40 °C. These pre-treated samples were then transformed into graphite targets with automated graphitization equipment (AGE) and measured with the MICADAS. Second, 63 samples of isolated macrocharcoal were purified with 0.5 mol/L HCl for 3 h at 40 °C, followed by 0.1 mol/L sodium hydroxide (NaOH) for 15 min at room temperature and another step of 0.5 mol/L HCl for 3 h at 40 °C. Because of their low dry weight after treatment (8–130 µgC with an average of 46 µgC), graphitization was replaced by combustion of the samples and direct injection of the resulting carbon dioxide (CO2) into the gas ion source of the MICADAS (Salazar et al., 2015). Zander et al. (2020) showed that the quality of a lake sediment chronology may improve with the implementation of small-sized gas samples, even though their individual age uncertainties are typically higher than for medium- to large-sized samples from graphite targets. Nevertheless, seven samples failed analysis due to their insufficient dry weight after chemical treatment. In LV1, there were two duplicated samples at 566 and 680 cm respectively, and in order to get the best age estimation, each sample was combined with its pair (from now on referred to as 'pooled dates') with OxCal 4.3 (R_combine, Bronk Ramsey C., 1994, 1995, 2001).

To assess chronological biases due to the ^{14}C reservoir effect, we constructed two age-depth models for each site: first, exclusively with dates originating from the palynomorph-bulk concentrate, which also contained algae cells such as Pediastrum and Botryococcus; and second, with dates originating solely from macrocharcoal. Then, we measured paired samples, and we calculated (i) the difference in ages of same depths between the 20–50 µm palynomorph concentrate and the microcharcoal and (ii) the mean and standard deviation of the differences of all three sites. The corrected ages of the 20–50 µm palynomorph concentrate and the terrestrial macrofossil ages were used to construct a combined model

with its 95% (2σ) probabilities using rbacon (Blaauw and Christen, 2011; Blaauw et al., 2021) in R software and the IntCal20 calibration curve (Reimer et al., 2020).

Subsequently, after developing the three independent chronologies, we used the biostratigraphy of each site to crosscheck the resulting ages. For instance, the bottom of the record was aligned with the population decrease of Amaranthaceae/Chenopodiaceae and an apparent regional appearance of *Acalypha* towards ca. 14,500 cal yr BP (see Section 3.3). Furthermore, during the Late Glacial, *Olea* pollen increases at 14,000–13,000 cal yr BP in all three records. Similarly, at 10,500 cal yr BP, *Alchornea* and *Acalypha* pollen increases at all sites. Moreover, *Celtis* pollen increases at ca. 8000 cal yr BP at all sites. Finally, at ca. 4500 cal yr BP, arboreal taxa such *Celtis* and Moraceae declined, and Poaceae increased at all three sites, signifying an expansion of open land. Our biostratigraphic comparison suggests that the three radiocarbon-based age-depth models provide robust and spatially reproducible chronologies.

Table 1. Radiocarbon dates of the Lake Victoria cores LV1 (LVC18_S1), LV2 (LVC18_S2) and LV4 (LVC18_S4) drilled in 2018.

Sample #	Laboratory code	Core	Sample ID	Composite core depth (cm)	Material	Carbon mass (µg)	^{14}C age (yr BP)*	Age corrected for ^{14}C reservoir effect for B and P (yr BP)*	Median ages (cal yr BP)	95 % C.I. (cal yr BP)	Model ages (cal yr BP)	Model age C.I.
1[1]	BE-13429	LVC18_S1	B1_20–22	022–024	C	12	-705 ± 170**	–	–	–	17	-63–201
2[1]	BE-13430	LVC18_S1	B1_24–26	026–028	C	14	-225 ± 150***	–	–	–	51	-51–260
3	BE-14379	LVC18_S1	B2_74–76	150–152	P	997	2250 ± 20	1680 ± 410	1635	751–2695	1540	1137–2070
4	BE-13425	LVC18_S1	B2_80–84	156–160	C	9	1410 ± 270	–	1317	743–1872	1633	1212–2227
5	BE-14384	LVC18_S1	B2_80–84	156–160	B	989	2300 ± 20	1730 ± 410	1689	828–2705	1633	1212–2227
6	BE-13418	LVC18_S1	B2_94–96	170–172	C	6	MEASUREMENT FAILED					
7	BE-15530	LVC18_S1	B3_70–72	246–248	P	989	3550 ± 30	2980 ± 410	3156	2120–4159	3327	2801–3737
8	BE-13420	LVC18_S1	C2_04–06	270–272	C	39	3540 ± 90	–	3826	3575–4084	3736	3401–3995
9	BE-14362	LVC18_S1	C2_30–32	296–298	C	52	3922 ± 100	–	4351	4003–4795	3996	3627–4301
10	BE-13416	LVC18_S1	C2_32–38	298–302	C	29	2780 ± 140	–	2920	2499–3334	4016	3635–4339
11	BE-15532	LVC18_S1	C2_34–36	300–302	P	994	4210 ± 30	3630 ± 410	3989	2883–5044	4023	3641–4339
12	BE-12182	LVC18_S1	B4_06–08	308–310	C	5	MEASUREMENT FAILED					
13	BE-13423	LVC18_S1	B4_18–20	322–324	C	9	2960 ± 300	–	3128	2358–3833	4183	3791–4531
14	BE-15533	LVC18_S1	B4_22–24	326–328	P	985	4380 ± 30	3800 ± 410	4208	3177–5315	4221	3833–4574
15	BE-13422	LVC18_S1	B4_26–28	330–332	C	8	3250 ± 320	–	3488	2745–4394	4263	3867–4621
16	BE-15534	LVC18_S1	B4_46–48	350–352	P	985	4680 ± 30	4100 ± 410	4596	3494–5596	4475	4082–4892
17	BE-15535	LVC18_S1	B4_72–74	376–378	P	990	5060 ± 30	4480 ± 410	5081	3980–6168	4767	4367–5274
18	BE-13421	LVC18_S1	B4_74–76	378–380	C	14	3980 ± 200	–	4439	3876–4691	4790	4381–5318

Sample #	Laboratory code	Core	Sample ID	Composite core depth (cm)	Material	Carbon mass (µg)	^{14}C age (yr BP)*	Age corrected for ^{14}C reservoir effect for B and P (yr BP)*	Median ages (cal yr BP)	95 % C.I. (cal yr BP)	Model ages (cal yr BP)	Model age C.I.
19	BE-15536	LVC18_S1	B5_09–11	402–404	P	990	5220 ± 30	4640 ± 410	5276	4242–6220	5209	4746–5764
20	BE-13424	LVC18_S1	B5_17–19	410–412	C	11	4390 ± 320	–	4989	4093–5840	5374	4896–5942
21	BE-13419	LVC18_S1	B5_39–41	432–434	C	3	MEASUREMENT FAILED					
22	BE-15537	LVC18_S1	B5_57–59	450–452	P	992	6200 ± 35	5630 ± 410	6443	5584–7418	6382	5736–7007
23	BE-15538	LVC18_S1	B5_83–85	476–478	P	987	6810 ± 35	6240 ± 410	7076	6214–7928	7053	6408–7625
24	BE-15531	LVC18_S1	B6_10–12	502–504	P	910	7380 ± 40	6810 ± 410	7663	6749–8424	7603	6982–8134
25	BE-15539	LVC18_S1	B6_36–38	528–530	P	996	7830 ± 40	7250 ± 410	8097	7312–9017	8123	7614–8618
26[2,3]	BE-14377	LVC18_S1	C5_01–03	546–548	C	18	13900 ± 430	–	16842	15681–18091	–	–
27	BE-12183	LVC18_S1	C5_23–25	566–568	C	56	8430 ± 120	–	9409	9029–9658	8920	8611–9346
28	BE-13417	LVC18_S1	C5_21–23	566–568	C	30	7300 ± 130	–	8119	7867–8376	8920	8611–9346
29	BE-12184	LVC18_S1	C6_07–09	624–626	C	2	MEASUREMENT FAILED					
30	BE-12185	LVC18_S1	C6_11–13	628–630	C	51	9490 ± 120	–	10801	10437–11182	10889	10392–11328
31	BE-12186	LVC18_S1	C6_39–41	656–658	C	4	MEASUREMENT FAILED					
32	BE-12187	LVC18_S1	C6_51–53	668–670	C	14	10550 ± 370	–	12295	11254–13114	12578	11939–13091
33	BE-12189	LVC18_S1	C6_63–65	680–682	W	38	11500 ± 170	–	13375	13095–13748	13140	12775–13433
34	BE-12188	LVC18_S1	C6_63–65	680–682	C,W,X	14	10000 ± 370	–	11599	10574–12689	13140	12775–13433
35	BE-12190	LVC18_S1	C6_79–81	696–698	C	13	11900 ± 480	–	13961	12840–15304	13414	13131–13780
36	BE-12191	LVC18_S1	C6_81–83	698–700	S, C	53	11600 ± 160	–	13465	13173–13781	13449	13157–13849
37	BE-12192	LVC18_S1	C6_89–91	706–708	W	3	MEASUREMENT FAILED					

Sample #	Laboratory code	Core	Sample ID	Composite core depth (cm)	Material	Carbon mass (µg)	^{14}C age (yr BP)*	Age corrected for ^{14}C reservoir effect for B and P (yr BP)*	Median ages (cal yr BP)	95 % C.I. (cal yr BP)	Model ages (cal yr BP)	Model age C.I.
38	BE-12193	LVC18_S1	C6_89–91	706–708	C	2	MEASUREMENT FAILED					
39	BE-15540	LVC18_S2	E2_34–36	126–128	P	920	1800 ± 30	1230 ± 410	1163	335–2094	1210	748–1748
40	BE-15541	LVC18_S2	E2_60–62	154–156	P	900	1980 ± 30	1410 ± 410	1343	557–2302	1500	1014–2065
41	BE-15542	LVC18_S2	E2_90–92	184–186	P	868	2260 ± 30	1690 ± 410	1646	787–2696	1848	1384–2405
42	BE-15543	LVC18_S2	E3_18—20	212–214	P	834	2620 ± 30	2050 ± 410	2043	1129–2998	2251	1739–2843
43	BE-15544	LVC18_S2	E3_46–48	240–242	P	718	2870 ± 40	2300 ± 410	2327	1396–3329	2692	2112–3381
44	BE-15545	LVC18_S2	F4_15–17	268–270	P	972	3310 ± 30	2740 ± 410	2860	1828–3848	3289	2619–4001
45	BE-14367	LVC18_S2	F4_67–73	320–326	C,R	37	4160 ± 100	–	4679	4416–4953	4705	4201–5062
46	BE-13426	LVC18_S2	F5_72–73	403–404	L	997	5360 ± 20	–	6144	6007–6273	6120	6006–6265
47	BE-14370	LVC18_S2	E5_80–82	432–434	C	92	5470 ± 80	–	6259	6004–6436	6378	6202–6679
48	BE-14372	LVC18_S2	E6_08–16	458–466	C	32	6170 ± 120	–	7054	6747–7318	7055	6709–7384
49	BE-14366	LVC18_S2	E6_16–20	466–470	C	28	6250 ± 140	–	7135	6796–7426	7144	6831–7461
50	BE-15546	LVC18_S2	F6_19–21	506–508	P	833	7280 ± 40	6710 ± 410	7560	6678–8367	7807	7332–8340
51	BE-14375	LVC18_S2	F7_33–35	550–552	C	46	7920 ± 110	–	8773	8455–9022	8746	8418–9110
52[2,3]	BE-14371	LVC18_S2	E7_34–38	588–592	C,W	21	7200 ± 180	–	8023	7688–8360	–	–
53	BE-15547	LVC18_S2	E7_50–52	604–606	P	862	8780 ± 40	8200 ± 410	9129	8207–10182	9609	9126–10115
54	BE-14364	LVC18_S2	E8_21–31	628–638	C	45	9030 ± 130	–	10156	9715–10503	10214	9818–10432
55	BE-15548	LVC18_S2	E8_27–29	634–636	P	871	9180 ± 40	8610 ± 410	9657	8554–10680	10249	10071–10410
56	BE-13427	LVC18_S2	E8_34–35	641–642	T	987	9243 ± 20	–	10416	10292–10504	10376	10262–10480

Sample #	Laboratory code	Core	Sample ID	Composite core depth (cm)	Material	Carbon mass (µg)	^{14}C age (yr BP)*	Age corrected for ^{14}C reservoir effect for B and P (yr BP)*	Median ages (cal yr BP)	95 % C.I. (cal yr BP)	Model ages (cal yr BP)	Model age C.I.
57	BE-14369	LVC18_S2	E8_35–37	642–644	C	136	9320 ± 300	–	10569	9609–11314	10391	10278–10500
58	BE-13428	LVC18_S2	E8_37–38	644–645	T	987	9230 ± 20	–	10393	10282–10499	10420	10306–10527
59	BE-14374	LVC18_S2	E8_47–53	654–660	C	43	9110 ± 130	–	10288	9821–10652	10561	10358–11153
60	BE-15549	LVC18_S2	E8_55–57	662–664	P	964	10100 ± 50	9560± 410	10923	9697–12434	10768	10507–11284
61	BE-14373	LVC18_S2	E8_75–77	682–684	C	40	10300 ± 150	–	12099	11404–12621	11798	10507–11284
62	BE-14368	LVC18_S2	E8_77–87	684–694	C	106	10200 ± 110	–	11878	11397–12466	11902	11387–12387
63	BE-15550	LVC18_S2	E8_83–85	690–692	P	813	10500 ± 50	9970 ± 410	11554	10421–12720	11936	11490–12332
64	BE-14365	LVC18_S2	E9_07–15	714–722	C	37	10400 ± 160	–	12240	11653–12723	12516	11986–12980
65	BE-15551	LVC18_S2	E9_11–13	718–720	P	927	11200 ± 50	10630 ± 410	12379	11249–13297	12537	12030–12951
66	BE-15552	LVC18_S2	E9_39–41	746–748	P	823	11900 ± 50	11360 ± 410	13274	12108–14308	13333	13022–13689
67	BE-14376	LVC18_S2	E9_41–43	748–750	C	70	11500 ± 140	–	13372	13104–13605	13413	13094–13778
68	BE-14363	LVC18_S2	E9_93–95	800–802	C,W,S	99	13000 ± 130	–	15557	15189–15944	15424	14405–15923
69	BE-16248	LVC18_S4	L2_31–35	116–118	C	32	2890 ± 100	–	3035	2781–3329	3051	2770–3344
70	BE-16249	LVC18_S4	L2_59–63	144–148	C	71	3290 ± 70	–	3517	3373–3690	3539	3293–3787
71	BE-16262	LVC18_S4	L2_61–63	146–148	P	968	3400 ± 25	2830 ± 410	2972	1932–3980	3557	3344–3787
72	BE-16250	LVC18_S4	L2_85–87	170–172	C	105	3670 ± 70	–	4004	3777–4233	4043	3832–4268
73	BE-16251	LVC18_S4	L3_03–05	188–190	C	37	3990 ± 90	–	4463	4156–4814	4404	4155–4649
74	BE-16252	LVC18_S4	L3_23–27	208–212	C	47	4190 ± 90	–	4706	4440–4959	4774	4488–5151
75	BE-16263	LVC18_S4	L4_18–20	272–274	P	995	5770 ± 30	5200 ± 410	5952	4883–6882	6273	5946–6564

Sample #	Laboratory code	Core	Sample ID	Composite core depth (cm)	Material	Carbon mass (µg)	^{14}C age (yr BP)*	Age corrected for ^{14}C reservoir effect for B and P (yr BP)*	Median ages (cal yr BP)	95 % C.I. (cal yr BP)	Model ages (cal yr BP)	Model age C.I.
76	BE-16253	LVC18_S4	L4_18–22	272–276	C	43	5500 ± 100	–	6294	6003–6492	6297	5946–6647
77	BE-16254	LVC18_S4	L5_09–11	334–336	C	55	6570 ± 100	–	7468	7273–7613	7498	7198–7773
78	BE-16255	LVC18_S4	L5_61–65	386–390	C	48	7910 ± 120	–	8763	8429–9023	8749	8413–9081
79	BE-16256	LVC18_S4	L5_93–97	418–422	C	53	8340 ± 110	–	9323	9029–9531	9296	8958–9585
80	BE-16264	LVC18_S4	L5_95–97	420–422	P	999	8510 ± 30	7940 ± 410	8843	7935–9883	9311	8978–9585
81	BE-16257	LVC18_S4	L6_58–60	484–486	C	62	9270 ± 120	–	10459	10201–10988	10325	9829–10657
82	BE-16258	LVC18_S4	L7_06–08	516–518	C	18	9000 ± 260	–	10103	9481–11058	10620	10167–11084
83	BE-16259	LVC18_S4	L7_36–38	546–548	C	31	9320 ± 190	–	10557	9974–11182	11056	10597–11626
84	BE-16265	LVC18_S4	L7_36–38	546–548	P	775	10200 ± 60	9660 ± 410	11068	9914–12476	11056	10597–11626
85	BE-16260	LVC18_S4	L8_30–32	594–596	C	25	10600 ± 230	–	12453	11755–13066	12263	11581–12850
86	BE-16261	LVC18_S4	L8_84–86	648–650	C	33	11500 ± 200	–	13379	13000–13795	13447	13034–13906
87	BE-15553	LVC18_S4	L9_10–12	674–676	C	50	12200 ± 190	–	14234	13614–14974	14097	13716–14565
88	BE-16266	LVC18_S4	L9_10–12	674–676	P	688	13000 ± 70	12300 ± 410	14478	13414–15667	14097	13716–14565
89	BE-15554	LVC18_S4	L9_20–24	684–686	C	60	12300 ± 170	–	14408	13808–15003	14299	13866–14791
90	BE-15555	LVC18_S4	L9_40–42	704–706	C	38	12000 ± 210	–	13920	13434–14828	14738	14108–15298
91	BE-15556	LVC18_S4	L10_02–04	762–764	C	194	13700 ± 170	–	16588	16081–17056	16386	15899–16826
92	BE-15557	LVC18_S4	L10_12–14	772–774	C	193	13700 ± 160	–	16589	16121–17045	16596	16106–17046
93	BE-16267	LVC18_S4	L10_12–14	772–774	P	248	14100 ± 110	13500 ± 410	16282	15046–17432	16596	16106–17046

Sample #	Laboratory code	Core	Sample ID	Composite core depth (cm)	Material	Carbon mass (µg)	^{14}C age (yr BP)∗	Age corrected for ^{14}C reservoir effect for B and P (yr BP)∗	Median ages (cal yr BP)	95 % C.I. (cal yr BP)	Model ages (cal yr BP)	Model age C.I.
94[2]	BE-16564	LVC18_CCS	L10–core catcher	Below last segment core	P	989	17200 ± 46	16600 ± 410	20044	19018–20970	–	–

∗Dates rounded following Stuiver & Polach (1977). ∗∗ F ^{14}C = 1.092 ± 0.023.∗∗∗F ^{14}C = 1.028 ± 0.019. [1]Samples containing bomb ^{14}C. [2]Sample not included in the age–depth models.[3]Outliers. B = Bulk, C = Charcoal, R = Terrestrial plant remains, L = Lakeshore plant root/stem (Poales), P = 20–50 µm palynomorph concentrate, S = Terrestrial seed (Carex spp.), T = Twig, W = Wood, X = Terrestrial seed coat, C.I. = Confidence Interval.

2.3.3 POLLEN ANALYSIS

We took a total of 80 sediment samples of 1 cm^3 at sampling intervals of ca. 35 cm at each site: 27 from LV1, 27 from LV2, and 26 from LV4. Lycopodium tablets were added to the samples prior to chemical treatment (Stockmarr, 1971). Samples were treated with HCl, KOH, HF, and acetolysis, following the standard methods for pollen extraction (Moore et al., 1991). For slide preparation, the samples were stained with fuchsine and diluted with glycerine. Pollen grains were identified under a light microscope at 400 × magnification and using palynological keys and photo atlases (Gosling et al., 2013; Reille, 1992; Roubik and Moreno, 1991; Schüler and Hemp, 2016) with the aid of the Mount Kilimanjaro reference collection at the palynological laboratory of the University of Göttingen, Germany. Pollen sums along the record range from 217 to 545 pollen grains per sample (mean = 390 pollen grains, standard deviation = 80).

Lake Victoria is located at a crucial ecological junction of three main biomes: the savanna, the rainforest, and the Afromontane forest. In this study, the grouping of the species by biome was made according to the Flora of Tropical East Africa (1955–2012), and only selected taxa from each biome were considered. All rainforest types mentioned in Section 2.1 were grouped in the rainforest category, and the two types of Afromontane forests under Afromontane, which have a more complex structure than the rainforests, require more precipitation, and start developing under cooler conditions at 1200–1300 m.a.s.l. (White, 1983). Taking into account these considerations, we included Moraceae, *Mussaenda*, *Macaranga*, *Alchornea*, and *Urera*-type in the rainforest category and *Celtis*, *Podocarpus*, *Juniperus*, *Olea* and *Allophylus* in the Afromontane category.

Accordingly, *Celtis* can develop starting from 300 up to 2000 m a.s.l and develops most strongly between 1000 and 1800 m a.s.l. (Schüler and Hemp, 2016). *Podocarpus* occurs at 900 m a.s.l. but is more abundant between 2500 and 3100 m a.s.l (Schüler and Hemp, 2016). *Juniperus* is part of the Afromontane undifferentiated forest. Interestingly, this ecosystem is very sensitive to drier conditions, in which it undergoes kaleidoscopic changes in structure, and after fires it is replaced by stands of single, dominant Afromontane species such as *Juniperus procera* or *Hagenia abyssinica*. These vegetational changes occur between 1250 and 2500 m a.s.l. (Kindt et al., 2015). *Olea* has its greatest abundances between 2000 and 2500 m a.s.l.,

even though some subspecies can also grow in riverine fringes at lower altitudes. Lastly, in the lowlands, the savanna vegetation includes Poaceae, Cyperaceae, *Cyperus*-type, *Cissampelos*, *Acalypha*, *Combretum*, and Amaranthaceae/Chenopodiaceae. The terrestrial and the pollen grains from aquatic *Cyperus* were summed in the Cyperaceae category.

2.4 NUMERICAL METHODS

2.4.1 STATISTICAL ANALYSES

The number of charcoal particles was resampled on a regular time bin, every 40 years based on the average accumulation rate. Then, we compared the three cores with a nonparametric two-sample Mann–Whitney test and the distribution of the charcoal influx (CHAR), as shown in boxplots (Fig. 5f). For each CHAR time series, we used a generalized additive model (GAM) to model and identify zones of similar trends. Additionally, to assess the trend change and highlight the phases of high, medium, or low values of CHAR, for each site we conducted a Bayesian change point analysis with the bcp v 4.0.5 package in R (Erdman and Emerson, 2007). The results between sites showed slight variations, but this was expected because the age uncertainty varies between models. Therefore, we decided to use only the change points of LV4, because their age uncertainty is the smallest of the three cores included in this study.

2.4.2 POLLEN ZONATION AND ORDINATION

To determine the local pollen assemblage zones (LPAZ), we used the optimal partitioning approach with minimum sum of squares and the broken stick model (Bennett, 1996; Birks and Gordon, 1985), and the subzones in zone 1 were based on visual criteria.

Then, we conducted a principal component analysis (PCA) using Canoco 5.10 (ter Braak and Šmilauer, 2018) to seek similarities in samples between sites and correlations with temperature records in the area and with our charcoal records. Because our response data are compositional and have a short length of the gradient (sd = 1.5), we applied a linear ordination method on the square-root-transformed pollen percentage data (ter Braak and Prentice, 1988). We grouped the samples and represented groups by colour according to their LPAZ and

by figure according to their sites of origin (Fig. 11). This ordination method was also performed site by site.

2.5 RESULTS AND INTERPRETATION

2.5.1 CHRONOLOGY

Of the three age–depth models constructed (Fig. 2, Fig. 3, Fig. 4), LV4 (the deepest site in the transect) turned out to have the most reliable chronology with the highest number of terrestrial dates and, thus, smaller uncertainties.

The calculated mean difference between the 20–50 palynomorph concentrate and the microcharcoal resulted in 573 years, which were taken as the ^{14}C reservoir effect value and subtracted from each one of the ^{14}C palynomorph-bulk dates to correct for too old dates (Olsson, 2009). The calculated standard deviation, sd = 410, was then taken as the uncertainty. The reservoir effect was taken as constant across the three cores because the calculations were based on measurements from all three.

Sedimentation rates are comparable in all cores (mean: LV1 = 0.07, LV2 = 0.06, LV4 = 0.05 cm/yr) with only minor variability (sd: LV1 = 0.04, LV2 = 0.02, LV4 = 0.01 cm/yr). However, there are two separate sedimentation periods in LV1 and LV2: the first from the start of the records up to ca. 5000–3000 cal yr BP with lower sedimentation rates and the second from then to the present with increased sedimentation rates (Fig. 2, Fig. 3). The latter may have increased by human impact in the catchment during the past 2000 years (Clark, 1962). LV4 does not show such a pattern, suggesting that in the deeper parts of the lake sedimentation rates remained more stable during the Late Glacial and the Holocene.

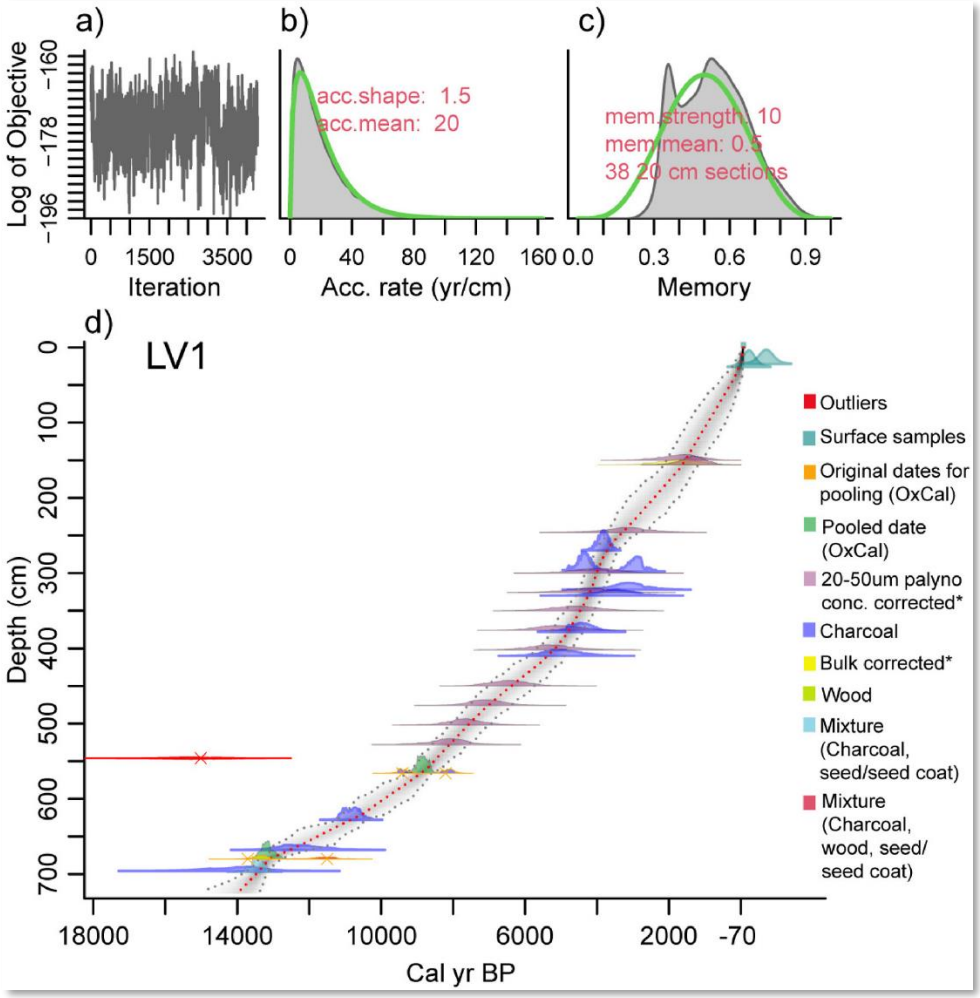

*Figure 2. Age-depth model of LV1, using the software Bacon (Blaauw and Christen, 2011; Blaauw et al., 2021) in cal yr BP (BP = 1950 CE; -70 = 2020 CE). (a) Markov Chain Monte Carlo random walk model iterations. (b) Prior (green) and posterior (grey) distribution of accumulation rate. (c) Prior (green) and posterior (grey) distribution of the age model. (d) Calibrated ^{14}C dates and age-depth model results. The red line indicates the best fit central tendency estimate for the model based on the weighted mean of all included iterations. The grey shade indicates a summary of the iterative walks, and the grey dotted line shows the 95% confidence intervals of these iterations. *20–50 µm palynomorph concentrate corrected for ^{14}C reservoir effect.*

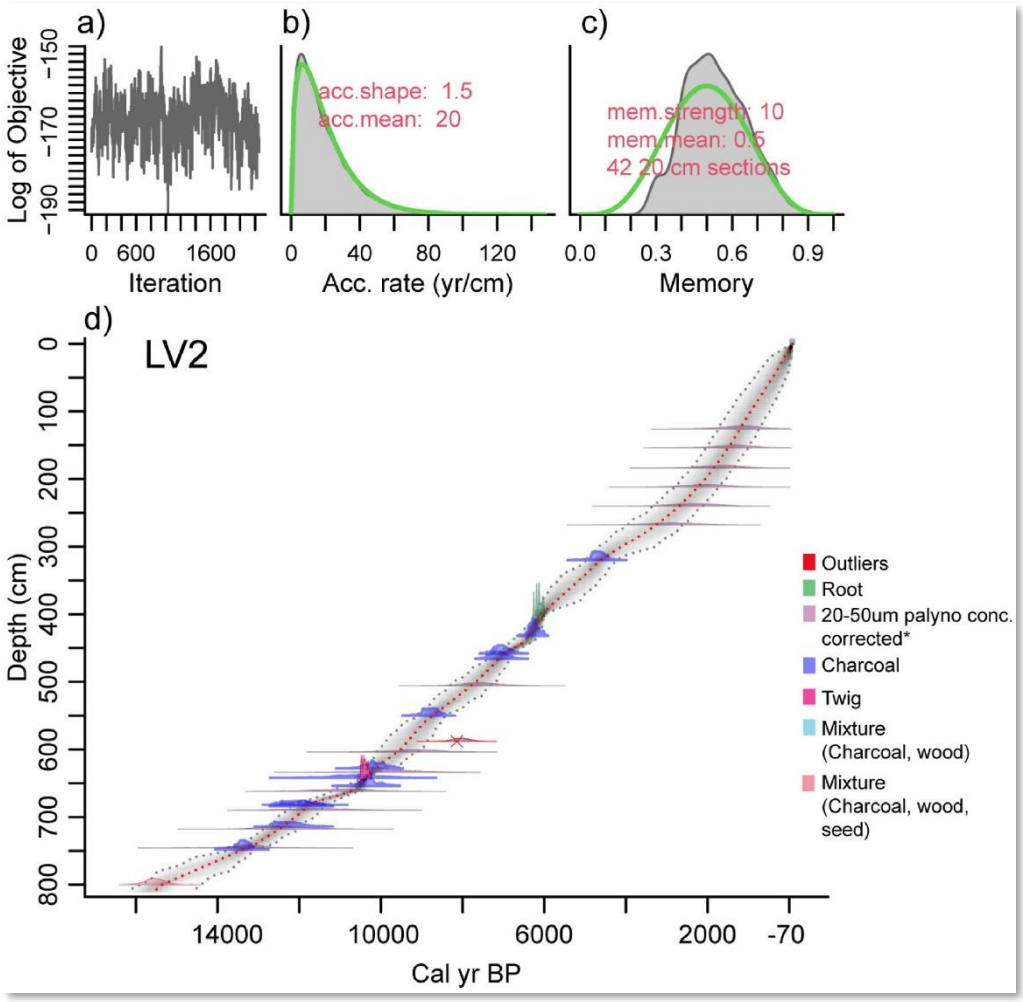

*Figure 3. Age-depth model of LV2 using Bacon software (Blaauw and Christen, 2011; Blaauw et al., 2021) in cal yr BP (BP = 1950 CE; -70 = 2020 CE). (a) Markov Chain Monte Carlo random walk model iterations. (b) Prior (green) and posterior (grey) distribution of accumulation rate. (c) Prior (green) and posterior (grey) distribution of the age model. (d) Calibrated ^{14}C dates and age-depth model results. The red line indicates the best fit central tendency estimate for the model based on the weighted mean of all included iterations. The grey shade indicates a summary of the iterative walks, and the grey dotted line shows the 95% confidence intervals of these iterations. *20–50 µm palynomorph concentrate corrected for ^{14}C reservoir effect.*

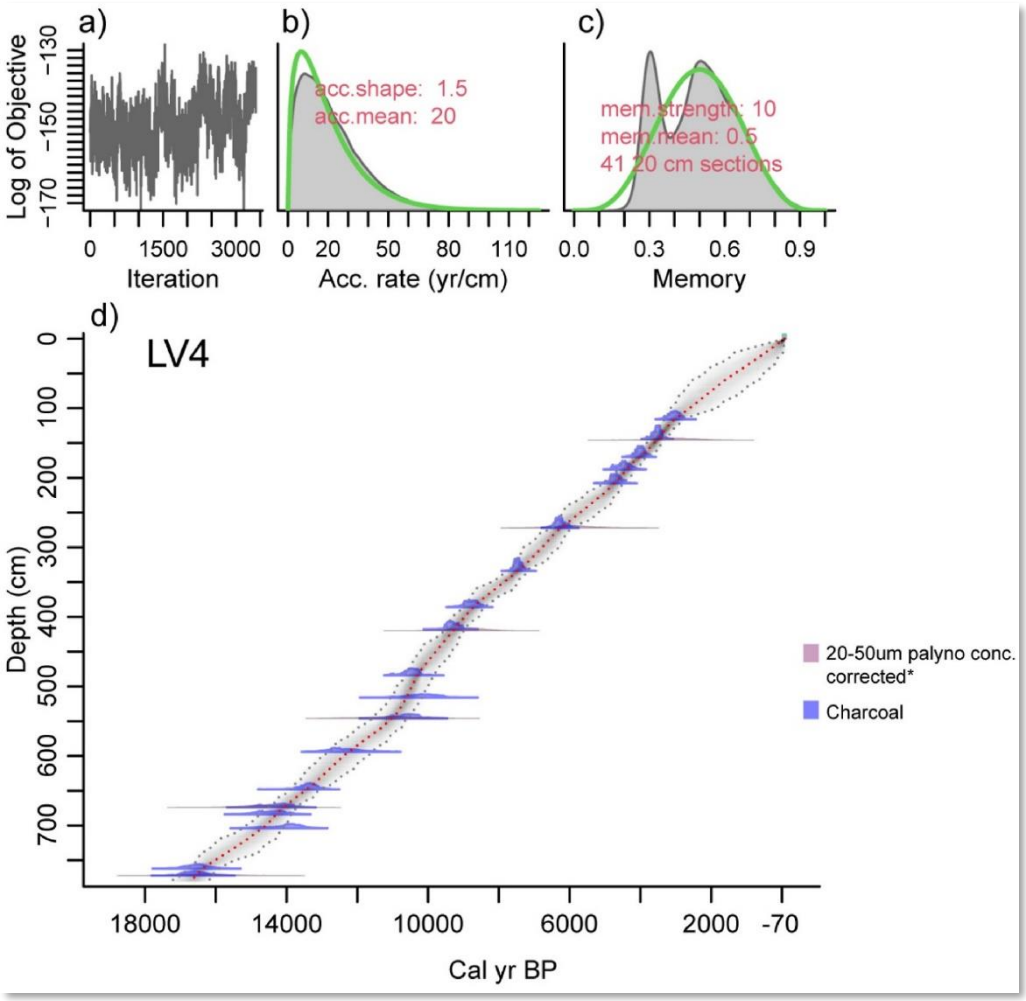

*Figure 4. Age-depth model of LV4, using the software Bacon (Blaauw and Christen, 2011; Blaauw et al., 2021) in cal yr BP (BP = 1950 CE; -70 = 2020 CE). (a) Markov Chain Monte Carlo random walk model iterations. (b) Prior (green) and posterior (grey) distribution of accumulation rate. (c) Prior (green) and posterior (grey) distribution of the age model. (d) Calibrated ^{14}C dates and age-depth model results. The red line indicates the best fit central tendency estimate for the model based on the weighted mean of all included iterations. The grey shade indicates a summary of the iterative walks, and the grey dotted line shows the 95% confidence intervals of these iterations. * 20–50 µm palynomorph concentrate corrected for ^{14}C reservoir effect. Dates coming from the 20-50 µm palynomorph concentrate appear in the diagram with larger uncertainties behind the charcoal dates.*

2.5.2 MACROSCOPIC CHARCOAL AND FIRE HISTORY

CHAR values differ between sites (Fig. 5f) showing p values < 0.05 (Mann–Whitney test) when compared with each other. Charcoal influx ranges at LV1 from 0 to 2.12 particles cm−2 yr −1, at LV2 from 0 to 0.89 and, at LV4 from 0 to 3.02, with means of 0.04, 0.08, and 0.15 particles cm−2 yr −1, respectively. The variability of records through time follows similar trends. LV1 shows more homogeneous and lower values than the other two sites possibly as a consequence of the morphology of the coring location and sediment resuspension (Fig. 5f). These moderate differences between sites might indicate that there are also various physical factors acting on charcoal transport and/or charcoal sources, such as water circulation, and depositional environments. In these terms, it has been demonstrated that, throughout the year Lake Victoria has a significant movement of waters across all its extension (Nyamweya et al., 2016). Therefore, we primarily attribute the deposition of the biggest charcoal particles at LV4 to sediment focusing in the deepest part of lake (Blais and Kalff, 1995).

At LV4, which is the chronologically best dated and the longest sequence, trend lines show CHAR maxima lasting from ca. 15,000–14,000, 11,500–10,500 and 5000–4000 cal yr BP. The latter maximum also occurs at the two other sites and is thus reproducible in space and time, attesting to a definite increase in biomass burning around 5000–4000 cal yr BP (Fig. 5). Declining trends in CHAR fluxes occur at all three sites from 13,000 to 11,500 cal yr BP, suggesting weakening burning during this time. From 10,000–5000 cal yr BP, CHAR fluxes remain low at all three sites, suggesting that fire events were reduced in the Lake Victoria basin during this time. A period with declining CHAR trends occurred again at all three sites from 4000 to 2000 cal yr BP, suggesting that after the fire peak at around 4500 cal yr BP, regional burning decreased for approximately two millennia. Change points occurred during periods showing divergent patterns of CHAR, being minima (e.g. 16,660 cal yr BP), increases (e.g. 15,090 cal yr BP), maxima (e.g. 11,150 cal yr BP), and declines (e.g. 2660 cal yr BP). In sum, LV4 CHAR change points occur at ca. 16,660, 15,090, 11,150, and 2660 cal yr BP (Fig. 5 d,e).

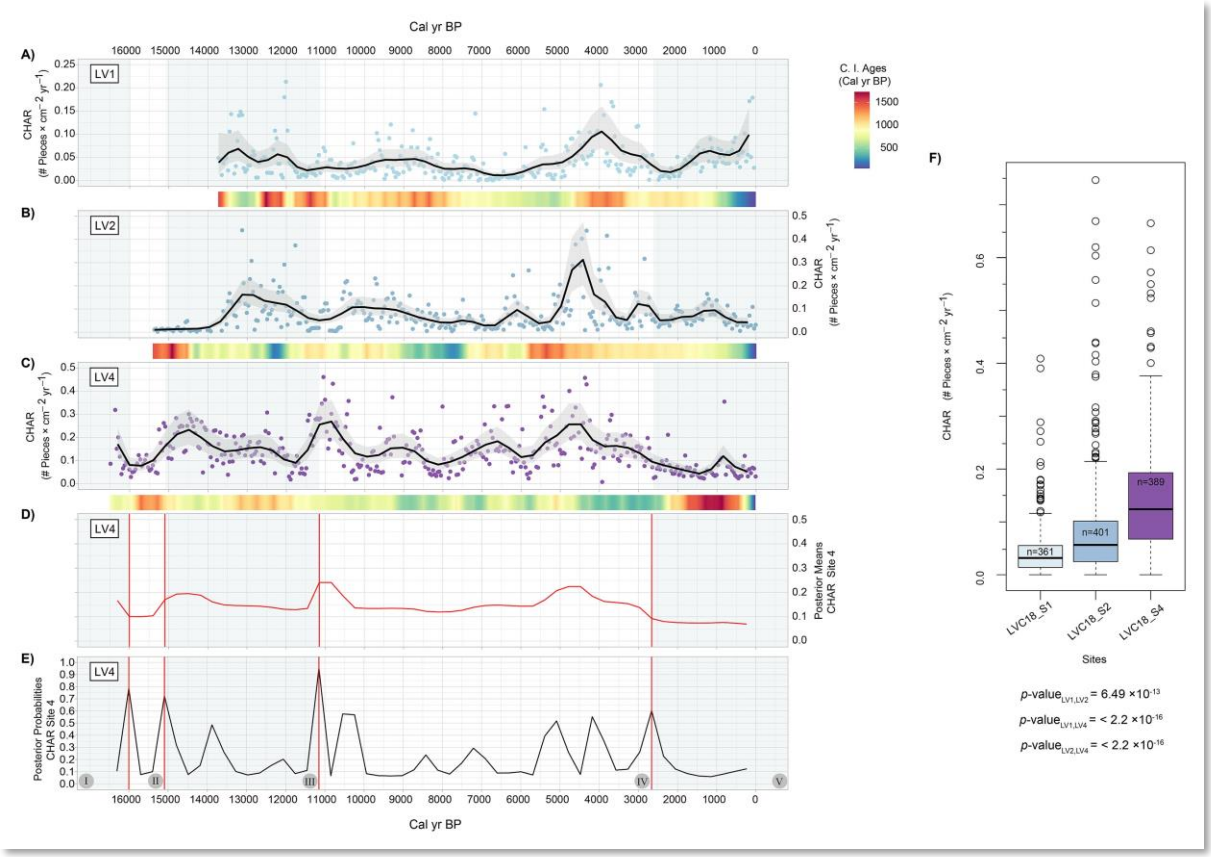

Figure 5. (a) Macrocharcoal record from LV1, (b) macrocharcoal record from LV2, (c) macrocharcoal record from LV4. For (a), (b), and (c), coloured points represent each sample, the black continuous line indicates a trend line based on a GAM, the grey shaded envelope represents the 95% confidence interval for the plotted trends, the grey shaded areas mark the time span between each change point, and coloured bars under each site represent the confidence interval (C.I.) age range for each point according to each age-depth model. (d) Posterior means for CHAR record from LV4 after Bayesian change point analysis. (e) Posterior probabilities of a change point for each position in the sequence of observations from ca. 16,600 cal yr BP to the present: red lines mark the exact position of each change point, and numbers in the grey circle indicate the number of each change point for reference in the text. (f) Boxplot showing the distribution of charcoal influx (CHAR) at the three sites.

2.5.3 PALYNOLOGY AND VEGETATION HISTORY

We identified three statistically significant local pollen assemblage zones (LPAZ), at all three sites (Fig. 6, Fig. 7, Fig. 8). A subzone boundary was added visually to LV2 and LV4, where the sequence is older. Pollen did not reach sufficient counts in the deepest sediments of LV4; specifically pollen grains and palynomorphs were absent at the bottom, and as we moved up core, a few corroded pollen grains and *Botryococcus* and *Pediastrum* occurred. After ca. 16,000 cal yr BP, the number of pollen grains was sufficient to reach statistically meaningful counts. The timing of the boundaries between sites differs slightly due to the variation in the

chronologies between sites, but these differences are within the limits of the age uncertainties. For this reason, the chronology taken into account to define the LPAZ is that belonging to LV4.

LPAZ LV2-1a, LV4-1a (LV2: 806–760 cm; LV4:778–640 cm, ca. 16,660–13,230 cal yr BP): Poaceae is the most abundant taxon (>65%), followed by Cyperaceae and *Cyperus*-type (ca. 10%) and Amaranthaceae/Chenopodiaceae (ca. 3%), suggesting open vegetation conditions during this period, most likely savanna ecosystems also characterized by genera such as *Combretum*. Afromontane components, mostly *Olea* and *Podocarpus*, likely built substantial stands after ca. 13,500 cal yr BP in the Lake Victoria area. The conspicuous presence of *Typha* pollen (>5%) suggests local swampy conditions at the sites LV2 and LV4, probably as a result of low lake levels and thus dry environments. CHAR suggests that fire burning was very low at ca. 16,000–15,000 cal yr BP, and started to increase between 15,000 and 14,000 cal yr BP.

LPAZ LV1-1, LV2-1b, LV4-1b (LV1: 722–611 cm; LV2: 804–656 cm; LV4:640–529 cm, ca. 13,230–10,750 cal yr BP): Poaceae (<50%), Cyperaceae (ca. 10%), and *Cyperus*-type (ca. 10%) pollen values remain high and stable, suggesting the persistence of savanna ecosystems. Taxa such as *Alchornea*, *Urera*-type and a very few trees such as *Celtis* and *Podocarpus* likely established locally, while Afromontane *Olea* (>15%) populations expanded during this time. The pollen data suggest that *Typha* populations decreased at the coring sites, likely because the local swamps or ponds were inundated. Moreover, the pollen data (e.g. Moraceae, *Celtis*, *Podocarpus*, *Olea*) suggest that transitional and river rainforest stands established when burning declined.

LPAZ LV1-2, LV2-2, LV4-2 (LV1: 611–296 cm; LV2: 656–305 cm; LV4: 529–223 cm, ca. 10,750–5020 cal yr BP): Poaceae pollen rapidly declines (<20%), as do Cyperaceae and *Cyperus*-type (<5%), while pollen of Moraceae, *Acalypha*, *Alchornea*, and *Urera*-type increases massively, suggesting that savanna ecosystems were replaced by rainforests during the early Holocene. Furthermore, the pollen data suggest that Afromontane forests also spread at the expense of grasslands and savanna during this period, although less pronounced than the rainforests. *Celtis* populations expanded, peaking at ca. 8000–6000 cal yr BP during the mid-Holocene (ca. 25%), while *Olea* gradually declined. The massive rainforest expansion was accompanied by steadily declining fire activity from 10,000–5000 cal yr BP, suggesting that

rainforest reduced regional burning. The fire minimum of the whole record was reached between ca. 9000 and 7000 cal yr BP, when Moraceae and thus the rain forests peaked.

LPAZ LV1-3, LV2-3, LV4-3 (LV1: 296–0 cm; LV2: 305–0 cm; LV4: 223–0 cm, ca. 5020 cal yr BP–Present): Pollen of rainforest taxa (e.g. Moraceae, *Urera*-type, *Alchornea*) declines and Poaceae and other savanna taxa (e.g. *Combretum*) increase from 25% to 50%, marking the onset of the late Holocene savanna re-expansion. The pollen data suggest that the Afromontane vegetation also declined, though less pronouncedly than the rainforest. Interestingly, close to the onset of this LPAZ at ca. 4800 cal yr BP, fire disturbance peaked, and *Podocarpus-Juniperus* forests expanded. The gradual decline of burning after a maximum at ca. 4500 to 3000 cal yr BP seems to be linked to the expansion of savanna ecosystems; it might thus be related to decreasing fuel availability during the late Holocene. However, fire incidence slightly increased after 1000 cal yr BP in connection with a further expansion of savanna, suggesting that the linkage between fuel availability and biomass burning does not always follow the same pattern.

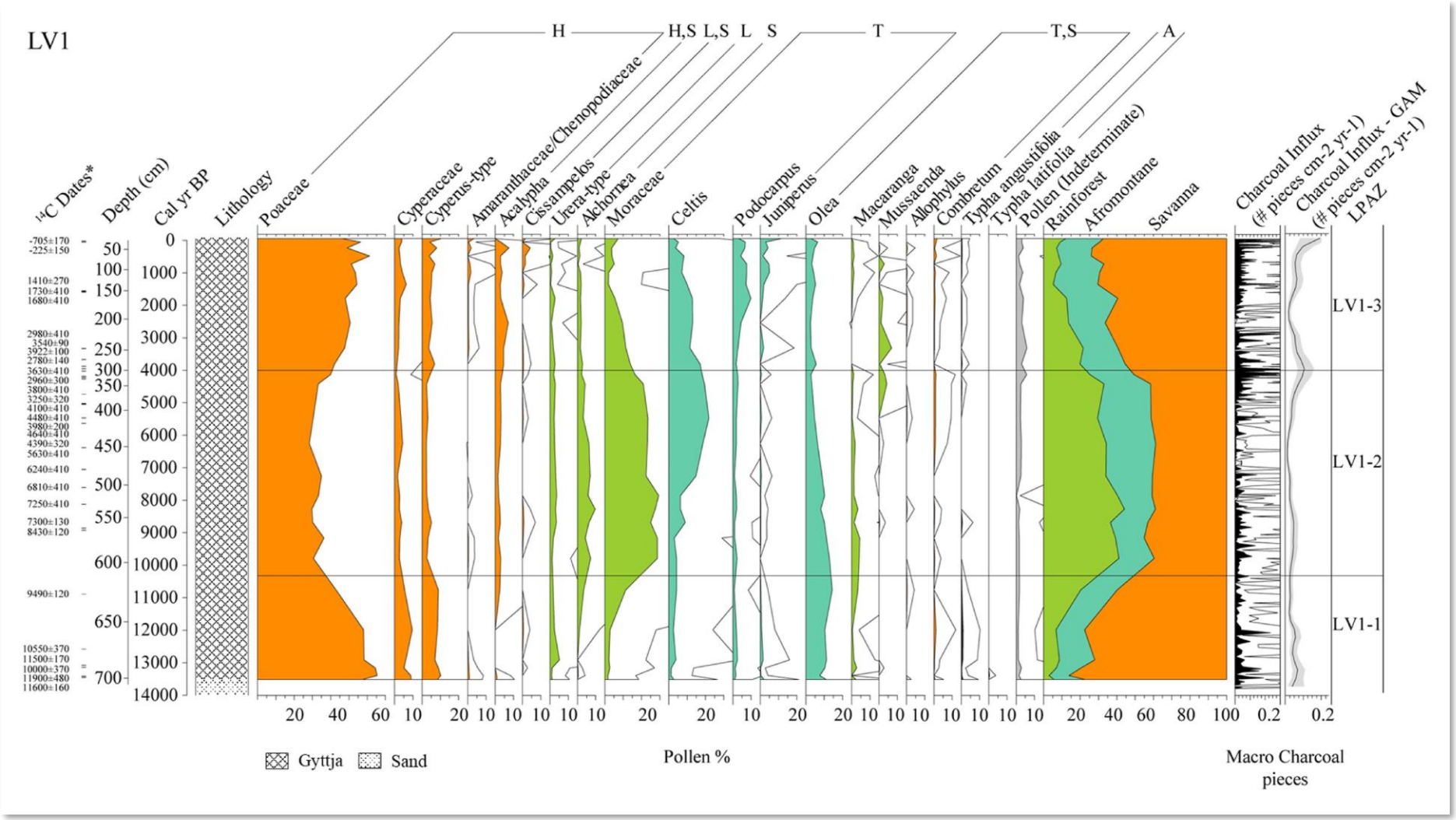

*Figure 6. Pollen percentages and macroscopic charcoal concentration values of the LV1 record. LPAZ = Local pollen assemblage zones, H = herbs, S = shrubs, L = lianas, T = trees, A = aquatic. Empty curves represent a 10 × exaggeration. In the charcoal influx GAM trend, the grey shaded envelope represents the 95% confidence interval. *Dates rounded following Stuiver and Polach (1977).*

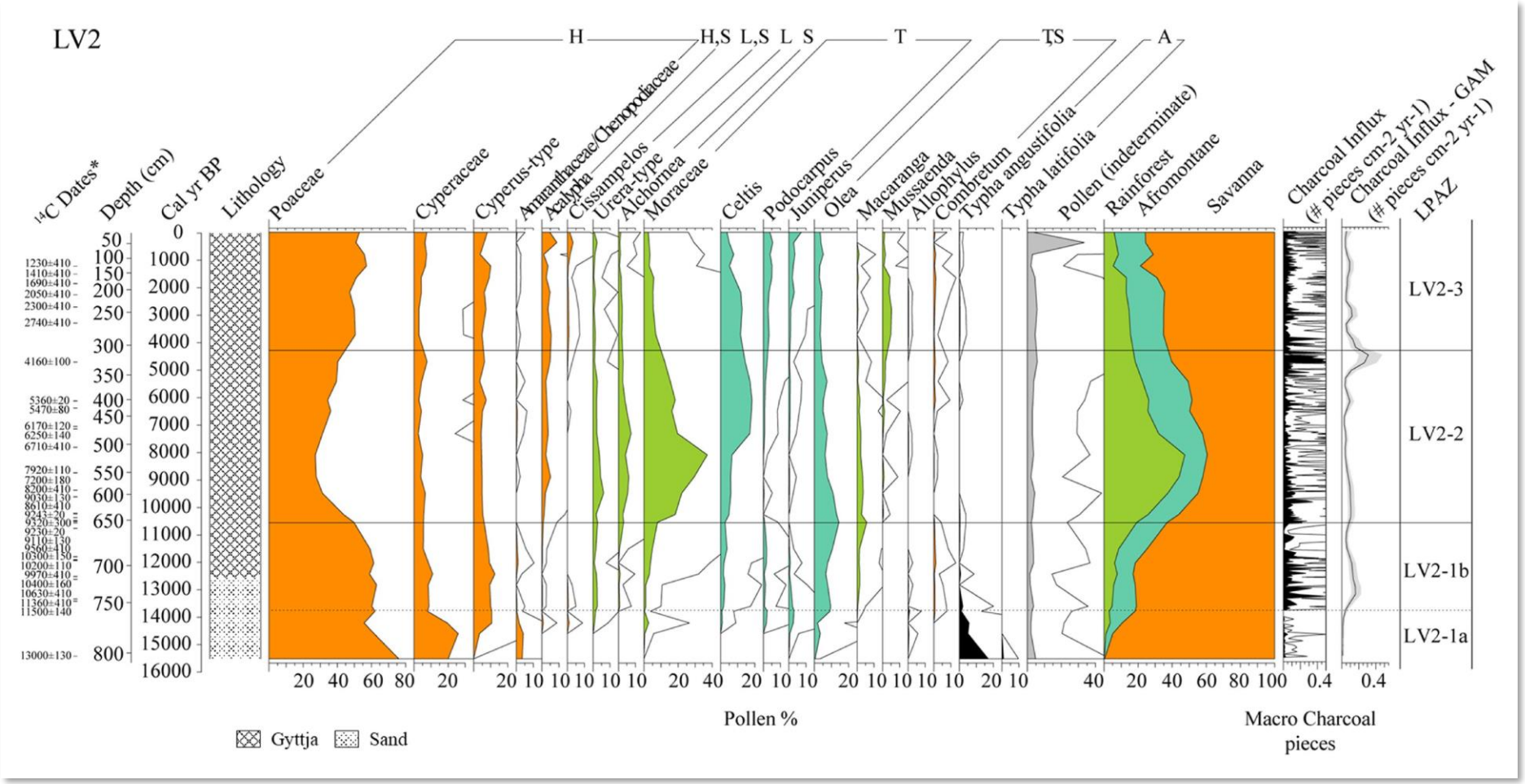

Figure 7. *Pollen percentages, and macroscopic charcoal concentration values of the LV2 record. LPAZ = Local pollen assemblage zones, H = herbs, S = shrubs, L = lianas, T = trees, A = aquatic. Empty curves represent a 10 × exaggeration. In the charcoal influx GAM trend, the grey shaded envelope represents the 95% confidence interval. * Dates rounded following Stuiver and Polach (1977).*

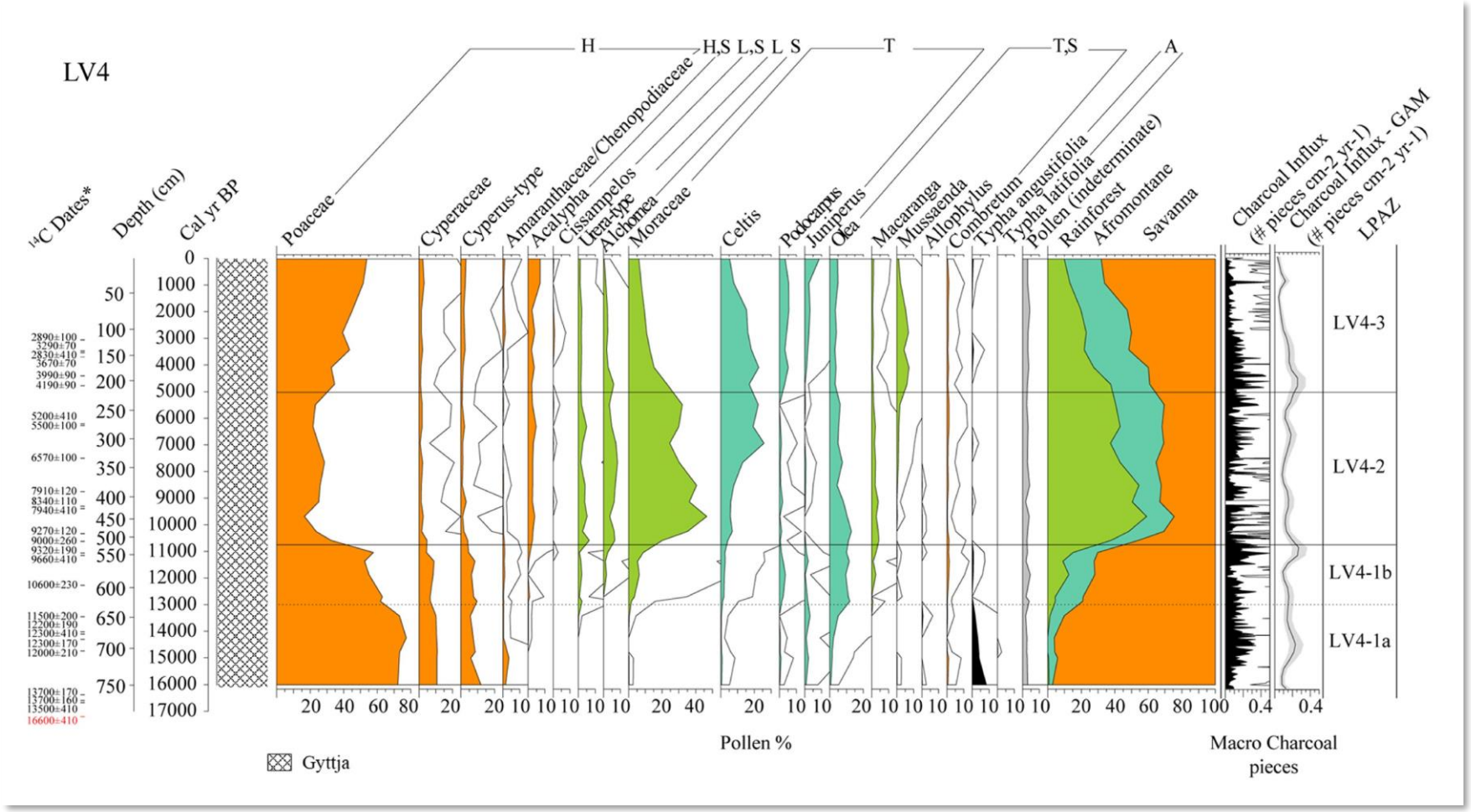

Fig. 8. *Pollen percentages, and macroscopic charcoal concentration values of the LV4 record. LPAZ = Local pollen assemblage zones, H = herbs, S = shrubs, L = lianas, T = trees, A = aquatic. Empty curves represent a 10 × exaggeration. In the charcoal influx GAM trend, the grey shaded envelope represents the 95% confidence interval. The radiocarbon date marked in red represents the dated sediment recovered from the core catcher below the last segment core (below 778 cm). *Dates rounded following Stuiver and Polach (1977).*

2.5.4 ORDINATION ANALYSES

When performing the analysis site by site, we obtained similar patterns to the ones shown in the PCA, which includes all sites. Therefore, we decided to show the one for LV4 (Fig. 10) because it includes a larger time span and a summary PCA including all sites (Fig. 11). For the PCA of LV4 (Fig. 10), the first two axes explain 85.48% of the total variance in the pollen data, of which 73.45% is explained by PC axis 1 and 12.03% by PC axis 2. For the summary PCA (Fig. 11), the first two axes explain 74.72% of the total variance, of which 59.33% is explained by PC axis 1 and 15.39% by PC axis 2.

For both PCAs, axis 1 spans a gradient from positive species scores such as Cyperaceae, *Juniperus*, *Typha angustifolia*, and *Cyperus*-type to negative species scores such as Moraceae, *Celtis*, and *Alchornea*. Thus, axis 1 may reflect an environmental gradient from warmer and wetter conditions (Moraceae, *Alchornea*, *Celtis*) to drier conditions (Amaranthaceae/Chenopodiaceae, Poaceae), with water plants such as *Typha* mirroring low lake levels. This interpretation is corroborated by the passively added TEX_{86} data in °C for Lakes Tanganyika, Victoria, and Chala (Fig. 10, Fig. 11). On axis 2, the most positive species scores belong to *Celtis*, *Mussaenda*, *Podocarpus*, and *Juniperus*, and the most negative are reached by *Macaranga*, *Olea*, and *Urera*. Therefore, we infer that axis 2 is connected to a gradient from denser (*Mussaenda*, *Podocarpus-Juniperus*) forest to more open (*Olea*) and pioneer communities (*Macaranga*), probably reflecting the importance of light availability. Interestingly, charcoal as a fire proxy is only weakly associated with axis 2, suggesting that at multimillennial scales vegetation and fire were linked at a secondary order of importance when compared to the linkage between vegetation and temperature.

2.6 DISCUSSION

2.6.1 CHRONOLOGICAL FRAMEWORK

Due to the size of Lake Victoria, it is difficult for big macrofossils to deposit there, thus it is challenging to find optimal material for radiocarbon dating. Various studies have used two distinct types of material for radiocarbon dating: 1) bulk lake sediment including filtered concentrates of 20–70 µm supposed to contain a mix of pollen, lignin, and charcoal (Kendall, 1969; Stager, 1984; Stager et al., 1986, 1997) and 2) charcoal (Beuning, 1999; Beuning et al.,

1997; Johnson et al., 1996). Even though the resulting chronological models provide the closest accuracy to the real ages of the lake deposits, several sources of contamination are known to affect the age determination of bulk and other non-terrestrial organic material (Walker, 2005). These include factors such as the reservoir effect, the mineral carbon error, and the presence of residues from aquatic organisms, which may have taken up old carbon from the water and sediments.

Several correction factors have been applied to account for the reservoir effect, all of them constant over time. In all studies, the reservoir effect was considered constant through time. Kendall (1969) proposed a 'zero error' of 400 years by extrapolation of the mean wet sediment rate of the surface muds from Lake Victoria's Pilkington Bay. However, Stager et al. (1997) reported a 600 year reservoir effect based on a linear extrapolation from the ages of a top core from Damba Channel, estimations for the P2 core (Stuiver, 1970). Later, Beuning et al. (1997) and Johnson et al. (1998) suggested a 500 year reservoir effect.

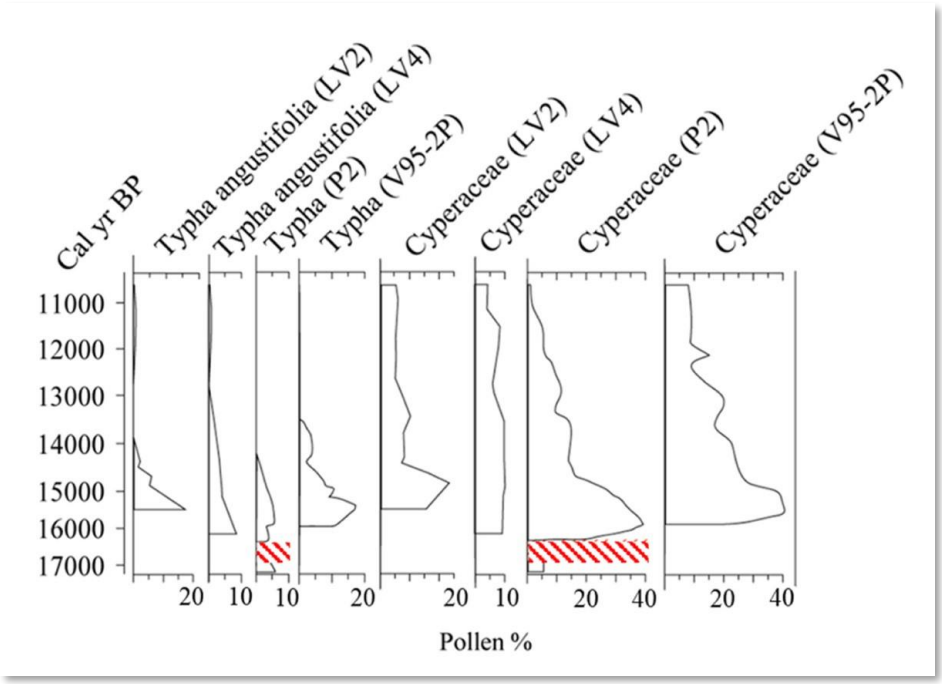

Figure 9. Pollen percentages of Typha and Cyperaceae from 11,000 to 17,000 cal yr BP of LV2 and LV4 (this study) compared with same pollen species from P2 (Kendall, 1969) and V95–2P (Beuning, 1999). Red lines represent the time gap of a sediment discontinuity reported by Kendall (1969).

Our estimations of a 573 years ^{14}C reservoir effect, which are based on multiple date comparisons across three cores, refines earlier estimates. The difference of 570 years falls between the corrections of 400 years for the P2 core (Kendall, 1969), 500 years for V95–2P

(Beuning et al., 1997), and 600 years for Ibis 2 (Stager et al., 1997). Kendall (1969) also mentions that the radiocarbon dates in his study were calculated with a ^{14}C half-life of 5568 years instead of 5730 as today, changing the value of the dates by a factor of 1.03. Such a good agreement implies that the previous chronological estimations were done carefully and are comparable with ours, having a correction of 500–600 years, or slightly less (400 years), given that the dating uncertainties often span several centuries (Table 1). For instance, the uncertainties of the reservoir effect were identified as 51–82 years (Beuning et al., 1997); 50–140 years (Johnson et al., 1998), 60–200 years (Kendall, 1969), and 80–300 years (Stager et al., 1997). However, the age gaps between the material dated are large, increasing the uncertainties of these models. Hence, this paper relies on many more charcoal dates than any other study to build the age–depth models, so that we can reduce the temporal uncertainties of the different events recorded in the lake sediments.

Kendall (1969) reported a stratigraphic discontinuity, which lasted until ca. 16,500 cal yr BP. However, this discontinuity layer was not present in the sediment of LV4. We know that in terms of time we are situated at the top of this layer because of the biostratigraphic relations that we can observe not only in this study but also in Beuning's (1999). These include the high values of *Typha*, *Olea* and Cyperaceae.

In contrast to the continuous gyttja layer that we see throughout the LV4 core, reaching the oldest dates of 16,100–17,000 cal yr BP for the core (19,000-21,000 cal yr BP for the sediment below it) (Table 1), Beuning (1999) found a 'vertisol' with rootlets and reed stems. That layer extended from 16,100 to ca. 15,500 cal yr BP with a peak in Cyperaceae and *Typha* that was found in our study in core LV4 (Fig. 9) and in core P2 (Kendall, 1969). Interestingly, a sandy layer also occurs in the shallower cores LV1 and LV2 presented here (Figs. 1, 6-9). This difference between LV4 and the other cores most likely indicates shallow water or swampy conditions at the profundal site, while probably shore conditions occurred at the shallower sites. Moreover, local shallower conditions inferred close to the other sites of coring, P2, V95–2P, LV1 and LV2, would then imply that the north and eastern parts of Lake Victoria were affected by very low water levels, whereas LV4 (deepest coring site) would have maintained relatively higher water tables around 16,100–17,000 cal yr BP. However, prior to 16,000 cal yr BP, lake levels must have been quite low also at LV4 (Fig. 9), as indicated by the high abundances of the swamp or lakeshore plant *Typha* (>5%). Higher water tables at LV4 than at

the other sites around 16,000 cal yr BP may explain the relatively low abundances of Cyperaceae, which was likely growing in marshy or swampy reeds close to the shore (<10 vs. 35–40%, Fig. 9).

The timing of the population peak of *Typha* at ca. 16,500–14,500 cal yr BP in the Lake Victoria records (Beuning, 1999; Kendall, 1969; this study, Fig. 9) coincides with that observed from 16,500 to 14,000 cal yr BP at Lake Rukwa (Vincens et al., 2005). Taken together, the available evidence suggests that a regional eastern African lake desiccation phase may have started before 18,500 cal yr BP and lasted until ca. 16,000–15,500 cal yr BP (*Typha* and Cyperaceae peaks in this study, Vincens et al., 2005). This dry phase was then followed by a wetter period that lasted until about 13,000 cal yr BP, when *Typha* and Cyperaceae began to decline.

2.6.2 BIOME INTERACTIONS WITH CLIMATE AND FIRES

The role that temperature, moisture, slopes, wind, and fuel play in the occurrence of fire events and the importance of human activities and vegetation as drivers of fire regimes have been extensively discussed (e.g. Archibald et al., 2009; Marlon, 2020). Whereas fire activity is co-modulated by fire-weather conditions involving heat, moisture, and wind, and vegetation composition and structure determines fuel availability, humans today are an important source of fire ignition (Conedera et al., 2009). Across the planet, the distribution of climatic mechanisms is broad, and throughout the late Pleistocene and the Holocene especially in the tropical regions, some climatically important events have occurred. In eastern Africa, past fire occurrence is likely to have been primarily driven by two factors: climatic conditions, which determine temperature, rainfall, the length of the dry and wet seasons and thus moisture availability (Nelson et al., 2012); and biomass availability, which depends on the climatically controlled biome type (e.g. Schüler et al., 2012) and within the Afromontane regions, the vegetation type (Hemp, 2005; Hemp and Beck, 2001; Mustaphi et al., 2021). However, even within the same kind of ecosystem, slight changes in moisture balance cause variations in fire propensity as observed previously in equatorial eastern Africa (Colombaroli et al., 2014; Gillson, 2004).

Major climatic changes altered past sea surface temperatures (SST) and with it, patterns in rainfall; for instance, during Heinrich Event 1, a megadrought occurred in the Afro–

Asian Monsoon region, which Stager et al. (2011) attributed to a movement of the Intertropical Convergence Zone (ITCZ) between 17,000 and 16,000 cal yr BP. This episode caused effects across eastern Africa, such as diatom-inferred low-water stands in Lake Tanganyika (Stager et al., 2011), the drying out of Lake Tana (Lamb et al., 2007), and swampy conditions in Lake Rukwa (Vincens et al., 2005). Moreover, climate may have influenced the fire regime through vegetation, for instance by promoting the growth of flammable dry savanna around Lake Victoria at ca. 15,000 to 14,000 cal yr BP. The flammable savanna persisted until the onset of the Holocene, although more mesophilous Afromontane taxa such as *Olea* and *Podocarpus* expanded between 16,000 and 12,000 cal yr BP. It is unclear whether this conspicuous Late Glacial expansion of subtropical Afromontane vegetation (Fig. 6, Fig. 7, Fig. 8; Kendall, 1969) was the consequence of colder-than-today conditions in the Lake Victoria area, or less likely, whether it was caused by increased wind transport of pollen from higher altitudes (Kendall, 1969; Beuning, 1999). Indeed, today Lake Victoria is only ca. 100–200 m below the lowest Afromontane forest stands, which implies that cooling of 1–2 °C would be enough to promote the expansion of subtropical vegetation close to the lake shores, if moisture is sufficient regionally, or locally along riverine fringes (Schüler and Hemp, 2016). Moreover, this cooling would partly push the rainforest vegetation below the site as subtropical Afromontane vegetation expanded. This cooler situation, besides the reduced moisture availability, may also explain the strong reduction in rain forest vegetation during the Late Glacial around Lake Victoria. Indeed, between 16,000 and 12,000 cal yr BP, annual mean temperatures oscillated between 19 and 23 °C in the Lake Victoria area (Berke et al., 2012), thus creating a suitable environment for Afromontane vegetation (see introduction). Further evidence for the temperature sensitivity of rainforests comes from our ordination analyses (Fig. 10, Fig. 11), which suggest that temperature primarily influenced tropical vegetation and that its influence on the fire regime was of secondary importance and/or mediated through vegetation.

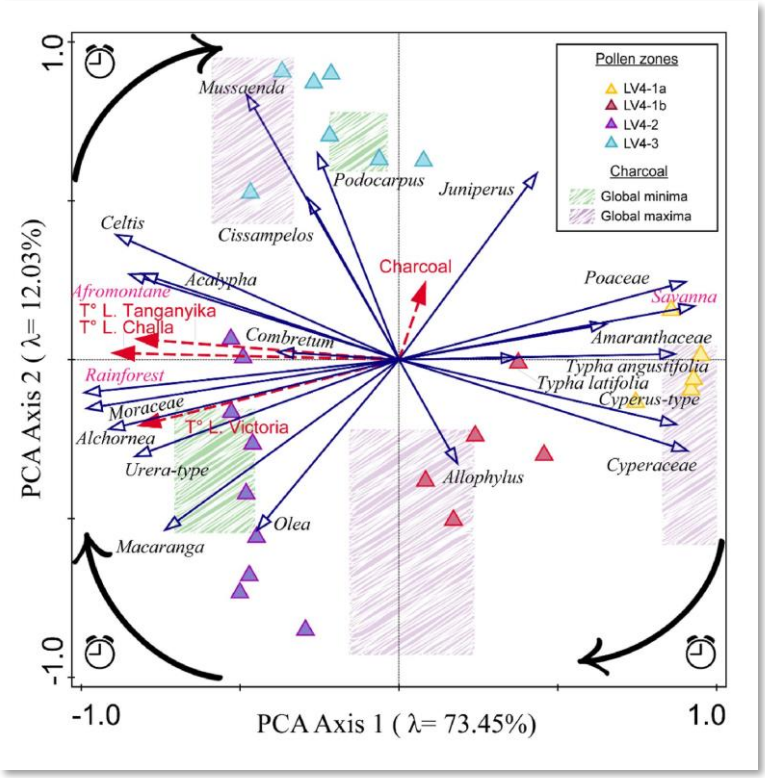

Figure 10. Principal component analysis (PCA) triplot of LV4 showing response variables (pollen taxa and biome sums, blue arrows), passive variables (temperature and charcoal, red arrows), and sample scores which are indicated with symbols. Different colours represent the local pollen zones and subzones. PCA axis 1 explains 73.45% of the variance, and PCA axis 2 explains 12.03% of the variance. Coloured rectangles represent localization of global maxima and minima in charcoal influxes in accordance with time (this study). Arrows represent the direction of time in the record according to the sample scores. Temperature records were obtained from TEX_{86} data for Lake Tanganyika (Tierney et al., 2008), Lake Victoria (Berke et al., 2012), and Lake Chala (Sinninghe Damsté et al., 2012).

From 12,000–9000 cal yr BP, biomass burning increased over Africa (Power et al., 2008). At the onset of the Holocene, atmospheric circulation was enhanced, which in eastern Africa resulted in a long-term increase in African monsoon activity and marked latitudinal shifts of the ITCZ (Garcin et al., 2007). In the equatorial tropics, this shift brought a pronounced increase in precipitation and a decrease in wind speed (Talbot et al., 2007). At Lake Victoria, this climatic shift resulted in a significant drop in fire occurrence, which persisted for several millennia through the early and mid-Holocene (Fig. 9). The decline of burning, which reached its lowest point at around 8000–6000 cal yr BP, was likely caused by warm and moist conditions, which also promoted the large-scale expansion of rainforests in the Lake Victoria area. We assume that during that time the fire regime shifted from fuel limited, due to the low biomass of dry savanna, to moisture limited due to the high biomass of humid rainforest. Most likely, the fire regime shift was accelerated by the reduced flammability of rainforest vegetation and positive feedbacks on moisture availability associated with the expansion of dense forest canopy (Ivory and Russell, 2016). During the Holocene, the African Humid Period

promoted the expansion of tall and partly shade-tolerant tropical rainforest trees and lianas such as Moraceae, *Macaranga*, *Alchornea*, *Acalypha*, and *Urera* at the expense of herbaceous savanna plants such as Poaceae and Amaranthaceae/Chenopodiaceae and shrubby trees such as *Combretum*. Afromontane trees such as *Olea* and *Podocarpus* likely moved several hundreds of meters upslope as a result of early and mid-Holocene climate warming. Increased moisture availability probably caused a general spread of *Celtis* to the lowlands around Lake Victoria, partly replacing the savanna during the mid-Holocene, a phase of low fire occurrence (Fig. 6, Fig. 7, Fig. 8; Schüler and Hemp, 2016).

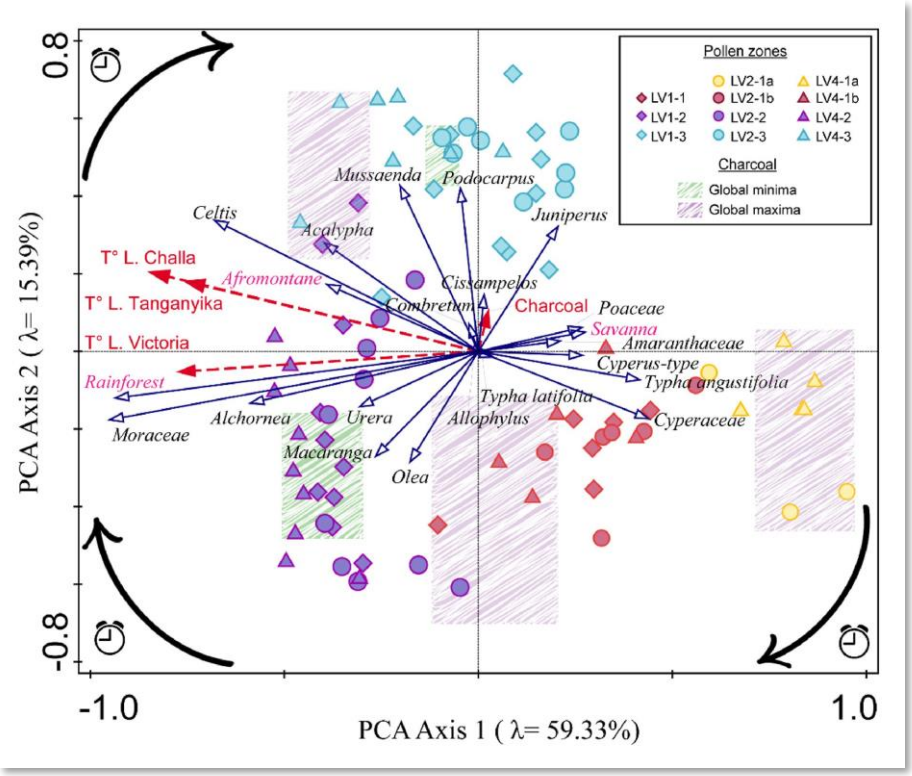

Figure 11. Principal component analysis (PCA) triplot of all sites showing response variables (pollen taxa and biome sums, blue arrows), passive variables (temperature and charcoal, red arrows), and sample scores which are indicated with symbols. Different symbols represent the sites, and colours represent the local pollen zones and subzones. PCA axis 1 explains 59.33% of the variance, and PCA axis 2 explains 15.39% of the variance. Coloured rectangles represent localization of global maxima and minima in charcoal influxes in accordance with time (this study). Arrows represent the direction of time in the record according to the sample scores. Temperature records were obtained from TEX_{86} data for Lake Tanganyika (Tierney et al., 2008), Lake Victoria (Berke et al., 2012), and Lake Chala (Sinninghe Damsté et al., 2012).

Towards the end of the mid-Holocene at 6000–5000 cal yr BP, the monsoonal circulation changed, likely as a result of a weakening of summer insolation in North and eastern Africa (Demenocal et al., 2000; Vincens et al., 2005; Wirrmann et al., 2001). Convective precipitation declined, resulting in drier climates in the surroundings of Lake Victoria and releasing the retreat of rainforests and the re-expansion of savanna vegetation. It is likely that this climatic

shift to drier conditions (e.g. Schüler et al., 2012) and the resulting vegetation change caused the biomass-burning maximum at ca. 5000 cal yr BP. By the midst of the late Holocene, as rainy conditions re-emerged across tropical Africa (Gasse, 2000), moisture reduced the development of fires, giving rise to the last minimum in the record between ca. 3000 and 2000 cal yr BP under a vegetation mix of savanna, rainforest, and Afromontane vegetation. Concurrently, metal-using agriculturalists spread in Eastern Africa (Clark, 1962; Kendall, 1969), likely contributing to major vegetation changes (Huffman, 1982; Humphris and Iles, 2013; Iles and Lane, 2015; M'Mbogori, 2021) and gradually resulting in the greatest landscape alterations by around 1500 cal yr BP (Schoenbrun, 1998). However, although this archaeological evidence is broadly accepted (e.g. Desmedt, 1991; Goldstein and Munyiri, 2017; Huffman, 1982; Marchant, 2021; Schoenbrun, 1993), palynological indicators for such a change have remained elusive (Beuning, 1999; Marchant et al., 2018). In our study, we focused on fire regime changes, and the vegetation overview used for biome reconstruction is too coarse to disentangle human modifications to ecosystems. Further high-resolution analyses are needed to better assess the human influence on the fire regime and vegetation.

2.7 CONCLUSION

This study provides a reliable chronological framework from an intensively dated transect across Lake Victoria. We conclude that climate was the main driver of fire in this area, at least until the early Iron Age (ca. 2400–1100 yr BP), when human impact became important. The regional fire regime and vegetation changes seem to function concomitantly. Fire occurrence may have been controlled by combined factors, such as fuel availability, heat, and moisture occurrence. Under dry and warm climates, when savanna expanded, fire occurrences increased; conversely, warm and humid climates promoted rain forests and reduced fire ignition and spread. The Lake Victoria basin, where tropical rainforest, savanna, and subtropical Afromontane vegetation co-occur, has been shown to be very sensitive to subtle climatic changes; even 1–2 °C may drive biome reorganizations. Thus, even minor future increases in temperature may provoke major ecosystem shifts, which may in turn affect the fire regime. Therefore, conservation measures are needed to prevent drastic impacts and reduce ecosystem vulnerability under global change conditions. Two plausible actions are to enhance the existing sinks (forests) in order to store greenhouse gasses and to develop appropriate land use strategies to allow society and wildlife to adjust to ongoing and future climate change.

APPENDIX A

Methodology Followed for Sieving

When starting to sieve, it is important to subsample first and to avoid letting the samples to sit for more than 3 days in the fridge because they dry out, which makes them more difficult to sieve. The sequence of subsampling and sieving is always done from the bottom to the top of the core.

- Sediment subsampling
  1. Clean all the surfaces before start working and do not take more than 1 core at a time.
  2. Take out from the fridge only the section core needed.
  3. Follow the composite file, which indicates the slices of 2 cm to be taken together.
  4. Make sure the containers for storing the samples are clean.

- Subsampling every centimetre (continuously) for pollen
  1. Label the container.
  2. Weight the empty container and tare the balance.
  3. Clean the surfaces of the sediment with a spatula.
  4. Take 1 cm^3 from the core with the volumetric subsampler (make sure you do not touch the edges).
  5. Weight the sample and record it.
  6. Put the lid on, and store it in zipper storage bags according to depth.
  7. Put the samples in the freezer.

- Subsampling for sieving
  1. Clean the surface of the core by removing the first millimetre of the sediment using a spatula.
  2. Mark slices of 2 cm according to the composite document.
  3. Take the corresponding container (already labelled) and rinse it with tap water.
  4. Cut the slice, taking care to not touch the edges of the pvc tube (leave at least 2–3 mm of the edges of the sediment that are in direct contact with the tube).
  5. Weight the container and tare.

6. Put the sediment into the container and record its weight.
7. Fill it up with water.
8. Put these samples in the fridge.

- Sieving for macrofossils and charcoal

Due to the sensitivity of fish macrofossils used for other studies, the use of chemicals for extracting charcoal particles is not feasible. Therefore, conventional methods for deflocculating the sediment (Millspaugh and Whitlock, 1995; Mooney and Tinner, 2011) cannot be used. And sieving was done only with water. For all depths, the sieving should be done with a tower of the 200µm and the 100µm sieve, with exception of samples located every 24 cm, where two extra sieves need to be added to the tower, 50µm and 20µm respectively.

To begin with the procedure, moisten all sieves (on both sides) with tap water, and proceed as follows:

1. Set up the sieving tower (accordingly)
    a. 200 and 100µm

    Or

    b. 200, 100, 50, and 20 µm
2. Put the sediment in the sieve.
3. Place the sieving tower into a wet sieving machine* and cover the uppermost sieve with the lid (make sure it is properly closed and the water hose is properly attached).

    * The use of the sieving machine is solely to soften the sediment a little while soaking in water.

4. Adjust settings for a smooth oscillatory movement:
    a. Interval time: 6 s
    b. Sieving time: 6 min
    c. Amplitude: 0.8 mm
5. Turn on the tap (IN 2 INTERVALS), the first and second time only during 10 s with a low to medium water flow and a stop flow interval of ~3min. Before activating the movement of the machine, make sure that the uppermost sieve has always water on it (this step is important, because it avoids any possible breakage of particles).

6. Turn on the sieving machine.
7. Once the time is due, you can finish the sieving by hand (fine sieving).
8. Recover the remaining material in containers properly labelled using tap water.
9. Rinse the lid of the sieving machine every time the sample is changed.
10. Put the samples in the freezer.

Note:

In order to make sure that the macrofossils were not damaged in the sieving machine, a test was carried out in a total of 162 samples. Two samples were analysed in each depth. One being sieved completely manually and the other one with the aid of the machine at the beginning of the sieving procedure. Then, samples were compared to check for particles or macrofossil's breakage or damage. There was no damage observed in chironomids, insect remains, fish scales, charcoal or fish teeth.

ACKNOWLEDGMENTS

The authors Yunuén Temoltzin–Loranca, Giulia Wienhues, and Moritz Muschick were supported by SNSF Sinergia grant number 183566 awarded to Ole Seehausen, Martin Grosjean, Tom Gilbert, and Blake Matthews. The coring in Lake Victoria was financed by the strategic pool of the Faculty of Natural Sciences of University of Bern (grant to Ole Seehausen, Anna Sapfo Malaspinas, Willy Tinner, Oliver Heiri, Martin Grosjean, and Flavio Anselmetti) and the Institute of Plant Sciences of University of Bern. We gratefully acknowledge the coring leaders Petra Boltshauser-Kaltenrieder, Moritz Muschick, Salome Mwaiko, and Willi Tanner and the coring team members Sandra Brügger and Alexander Bolland. We thank Edith Vogel and Gary Salazar for their contribution to the ^{14}C analysis. We acknowledge the lab assistance of Lara Zinkl and Sara Brechbühl. We are deeply indebted to TAFIRI and its coring members for looking after the team and the coring platform during the expedition: Edwin Sombe (boat captain), Harith Kalima (engineer), Boaz Jumbe (crew), Toto Mohammed (technician), Daniel Bwathondi † (crew), Daniel Chacha (crew), and Hamisi Ramadhani (cook). We thank TAFIRI for all the logistic support during the campaign. This research was supported by TAFIRI and conducted under COSTECH research permit No. 2018-237-NA-2018-57. We are grateful to Lisa Schüler for offering an introduction to East African pollen grains and for making available the pollen reference collection of the Mount Kilimanjaro area. Hermann Behling is gratefully acknowledged for hosting Yunuén Temoltzin-Loranca at the Department of Palynology and Climate Dynamics at the University of Göttingen. We thank Gianni Zanchetta and Richard Vachula for their careful reading of our manuscript and their insightful comments and suggestions.

References

Adolf, C., Wunderle, S., Colombaroli, D., Weber, H., Gobet, E., Heiri, O., van Leeuwen, J., Bigler, C., Connor,S.E, Gałka, M., La Mantia, T., Makhortykh, S., Svitavská-Svobodová, H., Vanniere, B. & Tinner W. (2018). The sedimentary and remote-sensing reflection of biomass burning in Europe. Global Ecology and Biogeography, 27(2), 199-212.

Andama, M. (2012). Holocene Climate and Environmental History of Lake Victoria basin: Evidence from Geochemical Proxies. Quaternary International, 279, 18.

Archibald, S., Roy, D. P., van Wilgen, B. W., & Scholes, R. J. (2009). What limits fire? An examination of drivers of burnt area in Southern Africa. Global Change Biology, 15(3), 613–630. https://doi.org/10.1111/j.1365-2486.2008.01754.x

Behling, H. (2002). South and southeast Brazilian grasslands during Late Quaternary times: a synthesis. Palaeogeography, Palaeoclimatology, Palaeoecology, 177(1–2), 19–27. https://doi.org/10.1016/S0031-0182(01)00349-2

Bennett, K. D. (1996). Determination of the number of zones in a biostratigraphical sequence. New Phytologist, 132(1), 155–170.

Berke, M. A., Johnson, T. C., Werne, J. P., Grice, K., Schouten, S., & Damsté, J. S. S. (2012). Molecular records of climate variability and vegetation response since the Late Pleistocene in the Lake Victoria basin, East Africa. Quaternary Science Reviews, 55, 59-74.

Beuning, K. R. M. (1999). A re-evaluation of the Late Glacial and Early Holocene vegetation history of the Lake Victoria region, East Africa. In E. M. van Zinderen Bakker & K. Heine (Eds.), Palaeoecology of Africa and the Surrounding Islands (First, pp. 115–136). Routledge.

Beuning, K. R., Kelts, K., Russell, J., & Wolfe, B. B. (2002). Reassessment of Lake Victoria–Upper Nile River paleohydrology from oxygen isotope records of lake-sediment cellulose. Geology, 30(6), 559-562.

Beuning, K. R. M., Kelts, K., Ito, E., & Johnson, T. C. (1997). Paleohydrology of Lake Victoria, East Africa, inferred from18O/16O ratios in sediment cellulose. Geology, 25(12), 1083–1086.

Beverly, E. J., White, J. D., Peppe, D. J., Faith, J. T., Blegen, N., & Tryon, C. A. (2020). Rapid Pleistocene desiccation and the future of Africa's Lake Victoria. Earth and Planetary Science Letters, 530, 115883. https://doi.org/10.1016/J.EPSL.2019.115883

Birks, H. J. B., & Gordon, A. D. (1985). Numerical methods in Quaternary pollen analysis. Academic Press.

Blaauw, M., Christen, J. A., & Aquino Lopez, M. A. (2021). Age-depth modelling using Bayesian statistics, package 'rbacon'.

Blaauw, M., & Christen, J. A. (2011). Flexible palaeoclimate age-depth models using an autoregressive gamma process. Bayesian Analysis, 6,457–474.

Blais, J. M., & Kalff, J. (1995). The influence of lake morphometry on sediment focusing. Limnology and Oceanography, 40(3), 582-588.

Bronk Ramsey C. (1994). Analysis of chronological information and radiocarbon calibration: the program OxCal. Archaeological Computing Newsletter, 41, 11–16.

Bronk Ramsey C. (1995). Radiocarbon calibration and analysis of stratigraphy: the OxCal program. Radiocarbon, 37(2), 425–430.

Bronk Ramsey C. (2001). Development of the radiocarbon calibration program OxCal. Radiocarbon, 43(2A), 355–363.

Burbridge, R. E., Mayle, F. E., & Killeen, T. J. (2004). Fifty-thousand-year vegetation and climate history of Noel Kempff Mercado National Park, Bolivian Amazon. Quaternary Research, 61(2), 215–230. https://doi.org/10.1016/j.yqres.2003.12.004

Clark, J. D. (1962). The spread of food production in sub-Saharan Africa. The Journal of African History, 3(2), 211-228.

Colombaroli, D., Ssemmanda, I., Gelorini, V., & Verschuren, D. (2014). Contrasting long-term records of biomass burning in wet and dry savannas of equatorial East Africa. Global Change Biology, 20(9), 2903–2914. https://doi.org/10.1111/GCB.12583

Colombaroli, D., van der Plas, G., Rucina, S., & Verschuren, D. (2018). Determinants of savanna-fire dynamics in the eastern Lake Victoria catchment (western Kenya) during the last 1200 years. Quaternary International, 488, 67–80. https://doi.org/10.1016/J.QUAINT.2016.06.028

Conedera, M., Tinner, W., Neff, C., Meurer, M., Dickens, A. F., & Krebs, P. (2009). Reconstructing past fire regimes: methods, applications, and relevance to fire management and conservation. Quaternary Science Reviews, 28(5-6), 555-576.

Demenocal, P., Ortiz, J., Guilderson, T., Adkins, J., Sarnthein, M., Baker, L., & Yarusinsky, M. (2000). Abrupt onset and termination of the African Humid Period: rapid climate responses to gradual insolation forcing. Quaternary science reviews, 19(1-5), 347-361.

Desmedt, C. (1991). Poteries anciennes décorées à la roulette dans la Région des Grands Lacs. African Archaeological Review 1991 9:1, 9(1), 161–196. https://doi.org/10.1007/BF01117220

Duane, W. J., Pepin, N. C., Losleben, M. L., & Hardy, D. R. (2008). General characteristics of temperature and humidity variability on Kilimanjaro, Tanzania. Arctic, Antarctic, and Alpine Research, 40(2), 323–334. https://doi.org/10.1657/1523-0430(06-127). [DUANE]2.0.CO;2

Erdman, C., & Emerson, J. W. (2007). bcp: An R Package for Performing a Bayesian Analysis of Change Point Problems. Journal of Statistical Software, 23(3), 1–13.

Garcin, Y., Vincens, A., Williamson, D., Buchet, G., & Guiot, J. (2007). Abrupt resumption of the African Monsoon at the Younger Dryas—Holocene climatic transition. Quaternary Science Reviews, 26(5–6), 690–704. https://doi.org/10.1016/j.quascirev.2006.10.014

Gasse, F. (2000). Hydrological changes in the African tropics since the Last Glacial Maximum. Quaternary Science Reviews, 19(1–5), 189–211. https://doi.org/10.1016/S0277-3791(99)00061-X

Genet, M., Daniau, A. L., Mouillot, F., Hanquiez, V., Schmidt, S., David, V., ... & Sánchez-Goñi, M. F. (2021). Modern relationships between microscopic charcoal in marine sediments and fire regimes on adjacent landmasses to refine the interpretation of marine paleofire records: An Iberian case study. Quaternary Science Reviews, 270, 107148.

Gillson, L. (2004). Testing non-equilibrium theories in savannas: 1400 years of vegetation change in Tsavo National Park, Kenya. Ecological Complexity, 1(4), 281-298.

Githumbi, E. N. (2017). Holocene environmental and human interactions in East Africa. (Doctoral dissertation, University of York).

Goldstein, S. T., & Munyiri, J. M. (2017). The Elmenteitan Obsidian Quarry (GsJj50): New Perspectives on Obsidian Access and Exchange During the Pastoral Neolithic in Southern Kenya. African Archaeological Review, 34(1), 43–73. https://doi.org/10.1007/S10437-016-9240-0/TABLES/4

Gosling, W. D., Miller, C. S., & Livingstone, D. A. (2013). Atlas of the tropical West African pollen flora. Review of Palaeobotany and Palynology, 199, 1–135. https://doi.org/10.1016/J.REVPALBO.2013.01.003

Hemp, A (2005) Climate change-driven forest fires marginalize the impact of ice cap wasting on Kilimanjaro. Global Change Biology 11: 1013–1023.

Hemp, A, Beck, E (2001) Erica excelsa as a fire-tolerating component of Mt. Kilimanjaro's forests. Phytocoenologia 31: 449–475.

Henne, P. D., Elkin, C., Franke, J., Colombaroli, D., Calò, C., La Mantia, T., ... & Tinner, W. (2015). Reviving extinct Mediterranean forest communities may improve ecosystem potential in a warmer future. Frontiers in Ecology and the Environment, 13(7), 356-362.

Huffman, T. N. (1982). Archaeology and ethnohistory of the African Iron Age. Annual Review of Anthropology, 11(1), 133–150.

Humphris, J., & Iles, L. (2013). Pre-colonial iron production in Great Lakes Africa: Recent research at UCL Institute of Archaeology. The world of iron, 56-65.

Iles, L., & Lane, P. (2015). Iron production in second millennium AD pastoralist contexts on the Laikipia Plateau, Kenya. Azania: Archaeological Research in Africa, 50(3), 372-401.

Ivory, S. J., & Russell, J. (2016). Climate, herbivory, and fire controls on tropical African forest for the last 60ka. Quaternary Science Reviews, 148, 101–114. https://doi.org/10.1016/j.quascirev.2016.07.015

Johnson, T. C., Scholz, C. A., Talbot, M. R., Kelts, K., Ricketts, R. D., Ngobi, G., Beuning, K. R. M., Ssemmanda, I., & McGill, J. W. (1996). Late Pleistocene desiccation of Lake Victoria and rapid evolution of cichlid fishes. Science, 273(5278), 1091–1093.

Johnson, T. C., Chan, Y., Beuning, K., Kelts, K., Ngobi, G., & Verschuren, D. (1998). Biogenic silica profiles in Holocene cores from Lake Victoria: implications for lake level history and initiation of the Victoria Nile. In Environmental change and response in East African lakes (pp. 75-88). Springer, Dordrecht.

Kendall, R. L. (1969). An Ecological History of the Lake Victoria Basin. Ecological Monographs, 39(2), 121–176.

Kindt, R., van Breugel, P., Orwa, C., Lillesø, J. P. B., Jamnadass, R., & Graudal, L. (2015). Useful tree species for Eastern Africa: a species selection tool based on the VECEA map.

Köppen W (1936) Das geographische System der Klimate. In: Köppen W, Geiger R (eds) Handbuck der Klimatologie Bd. 1, Teil C. Gebrüder Bornträger, Berlin.

Lamb, H. F., Bates, C. R., Coombes, P. V., Marshall, M. H., Umer, M., Davies, S. J., & Dejen, E. (2007). Late Pleistocene desiccation of Lake Tana, source of the Blue Nile. Quaternary Science Reviews, 26(3–4), 287–299. https://doi.org/10.1016/j.quascirev.2006.11.020

Long, C. J., Whitlock, C., Bartlein, P. J., & Millspaugh, S. H. (1998). A 9000-year fire history from the Oregon Coast Range, based on a high-resolution charcoal study.

Loomis, S. E., Russell, J. M., Verschuren, D., Morrill, C., De Cort, G., Sinninghe Damsté, J. S., ... & Kelly, M. A. (2017). The tropical lapse rate steepened during the Last Glacial Maximum. Science advances, 3(1), e1600815.

Marchant, R. (2021). East Africa's Human Environment Interactions. In East Africa's Human Environment Interactions (pp. 39–114). Palgrave Macmillan. https://doi.org/10.1007/978-3-030-88987-6_2

Marchant, R., Mumbi, C., Behera, S., & Yamagata, T. (2007). The Indian Ocean dipole–the unsung driver of climatic variability in East Africa. African Journal of Ecology, 45(1), 4-16.

Marchant, R., Richer, S., Boles, O., Capitani, C., Courtney-Mustaphi, C. J., Lane, P., ... & Wright, D. (2018). Drivers and trajectories of land cover change in East Africa: Human and

environmental interactions from 6000 years ago to present. Earth-Science Reviews, 178, 322-378.

Marlon, J. R. (2020). What the past can say about the present and future of fire. Quaternary Research, 96, 66–87. https://doi.org/10.1017/qua.2020.48

Millspaugh, S. H., & Whitlock, C. (1995). A 750-year fire history based on lake sediment records in central Yellowstone National Park, USA. The Holocene, 5(3), 283-292.

Mooney, S. D., & Tinner, W. (2011). The analysis of charcoal in peat and organic sediments. Mires and Peat, 7(9), 1-18.

Moore, P., Webb, J. A., & Collinson M.E. (1991). Pollen Analysis (Second). Blackwell Scientific Publications.

Mustaphi, C. J. C., Kinyanjui, R., Shoemaker, A., Mumbi, C., Muiruri, V., Marchant, L., ... & Marchant, R. (2021). A 3000-year record of vegetation changes and fire at a high-elevation wetland on Kilimanjaro, Tanzania. Quaternary Research, 99, 34-62.

M'Mbogori, F. N. (2021). Human and Environmental Interactions in Late Iron Age Kenya. In Oxford Research Encyclopedia of Anthropology.

Nakintu, J., & Lejju, J. (2016). Environmental Dynamics of Lake Victoria: Evidence from a 10,000 14C yr Diatom Record from Napoleon Gulf and Sango Bay. Journal of Environmental Science and Engineering, 5, 626-637.

Nelson, D. M., Verschuren, D., Urban, M. A., & Hu, F. S. (2012). Long-term variability and rainfall control of savanna fire regimes in equatorial East Africa. Global Change Biology, 18(10), 3160–3170. https://doi.org/10.1111/j.1365-2486.2012.02766.x

Nicholson, S. E. (2018). The ITCZ and the Seasonal Cycle over Equatorial Africa. Bulletin of the American Meteorological Society, 99(2), 337–348. https://doi.org/10.1175/BAMS-D-16-0287.1

Nyamweya, C., Desjardins, C., Sigurdsson, S., Tomasson, T., Taabu-Munyaho, A., Sitoki, L., & Stefansson, G. (2016). Simulation of Lake Victoria circulation patterns using the regional ocean modeling system (ROMS). PLoS One, 11(3), e0151272.

Okungu, J. ., Njoka, S., Abuodha, J. O. Z., & Hecky, R. E. (2005). Lake Victoria Environment Report Water Quality and Ecosystem Status: Kenya National Water Quality Synthesis Report.

Olsson, I. U. (2009). Radiocarbon dating history: early days, questions, and problems met. Radiocarbon, 51(1), 1-43.

Pedrotta, T., Gobet, E., Schwörer, C., Beffa, G., Butz, C., Henne, P. D., ... & Tinner, W. (2021). 8,000 years of climate, vegetation, fire and land-use dynamics in the thermo-mediterranean

vegetation belt of northern Sardinia (Italy). Vegetation History and Archaeobotany, 30(6), 789-813.

Power, M. J., Marlon, J., Ortiz, N., Bartlein, P. J., Harrison, S. P., Mayle, F. E., ... & Zhang, J. H. (2008). Changes in fire regimes since the Last Glacial Maximum: an assessment based on a global synthesis and analysis of charcoal data. Climate dynamics, 30(7), 887-907.

Reille, M. (1992). Pollen et spores d'Europe et d'Afrique du nord. Laboratoire de Botanique Historique et Palynologie.

Reimer, P. J., William, Austin, E. N., Bard, Edouard, Bayliss, A., Paul, Blackwell, G., Christopher, Ramsey, B., Butzin, M., Cheng, H., Lawrence Edwards, R., Friedrich, Michael, Pieter, Grootes, M., Thomas, Guilderson, P., Hajdas, I., Heaton, T. J., … Talamo, S. (2020). Chronos 14 Carbon-Cycle Facility, the Changing Earth Research Centre, and School of Biological. Earth and Environmental Sciences, 62, 23. https://doi.org/10.1017/RDC.2020.41

Roubik, D. W., & Moreno P., J. E. (1991). Pollen and spores of Barro Colorado Island [Panama].

Rucina, S. M., Muiruri, V. M., Kinyanjui, R. N., McGuiness, K., & Marchant, R. (2009). Late Quaternary vegetation and fire dynamics on Mount Kenya. Palaeogeography, Palaeoclimatology, Palaeoecology, 283(1–2), 1–14. https://doi.org/10.1016/j.palaeo.2009.08.008

Salazar, G., Zhang, Y. L., Agrios, K., & Szidat, S. (2015). Development of a method for fast and automatic radiocarbon measurement of aerosol samples by online coupling of an elemental analyzer with a MICADAS AMS. Nuclear Instruments and Methods in Physics Research Section B: Beam Interactions with Materials and Atoms, 361, 163-167.

Schoenbrun, D. L. (1993). We Are What We Eat: Ancient Agriculture Between the Great Lakes. The Journal of African History, 34(1), 1–31.

Schoenbrun, D. L. (1998). A green place, a good place: Agrarian change, gender, and social identity in the Great Lakes region to the 15th century. Portsmouth: Heinemann.

Schüler, L., & Hemp, A. (2016). Atlas of pollen and spores and their parent taxa of Mt Kilimanjaro and tropical East Africa. Quaternary International, 425, 301–386. https://doi.org/10.1016/J.QUAINT.2016.07.038

Schüler, L., Hemp, A., Zech, W., & Behling, H. (2012). Vegetation, climate and fire-dynamics in East Africa inferred from the Maundi crater pollen record from Mt Kilimanjaro during the last glacial-interglacial cycle. Quaternary Science Reviews, 39, 1–13. https://doi.org/10.1016/j.quascirev.2012.02.003

Stager, J. C. (1984). The diatom record of Lake Victoria (East Africa): the last 17,000 years. Proceedings of the Seventh International Diatom Symposium, 455–476.

Stager, J. C., Cumming, B., & Meeker, L. (1997). A high-resolution 11,400-Yr diatom record from Lake Victoria, East Africa. Quaternary Research, 47(1), 81–89. https://doi.org/10.1006/qres.1996.1863

Stager, J. C., & Johnson, T. C. (2000). A 12,400 14C yr offshore diatom record from east central Lake Victoria, East Africa. Journal of Paleolimnology, 23(4), 373-383.

Stager, J. C., Reinthal, P. N., & Livingstone, D. A. (1986). A 25,000-year history for Lake Victoria, East Africa, and some comments on its significance for the evolution of cichlid fishes. Freshwater Biology, 16(1), 15–19. https://doi.org/10.1111/j.1365-2427.1986.tb00944.x

Stager, J. C., Ryves, D. B., Chase, B. M., & Pausata, F. S. R. (2011). Catastrophic drought in the Afro-Asian monsoon region during Heinrich event 1. Science, 331(6022), 1299–1302. https://doi.org/10.1126/science.1198322

Stockmarr, J. (1971). Tablets with spores used in absolute pollen analysis. Pollen Spores, 13, 615–621.

Stuiver, M. (1970). Oxygen and carbon isotope ratios of fresh-water carbonates as climatic indicators. Journal of Geophysical Research, 75(27), 5247-5257.

Stuiver, M., & Polach, H. A. (1977). Discussion reporting of 14C data. Radiocarbon, 19(3), 355-363.

Szidat, S., Salazar, G. A., Vogel, E., Battaglia, M., Wacker, L., Synal, H. A., & Türler, A. (2014). 14C analysis and sample preparation at the new Bern Laboratory for the Analysis of Radiocarbon with AMS (LARA). Radiocarbon, 56(2), 561-566.

Talbot, M. R., Filippi, M. L., Jensen, N. B., & Tiercelin, J.-J. (2007). An abrupt change in the African monsoon at the end of the Younger Dryas. Geochemistry, Geophysics, Geosystems, 8(3), 1–16. https://doi.org/10.1029/2006GC001465

Talbot, M. R., & Lærdal, T. (2000). The Late Pleistocene-Holocene palaeolimnology of Lake Victoria, East Africa, based upon elemental and isotopic analyses of sedimentary organic matter. Journal of Paleolimnology, 23(2), 141-164.

Talbot, M. R., & Livingstone, D. A. (1989). Hydrogen index and carbon isotopes of lacustrine organic matter as lake level indicators. Palaeogeography, Palaeoclimatology, Palaeoecology, 70(1-3), 121-137.

ter Braak, C. J. F., & Prentice, I. C. (1988). A theory of gradient analysis. In M. Begon, A. H. Fitter, E. D. Ford, & A. Macfadyen (Eds.), Advances in Ecological Research (pp. 271–317). Academic Press.

ter Braak, C. J. F., & Šmilauer, P. (2018). Canoco Reference Manual and User's Guide: Software for Ordination (5.10). Biometris.

Thevenon, F., Williamson, D., Vincens, A., Taieb, M., Merdaci, O., Decobert, M., & Buchet, G. (2003). A late-Holocene charcoal record from Lake Masoko, SW Tanzania: climatic and anthropologic implications. The Holocene, 13(5), 785–792. https://doi.org/10.1191/0959683603hl665rr

Vincens, A., Buchet, G., Williamson, D., & Taieb, M. (2005). A 23,000 yr pollen record from Lake Rukwa (8°S, SW Tanzania): New data on vegetation dynamics and climate in Central Eastern Africa. Review of Palaeobotany and Palynology, 137(3–4), 147–162. https://doi.org/10.1016/j.revpalbo.2005.06.001

Walker, M. (2005). Quaternary dating methods. John Wiley and Sons.

White. (1983). The Vegetation of Africa. A Descriptive Memoir to Accompany the Unesco/AETFAT/UNSO Vegetation Map of Africa. UNESCO.

Whitlock, C., Higuera, P. E., McWethy, D. B., & Briles, C. E. (2010). Paleoecological perspectives on fire ecology: revisiting the fire-regime concept. The Open Ecology Journal, 3(1).

Wirrmann, D., Bertaux, J., & Kossoni, A. (2001). Late Holocene Paleoclimatic Changes in Western Central Africa Inferred from Mineral Abundance in Dated Sediments from Lake Ossa (Southwest Cameroon). Quaternary Research, 56(2), 275–287. https://doi.org/10.1006/qres.2001.2240

Zander, P. D., Szidat, S., Kaufman, D. S., Żarczyński, M., Poraj-Górska, A. I., Boltshauser-Kaltenrieder, P., & Grosjean, M. (2020). Miniature radiocarbon measurements (< 150 µg C) from sediments of Lake Żabińskie, Poland: effect of precision and dating density on age–depth models. Geochronology, 2(1), 63-79.

Zhao, Y., & Yu, Z. (2012). Vegetation response to Holocene climate change in East Asian monsoon-margin region. Earth-Science Reviews, 113(1–2), 1–10. https://doi.org/10.1016/j.earscirev.2012.03.001

Chapter III: Ecological Long-Term Successions Around Lake Victoria in Response to the Latest Pleistocene and Early Holocene Climatic Changes

Declaration of contribution

The following study is to be submitted to Palaeogeography, Palaeoclimatology, Palaeoecology. Yunuén Temoltzin Loranca, Willy Tinner and Erika Gobet conceptualized the study, Boris Vannière provided guidance for the fire reconstructions. Jacqueline van Leeuwen and Yunuén Temoltzin Loranca conducted the palynological investigations. Yunuén Temoltzin Loranca did the numerical investigations, the data visualization and wrote the draft of the manuscript. Erika Gobet, Boris Vannière, Jacqueline van Leeuwen, Giulia Wienhues, Colin Courtney-Mustaphi, Mary Kishe, Moritz Muschik, Leighton King, Nare Ngoepe, Blake Matthews, Hendrik Vogel, Oliver Heiri, Ole Seehausen, Martin Grosjean and Willy Tinner discussed the results and commented on the manuscript. Ole Seehausen and Martin Grosjean acquired the funding. All authors agree on the science and the style of the manuscript.

Ecological long-term successions around Lake Victoria in response to the latest Pleistocene and Early Holocene climatic changes.

Yunuen Temoltzin-Loranca*[a,b], Erika Gobet[b], Boris Vannière[b,c], Jacqueline F.N. van Leeuwen[b], Giulia Wienhues[a], Colin Courtney-Mustaphi[d], Mary Kishe[e], Moritz Muschick[f,g], Leighton King[f,g], Pavani Misra[f,g], Nare Ngoepe[f,g], Blake Matthews[f,g], Hendrik Vogel[h], Oliver Heiri[d], Ole Seehausen[f,g], Martin Grosjean[a], Willy Tinner[b]

[a] Institute of Geography and Oeschger Center for Climate Change Research, University of Bern, Bern, Switzerland
[b] Institute of Plant Sciences and Oeschger Center for Climate Change Research, University of Bern, Bern, Switzerland
[c] MSHE, Chrono-environnement, CNRS, Université de Franche Comté, Besançon, France
[d] Department of Environmental Sciences, Geoecology, University of Basel, Basel, Switzerland
[e] Tanzania Fisheries Research Institute, Dar es Salaam, Tanzania
[f] Department of Fish Ecology and Evolution, Center for Ecology, Evolution, and Biogeochemistry, Swiss Federal Institute for Aquatic Science and Technology (EAWAG), Kastanienbaum, Switzerland
[g] Aquatic Ecology and Evolution, Institute of Ecology and Evolution, University of Bern, Bern, Switzerland
[h] Institute of Geological Sciences and Oeschger Center for Climate Change Research, University of Bern, Bern, Switzerland

* Correspondence to: Yunuén Temoltzin Loranca (yunuen.temoltzin@unibe.ch)

Keywords:

Pollen, Late Pleistocene, Early Holocene, East Africa, Vegetation dynamics.

3.1 ABSTRACT

Climate and ecosystem dynamics in tropical East Africa during the latest Pleistocene and the Holocene, including the African Humid Period (AHP, ca. 14,800 to 5500 cal yr BP) have been widely investigated. Nevertheless, there are only a few, and often incomplete terrestrial palaeorecords in tropical East Africa encompassing these periods. Novel and highly resolved palaeovegetation datasets may provide new insights into past ecosystem dynamics, disclosing long-term responses of vegetation to climate change. In this study, we present the first high-resolution pollen record from the Lake Victoria basin, covering the period from 16,600 to 9000 cal yr BP, when Afromontane forests and rainforests gradually replaced the savanna. We discuss this original dataset alongside published palaeoclimate data, TEX_{86} inferred temperature and $\delta D_{leaf\ wax}$ inferred precipitation records, to assess long-term ecological successions and their potential causes around Lake Victoria. By ca. 16,500 cal yr BP, the movement of the Afrotropical rainbelt not only brought an increase in temperature and

moisture into the Lake Victoria basin but also promoted the spread of arboreal taxa, such as *Celtis* and *Podocarpus*, at the expense of the savanna. At that time fires were prominent in Afromontane stands. Later at ca. 15,500-15,000 cal yr BP temperatures and humidity rose and Afromontane elements, such as *Olea* and *Macaranga* spread faintly, while grasses were burning in the savanna. During the period from 13,250 to 10,700 cal yr BP, Afromontane vegetation dominated by *Olea* became more prominent and expanded towards the lowlands where the first rainforest or gallery forest stands established, however, the savanna only marginally retreated. An initial spread of rainforests occurred at ca. 11,500-11,100 cal BP at the onset of the Holocene, when temperatures and moisture further increased. Subsequently, between 10,700 and 10,300 cal yr BP the tropical savanna was largely replaced by the rainforest, while the Afromontane forest probably spread to higher elevations, as is the case today. Our high temporal resolution record demonstrates the dynamic response of African tropical ecosystems to major temperature and humidity variations from 16,600 to 9000 cal yr BP, including some of the most important landscape transformations in East Africa in the past 20,000 years.

3.2 INTRODUCTION

Climate change is expected to significantly impact East African ecosystems in the coming years, including biodiversity and provisioning services in regions such as the Lake Victoria basin (Chapman et al., 2008; Lejju, 2012). The frequency and intensity of rainfall is expected to increase, and temperature is predicted to rise (Luhunga & Songoro, 2020), both of which will consequently impact commercial activities, agriculture, water stress, health, and food security in the region (IPCC, 2022). The climate of the East African region is complex due to the influence of the Atlantic and the Indian Ocean (Liu et al., 2017; Marchant et al., 2007; Nicholson & Kim, 1997). Changes in temperature, rainfall, fire regime, herbivory and human activities are among the most important factors altering the landscape. Some of these environmental drivers, have been studied in the Lake Victoria basin since the late 1960s with special focus on vegetation dynamics, uncovering important changes since the Pleistocene to modern times (Beuning, 1999; Colombaroli et al., 2014; Kendall, 1969; Ssemmanda & Vincens, 2002, 2018; Temoltzin-Loranca et al., 2023).

Lake Victoria is the largest tropical lake on Earth; thus, both aquatic and terrestrial habitats in its basin represent important reservoirs of biodiversity (Sayer et al., 2018; UN-Habitat, 2008). One of the most significant impacts for the vegetation on both historical and palaeoenvironmental (Late Quaternary) scales has been the change in precipitation regimes, which results in variable drought frequency, changes in lake water level and changes to the surrounding vegetation (Nicholson & Yin, 2001).

In the past 17,000 years, rainfall and temperature have played an important role in shaping the landscape. In this context, palynological records from Lake Victoria have allowed us to examine general trends in vegetation dynamics and reported considerable biome changes (Kendall, 1969; Temoltzin-Loranca et al., 2023). Namely, the expansion of Afromontane vegetation at ca. 13,250 cal yr BP, the expansion of the rainforest at ca. 10,600 cal yr BP, and the re-expansion of the savanna after 4500 cal yr BP (Kendall, 1969; Temoltzin-Loranca et al., 2023). While these major biome shifts have been documented in past studies, the temporal resolution of available records remained rather low (for instance, every ca. 340 years in Kendall, 1969 or ca. 410 years in Beuning, 1999 and ca. 700 years in Temoltzin-Loranca et al., 2023), which impeded to thoroughly address the involved ecological processes.

The analysed timespan covers some major climate and ecosystem reorganizations during the latest Pleistocene and the Early Holocene, including the onset of the African Humid Period (AHP) – the most notable climatic period for the African continent since the Pleistocene to modern times – which extends from ca. 14,800 to 5,500 cal yr BP (deMenocal et al., 2000; Shanahan et al., 2015). More specifically, humidity peaked during the Early and Mid-Holocene, triggering important vegetation changes, such as the decline of savanna and the expansion of forests in East Africa (Ssemmanda & Vincens, 1993; Van Zinderen Bakker & Coetzee, 1988; Vincens et al., 2005). Considering the importance of such ecological reorganizations, in this manuscript we refer to this humid-warm period at ca. 11,500-5500 cal yr BP as the Holocene AHP.

The major biome reorganizations observed in previous palaeoecological investigations opened major questions regarding the precise timing of changes and the ecological processes involved. For instance, the timing of the spread of the Moraceae rainforest in the surroundings of Lake Victoria was debated, mainly due to differences in the accuracy of the chronologies

previously published. While Kendall (1969) reported the expansion at ca. 9500 ^{14}C yr BP (10,900 cal yr BP) during the Holocene African Humid Period (AHP), Beuning (1999) suggested it occurred in the Late Pleistocene at ca. 11,200 ^{14}C yr BP (13,100 cal yr BP). Three independently dated pollen records collected from sediment cores along a transect from the lake shore to the deep water presented in Temoltzin-Loranca et al. (2023) provided robust evidence that the rainforest spread between 11,500 and 10,000 cal yr BP, confirming the Early Holocene age of this important vegetation reorganization. However, the low temporal resolution of that study (ca. 550 years on average in sediment cores LV1, LV2 and LV4) impeded a chronologically and ecologically precise assessment. For instance, it remains unclear whether the rainforest spread solely in response to moisture conditions, or if the Early Holocene warming also played a role. Similarly, the ecological processes that led to the expansion of Afromontane vegetation at ca. 13,250 cal BP are elusive, and the source of fire remained unexplored (Temoltzin-Loranca et al. 2023). Here, we aim to merge this gap by investigating the changes observed during the savanna-forest transition from the latest Pleistocene (16,600 cal yr BP) to the Early Holocene (9000 cal yr BP) at a high temporal resolution (every 40 years).

This study seeks to: (I) provide the first high–resolution pollen record for the Lake Victoria basin during the latest Pleistocene and Early Holocene; (II) to assess the major vegetation and ecosystem changes including the source of the biomass burning; and (III) to elucidate the ecosystem responses to climate, by comparing our palaeoecological time series with independent palaeoclimate proxies, reflecting rainfall amount and temperature (Berke et al., 2012). We are particularly interested in the factors that allowed Afromontane and rainforest vegetation to gradually replace the savanna during the period from 16,600 to 9000 cal yr BP.

3.3 SITE AND METHODS

3.3.1 STUDY SITE

Lake Victoria is the second-largest freshwater lake in the world (surface area = 68,800 km^2). As part of the East African Rift System (EARS), it was formed as a result of faulting (Odada & Olago, 2006). It is located at an altitude of 1135 m above sea level (m a.s.l). Rainfall is the biggest contributor to Lake Victoria's water balance accounting for ca. 80%, the remaining ca. 20% come from 17 tributaries of which the largest is the Kagera River (Yin & Nicholson, 1998). Both rainfall and the wind regime follow a bimodal pattern with two rainy seasons occurring

from March to June, and from October to December (Okungu et al., 2005). Today's precipitation ranges from 1000 to 1500 mm/year, mainly controlled by the migration of the Afrotropical rainbelt and the Congo Air Boundary (CAB) across the equator (Colombaroli et al., 2018; Okungu et al., 2005; Tierney et al., 2011; Verschuren et al., 2009). The wind direction from January to March is regulated by the Northeast Monsoon, whereas from August to September it is influenced by the Southeast Monsoon (Nieuwolt, 1979). The times between April and July, and October and December are transitional periods (Okungu et al., 2005).

The three main biomes or vegetation types around Lake Victoria are the tropical rainforests which develop in warm-humid conditions, the Afromontane forests which expand at higher and cooler altitudes at ca. 1200 – 2500 m a.s.l., and the tropical savanna, rich in evergreen to semi–evergreen bushlands, which extend over warm to arid conditions (Lillesø et al., 2011). More specifically, the vegetation types include the Guineo–Congolian rainforest, the transitional rainforest, the swamp forest, the scrub forest, and the evergreen and semi–evergreen bushland and thicketed derived communities (White, 1983) as well as several transitional plant communities between these major units. In addition to the zonal vegetation types, azonal vegetation can occur in areas such as wetlands (FTEA, 1952–2012). Today, the lake basin is surrounded by the ecosystems mentioned above, having the closest stands of Afromontane taxa at Mount Elgon, the Mau escarpment, and the Ngorongoro crater (Hedberg, 1955). Outside the study region, subtropical to temperate Afromontane forests grow in disjunct zones of the mountains of East, West and South Africa (Allen et al., 2021; Bekele, 1993; Mucina & Geldenhuys, 2016; Powell et al., 2023). Striking floristic (e.g. *Olea*, *Podocarpus*, *Celtis*, *Juniperus*, Erica) and faunal similarities, as well as ecological niche models, suggest that these isolated mountain forest communities were connected in the past during cold periods of the Pleistocene that allowed taxa to spread to lower altitudes (Allen et al., 2021).

3.3.2 Sediment Cores, Chronology and XRF

As part of a campaign organized by the University of Bern and the Tanzanian Fisheries Institute (TAFIRI), four sediment cores located at water depths ranging from 13.4 to 63 m were retrieved near the Shirati Bay. In this study, we focus on core LVC18_S4, hereafter referred to as LV4, located at 01°02.966'S / 33°47.768'E, ca. 30 km away from the shore at a water depth of 63 m (Fig. 1). The chronology and full details of the coring campaign are described in

Temoltzin-Loranca et al. (2023). Scanning X-ray fluorescence (XRF) was performed at 5mm intervals with an ITRAX core scanner using a Mo- and Cr- anode X-ray tube at 50 mA, 30 kV and 30 seconds integration time. Here, we display only 2 elemental ratios, Rb/K as an indicator of chemical weathering (Wienhues, et al. submitted), and Zr/Ti as a grain size proxy (Davies et al. 2015).

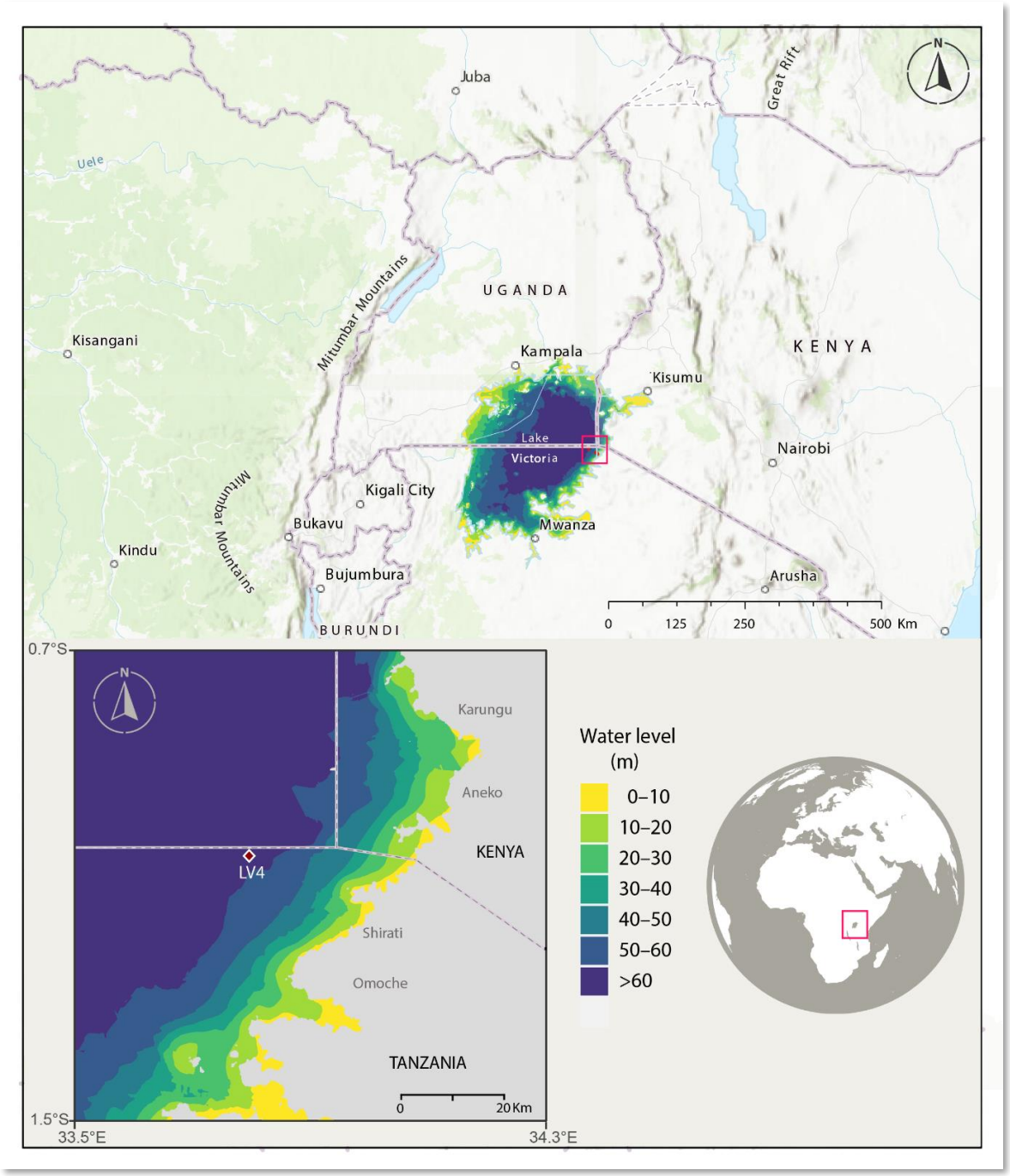

Figure 1. Location of Lake Victoria and core LV4. The colour chart shows the water depth in 2017. Datapoints for elaborating both maps were extracted from Hamilton et al. (2022).

3.3.3 POLLEN AND CHARCOAL ANALYSES

We took 153 sediment samples of 1 cm^3 which were collected at 2 cm intervals (ca. every 40 years) throughout the lower portion of LV4 (depths= 463–777). The samples were prepared for pollen analyses following standard procedures using HCl, KOH, HF and acetolysis (Moore et al., 1991). *Lycopodium clavatum* tablets (Batch number 3862 with n= 9666± 671 spores per tablet) provided by the University of Lund (Maher, 1981) were added to the samples prior to chemical treatment in order to calculate microfossil concentrations and influx (Stockmarr, 1971). Samples were stained with fuchsine and diluted with glycerine for mounting. The slides were analyzed under a light microscope (Leica 2500) at 400× magnification. We used palynological keys, atlases (Gosling et al., 2013; Reille, 1992; Roubik & Moreno P., 1991; Schüler & Hemp, 2016) and the pollen reference collection of the Kilimanjaro region located at the palynological laboratory of the University of Göttingen, Germany. Pollen sums ranged from 98 (deepest sample of the record where grains were rare to find) to 588 grains per sample (mean= 375 pollen grains, standard deviation= 95). Eight samples above the lowermost sample were sterile (ca. 300 years).

For biomass burning assessment, we analysed macrocharcoal for a total of 389 sediment samples (whole core) of ca. 9 cm^3 taken continuously at 2 cm intervals and sieved through a mesh size of 200 µm (see Temoltzin-Loranca et al., 2023). In this paper we only display the samples corresponding to the lower portion of LV4 (depths= 463 –777). The samples were analysed under a stereomicroscope (Leica M125) at 40× magnification, and the charcoal was picked. Additionally, charcoal morphotypes (wood vs grass) were determined following Colombaroli et al.'s (2014) approach. Charcoal particles with a length–width ratio ≥ 3:1 and stomata within the rows of epidermal cells (Colombaroli et al., 2014; Jensen et al., 2007) were considered to originate from grass, whereas particles with thicker structure and a length–width ratio of ≤3:1 were identified as wood charcoal pieces (Umbanhowar & McGrath, 1998). For the calculation of macroscopic charcoal influx, charcoal particle numbers were standardized to 1 cm^3 respectively to 1 cm^2/year using the age-depth model from Temoltzin-Loranca et. al (2023).

3.3.4 NUMERICAL METHODS

3.3.4.1 POLLEN ZONATION AND ORDINATION

We assigned Local Pollen Assemblage Zones (LPAZ) by using the optimal partitioning approach with a minimum sum of squares (Birks and Gordon, 1985) and determined the number of significant zones with the aid of the broken-stick model (Bennet, 1996). In order to retain the original low-resolution subdivision (LPAZ) of Temoltzin-Loranca et al. (2023), the new significant zone limits, resulting from the additional pollen samples analysis, were used to delimit subzones.

To identify gradients in vegetation composition, we analysed the pollen percentage data with a Detrended Correspondence Analysis (DCA; Legendre & Birks, 2012; Lepš & Šmilauer, 2003; ter Braak & Prentice, 1988) using Canoco 5.10 (ter Braak & Šmilauer, 2018). The gradient length of the first axis of the DCA was 1.71 standard deviations, indicating that Principal Component Analysis (PCA) would be suitable to analyse the data. However, PCA displayed a strong horseshoe effect, and we decided to proceed with DCA to reduce this effect (Legendre & Birks, 2012; ter Braak & Prentice, 1988). Pollen percentage data was detrended by segments, and we applied a squared-root transformation to stabilize the variance. Additionally, the rare types were down-weighted and only the 35 species with the largest contribution to the total variance explained along axis 1 and 2 are shown in the final figure.

3.3.4.2 SPECIES RESPONSE CURVES

In order to explore the response of selected species to climate, specifically rainfall and temperature, we fitted generalized additive models, GAMs (Hastie TJ & Tibshirani RJ, 1990; Šmilauer & Lepš, 2014) assuming a Poisson distribution for the response variables and using a log link function with a maximum of 2 degrees of freedom (DF). Then, we chose the most parsimonious model using stepwise selection based on the Akaike Information Criterion (AIC) value. Response curves were fitted in Canoco 5 (ter Braak & Šmilauer, 2018). In our study, we used the previously published data from TEX_{86}, and $\delta D_{\text{leaf wax}}$ (Berke et al. 2012) to represent past changes in temperature and rainfall amount in the study region. Additionally, we tested the response of vegetation to fire (charcoal), however, as the response curves did not exhibit noteworthy responses, we decided to stop further analysis.

3.4 RESULTS AND INTERPRETATION

3.4.1 VEGETATION AND FIRE HISTORY

The palaeoecological record of Lake Victoria (LV4) starts at 16,600 cal yr BP and the whole examined sequence includes 7600 years (16,600-9,000 cal yr BP). However, in the bottom part of the core, pollen grains were very rare or absent from 16,600 to 16,300 cal yr BP. We found a total of 128 pollen taxa that were identified to the most detailed taxonomic level possible. Due to the higher temporal resolution of this record, the subzones LV4-1a and LV4-1b previously determined by visual criteria (Temoltzin-Loranca et al., 2023) were now statistically significant. Moreover, LV4-2 resulted in two additional statistically significant subzones: LV4-2a and LV4-2b.

LV4-1a (16,600-13,250 cal yr BP); flourishment of the savanna grasslands (Fig. S1). Herbs dominated the landscape with values close to 90% of abundance. The most frequent taxa are Poaceae, which maintains pollen values between 50% and 60%, as well as Cyperaceae, with values around 10 to 20 %. Plant species belonging to the Amaranthaceae, Brassicaceae and Cichorioideae families and taxa such as *Artemisia* and *Senecio* were also important (5-10%). Additionally, our pollen data suggest the presence of savanna trees such as *Acacia*-type, *Combretum*, *Indigofera* and *Lannea* (Figs. 2, 3 and 4). The pollen assemblage also indicates the presence of Afromontane vegetation, which formed isolated stands in the surroundings of the lake (e.g. trees and shrubs such as *Podocarpus*, *Celtis*, *Olea*, and *Juniperus*, as well as herbs such as *Conyza*, and *Rumex*). *Olea* expanded for the first time around 15,000 cal yr BP but remained rather low until ca. 13,800 cal yr BP. During this period, the lake was most likely shallow, the presence of *Typha* (>3%) suggests the proximity of our coring spot (today at 69 m water depth) to a lake shore or wetland, until ca. 13,800 cal yr BP, when aquatic taxa (*Lemna*, *Potamogeton*, *Nymphaea caerulea*, *Nymphaea lotus*) fainted.

Biomass burning inferred by macrocharcoal influx peaks occurred between 16,600 and 16,000 cal yr BP. The higher influx in woody charcoal particles suggests that most fires occurred in the Afromontane stands (*Olea*, *Podocarpus*, *Juniperus*). Around 15,500 cal yr BP, grassland burning started to increase steadily, resulting in maximum values in the grass charcoal influx around 14,500 cal yr BP. Towards the end of this zone (around 14,000 cal yr BP), the amount of grassland savanna fires declined and remained at a low level.

LV4-1b (13,250-10,700 cal yr BP); the spread of Afromontane vegetation, first rainforest or gallery forest stands (Fig. S1). Pollen of herbs continues to dominate the record;

however, it decreases to ca. 65%. Woody taxa characteristic of the thicket clumps, such as *Allophylus*, *Trema*, *Scutia*, *Grewia* and *Syzygium* expanded in the savanna (Figs. 2, 3, 4 and 5). Subtropical Afromontane vegetation spread rather abruptly at around 13,250 cal yr BP. Specifically, *Olea* became important (>15%) together with *Podocarpus*, *Celtis* and *Macaranga* (ca. 5%). Moreover, concurrent with the mass expansion of *Olea*, an initial establishment of tropical rainforest or gallery forest taxa occurred. Moraceae, *Alchornea* and *Urera*-type established the first isolated stands, likely in sheltered micro-habitats where temperature and moisture conditions were favourable. At around 11,500-11,100 cal BP the rainforest taxon Moraceae increased to reach a first peak (>10%), while moderate minima of Moraceae occurred around 12,500, 11,700 and 10,800 cal yr BP. From ca. 11,100 to 10,700 cal yr BP, higher macroscopic charcoal influx dominated by woody species suggests frequent fire events in the Afromontane and rainforest stands.

LV4-2a (10,700-10,300 cal yr BP); the expansion of the rainforest and the vanishing of the savanna (Fig. S1). Pollen percentages of herbs (particularly Poaceae and Cyperaceae) decrease markedly (Figs. 2, 3 and 5), while arboreal pollen percentages increase (>60%). Rainforest taxa spread around Lake Victoria during this period, such as Moraceae (>20%), *Alchornea* (ca. 5%) and *Acalypha* (2%). Changes in the Afromontane forests comprised the expansion of *Olea*, *Celtis* and *Macaranga*, while *Podocarpus* remained rare and others such as Myrica, *Juniperus*, Ericaceae and *Hagenia* decreased markedly. A remarkable change in savanna trees and shrubs communities and thicket clumps occurred during LV4-2a, with a shift from *Combretum* to *Trema*, likely indicating the expansion of evergreen *Trema* trees on the costs of drought-adapted *Combretum* shrublands. Subtropical and tropical trees or shrubs such as *Phoenix*-type and *Alchornea* spread during this phase with distinct pollen peaks at around 10,300 cal yr BP at the transition to zone LV4-2b. Interestingly, *Tetrorchidium* appeared for the first time in the pollen record. At the onset of this subzone around 10,700 cal yr BP macroscopic charcoal originating from trees starts to decline after a last peak, suggesting that forest fires became less frequent than before.

LV4-2b (10,300-9000 cal yr BP); further spread of tropical rainforests and persistence of Afromontane vegetation (Fig. S1). At ca. 10,300 cal yr BP the dominance of Moraceae (2 pore pollen type) rapidly increases from 30 to 40 % suggesting that rainforests spread abruptly (in less than 40 years; Figs. 2, 3 and 5). Around 10,000 cal yr BP Moraceae (2 pore pollen type)

was partly replaced during 100-200 years by tropical rainforest taxa such as *Alchornea* (ca. 5%), *Acalypha* (ca. 3%) and the triporate Moraceae pollen type. Furthermore, pollen types such as *Phoenix* and *Tetrorchidium* are lacking during this phase, indicating a decline of these palms, shrubs or trees in the lake catchment. Fluctuations among the rainforest tree taxa may indicate minor reorganizations of vegetation composition and successional processes toward closed forest canopy. Indeed, after 10,000 cal yr BP, arboreal pollen (AP) dominated by Moraceae, reaches peak values around 75%, suggesting the occurrence of rather dense forest in the Lake Victoria area. Although declining, the pioneer tree *Musanga* persisted, while *Urera*-type, possibly in the form of lianas reaching the forest canopy, spread. The expansion of rainforest was not at the expense of Afromontane taxa with stable populations of *Olea* (ca.10%) and *Macaranga* (ca. 5%), but rather savanna vegetation almost collapsed. Specifically, herb taxa such as Poaceae (ca. 20%), Cyperaceae, *Artemisia* (ca. 2%), as well as savanna woody taxa such as *Combretum* and *Indigofera* reached lowest abundances. Macroscopic herbaceous and woody charcoal influx suggests fewer fires when compared to previous zones.

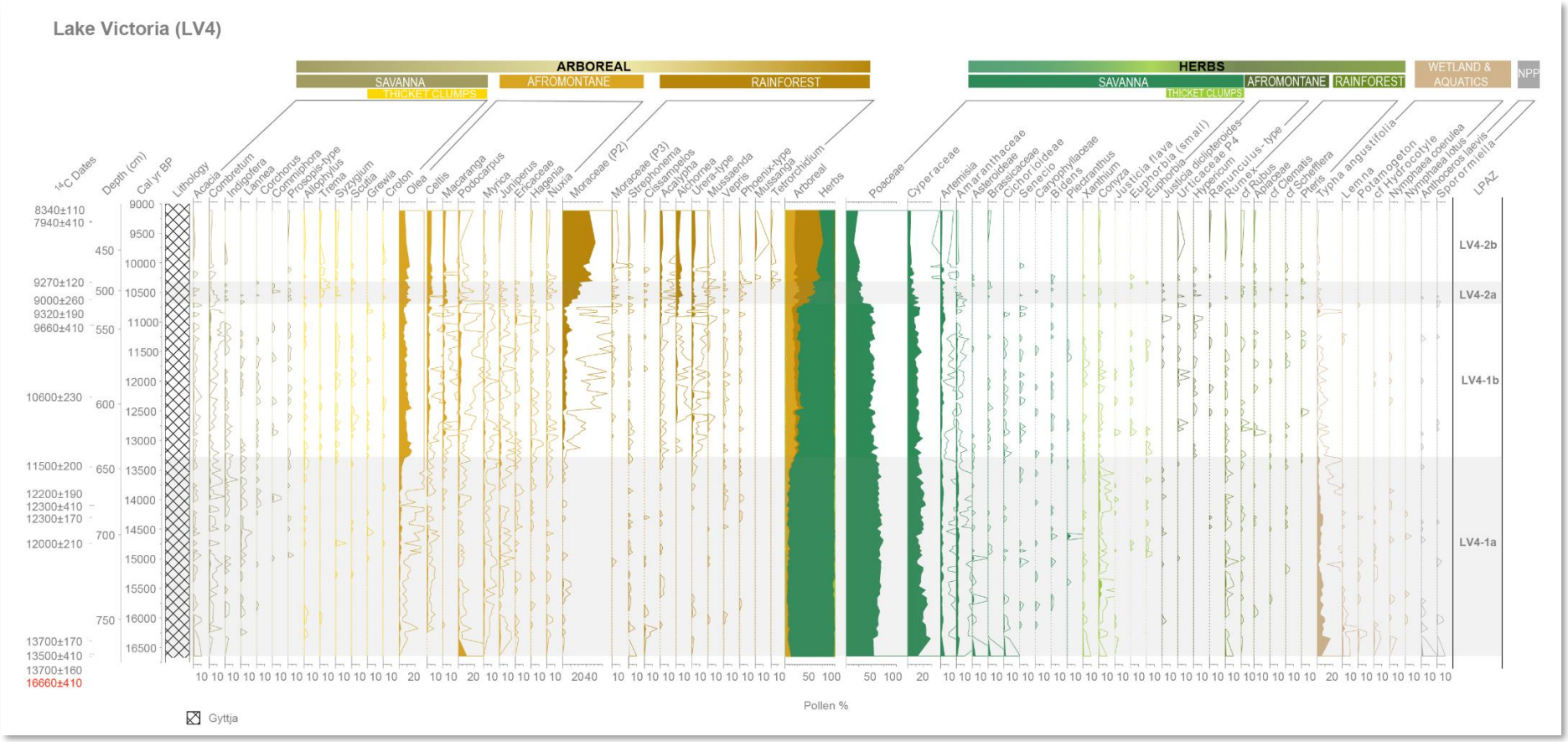

Figure 2. *Pollen record from Lake Victoria (LV4). Arboreal species are plotted on the left side in different shades of yellow according to each biome indicated by the bands on top. Herb species are plotted on the right side in different shades of green according to each biome. indicated by the bands on top. LPAZ= Local pollen assemblage zones. Empty curves represent a 10x exaggeration.*

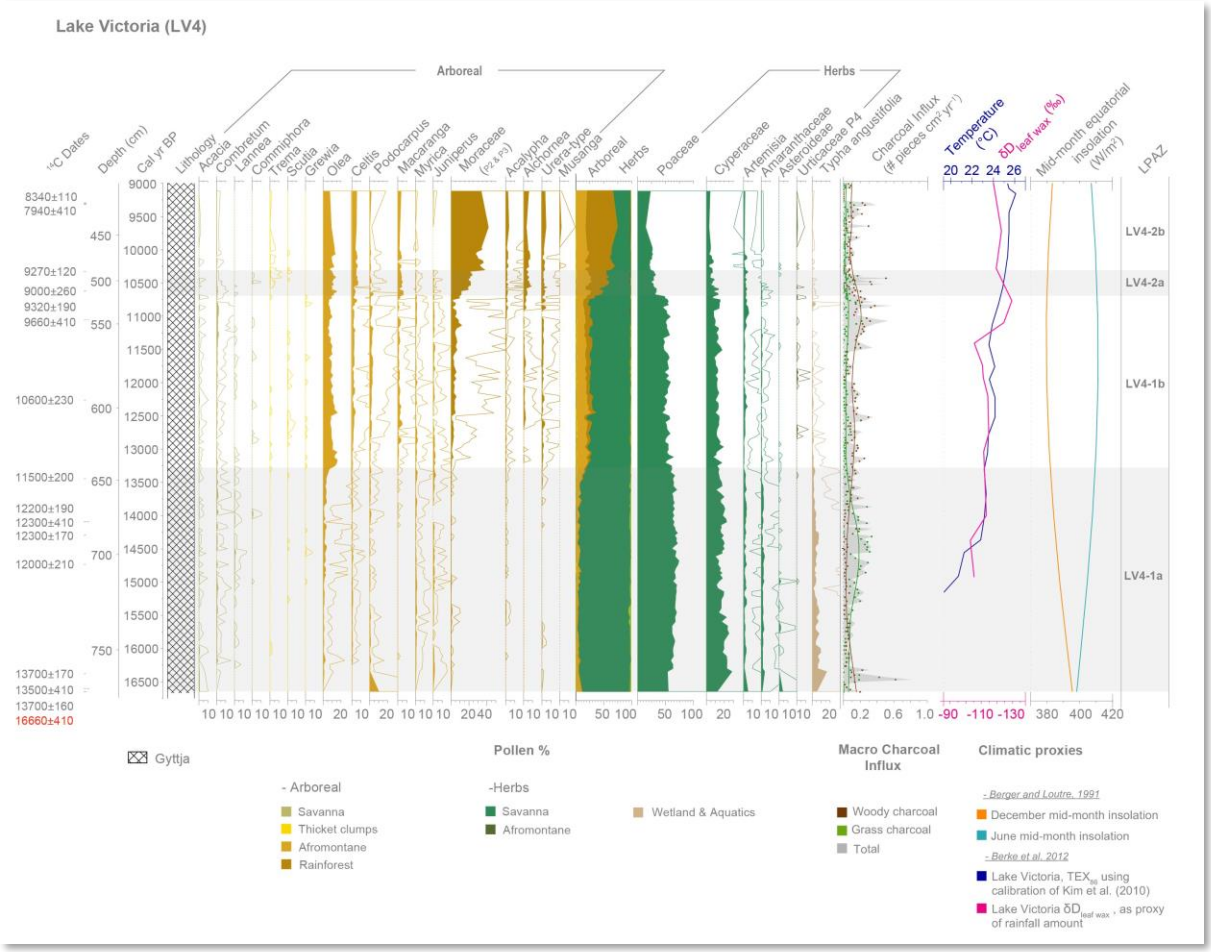

Figure 3. Selected pollen taxa from Lake Victoria core LV4, charcoal influx, temperature, $\delta D_{leaf\ wax}$, and Equatorial insolation. For the pollen record, the woody species are plotted on the left side of the summary curve, in diverse yellow shades representing a different ecosystem: Savanna (dark khaki), thicket clumps (gold), Afromontane (dark gold) and rainforest (dark goldenrod). Herb species on the right side of the summary curve are plotted in diverse green shades representing a different ecosystem: Savanna (sea green) and Afromontane (olive green). Wetland and aquatics are represented in sand colour. LPAZ= Local pollen assemblage zones. Empty curves represent a 10x exaggeration. For the charcoal record, the points represent the herb charcoal influx (lime green) and the woody charcoal influx (brown). Continuous lines superimposed on the charcoal data indicate LOWESS smoothing used only for visualization purposes. The gray curve represents the total charcoal influx. Temperature record of Lake Victoria is plotted in °C inferred from TEX_{86} using the calibration of Kim et al. (2010), obtained from Berke et al. (2012). $\delta D_{leaf\ wax}$ record from Lake Victoria in ‰, used as proxy of rainfall amount (Berke et al. 2012), more negative values indicate more rainfall. Equatorial insolation of June (blue) and of December (orange) in W/m^2 (Berger and Loutre, 1991).

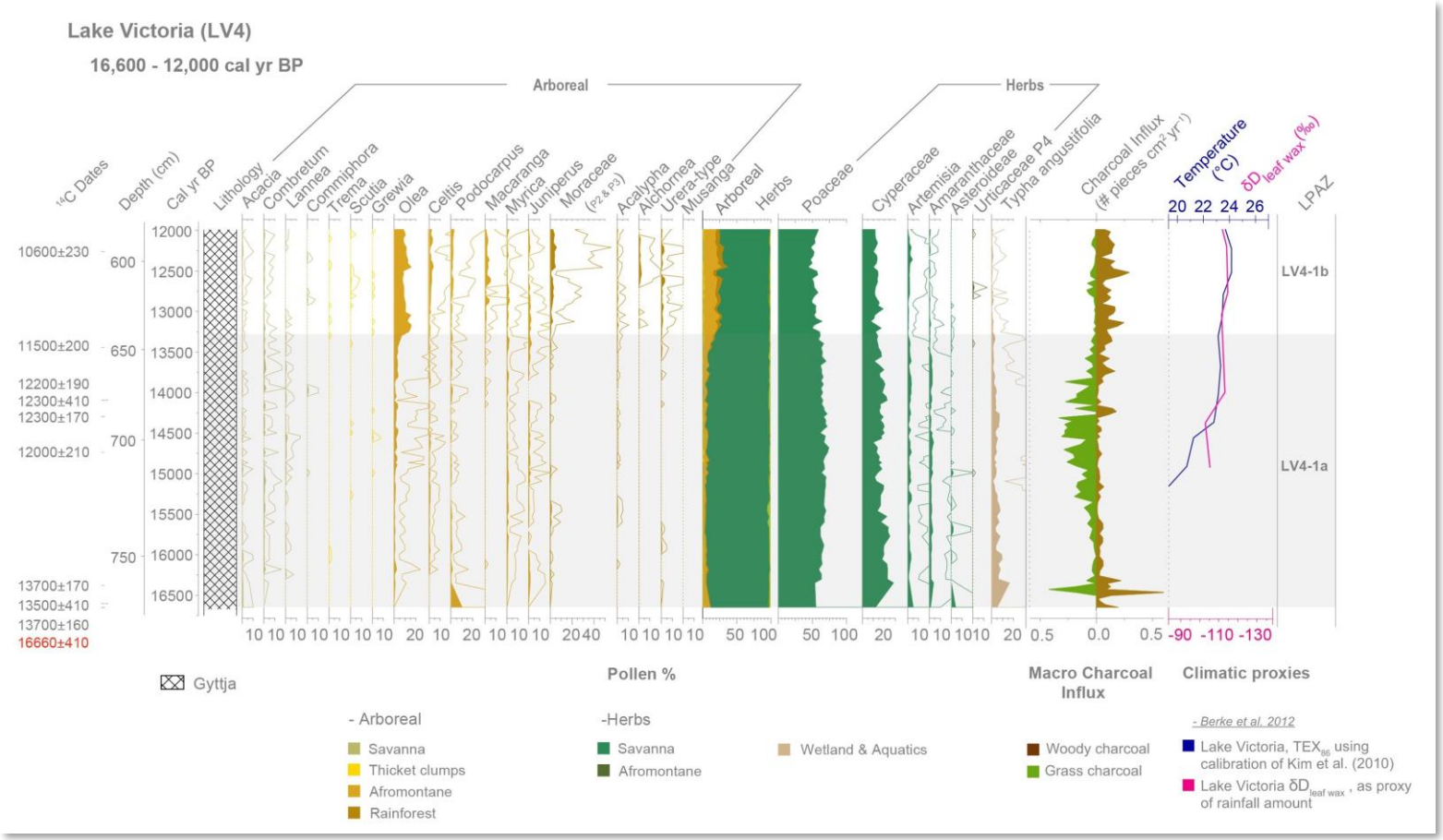

Figure 4. Selected pollen taxa from Lake Victoria core LV4 from 16,600 to 12,000 cal yr BP together with charcoal influx, temperature and the δD $_{leaf\ wax}$ record. For the pollen record, the woody species are plotted on the left side of the summary curve, in diverse yellow shades representing a different ecosystem: Savanna (dark khaki), thicket clumps (gold), Afromontane (dark gold) and rainforest (dark goldenrod). Herb species on the right side of the summary curve are plotted in diverse green shades representing a different ecosystem: Savanna (sea green) and Afromontane (olive green). Wetland and aquatics are represented in sand colour. LPAZ= Local pollen assemblage zones. Empty curves represent a 10x exaggeration. The herb charcoal influx is plotted in green and the woody charcoal influx in brown. The temperature record of Lake Victoria is plotted in °C inferred from TEX$_{86}$ using the calibration of Kim et al. (2010), obtained from Berke et al. (2012). δD $_{leaf\ wax}$ record from Lake Victoria in ‰, used as proxy of rainfall amount (Berke et al. 2012).

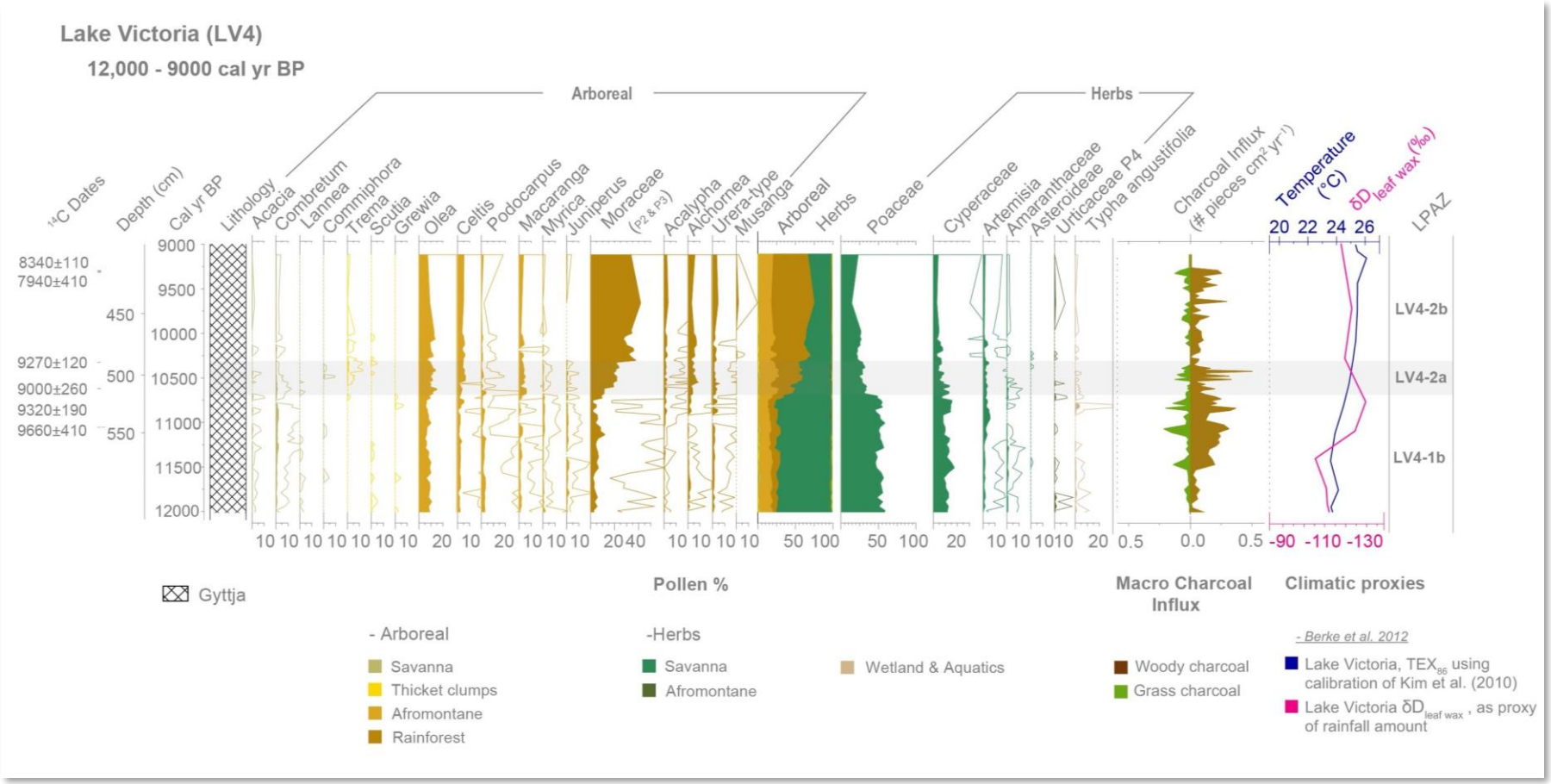

Figure 5. Selected pollen taxa from Lake Victoria core LV4 from 12,000 to 9000 cal yr BP together with the charcoal influx, temperature and the δD $_{leaf\ wax}$ record. For the pollen record, the woody species are plotted on the left side of the summary curve, in diverse yellow shades representing a different ecosystem: Savanna (dark khaki), thicket clumps (gold), Afromontane (dark gold) and rainforest (dark goldenrod). Herb species on the right side of the summary curve are plotted in diverse green shades representing a different ecosystem: Savanna (sea green) and Afromontane (olive green). Wetland and aquatics are represented in sand colour. LPAZ= Local pollen assemblage zones. Empty curves represent a 10x exaggeration. The herb charcoal influx plotted in green and the woody charcoal influx in brown. The temperature record of Lake Victoria is plotted in °C inferred from TEX$_{86}$ using the calibration of Kim et al. (2010), obtained from Berke et al. (2012). δD $_{leaf\ wax}$ record from Lake Victoria in ‰, used as proxy of rainfall amount (Berke et al. 2012).

3.4.2 Ordination and Species Response Curves

The ordination results are displayed in a species and sample scatterplot (Figs. 6A and 6B), and as variations in DCA axis 1 over time (Fig. 7B). The species scores indicate that DCA axis 1, explaining 21.07% in the species data, represents a gradient of temperature and moisture requirements from warm and wet (e.g. Moraceae, *Acalypha*, *Urera*-type) to cool and dry (e.g. Amaranthaceae, *Rumex*, *Acacia*-type, Indigofera). For DCA axis 2, explaining only 4.04 % of the variance, species scores suggest a weak gradient from eroding shale habitats (e.g. *Thalictrum*, *Hypericum*, *Lannea*, *Euphorbia*) to more stable landscapes (e.g. Asteroideae, *Lemna*, *Acacia*-type). In the sample scatterplot, the sample scores are grouped according to the statistically significant pollen assemblage zones LV4-1a to LV4-2b. When plotting variations in DCA axis 1 along time, together with changes in temperature, rainfall amount, and proxy measurements for chemical weathering (Rb/K; Wienhues et al. submitted) and grain size (Zr/Ti), axis 1 scores follow changes in climatic conditions from cool and dry to warm and wet. Until ca. 10,700 cal BP, before Moraceae rainforest became dominant, cool and dry conditions were associated with low or shallow erosion, while warm and wet conditions with enhanced or more deeply incised erosion (Fig. 8). With the mass expansion of rainforest, the erosion declined.

The response curves (GAMs; Figs. 7, S2, S3) of Afromontane taxa such as *Podocarpus*, *Macaranga* and *Olea* provide evidence that these taxa were advantaged by warm conditions and responded positively to high moisture availability. The rainforest and riverine forest taxa (Moraceae and *Urera*-type) responded similarly. In contrast, Afromontane *Juniperus* was favoured by drier and cooler conditions, similar to savanna taxa such as Poaceae and Amaranthaceae. Moraceae and *Olea* responded most positively to warming, while grasses (Poaceae, Cyperaceae) benefitted mostly from cool conditions. In contrast to the generally positive response to temperature, Moraceae and *Olea* were advantaged by moister conditions only until a certain level, after which they started to decline. Poaceae and Amaranthaceae were strongly advantaged by drier conditions.

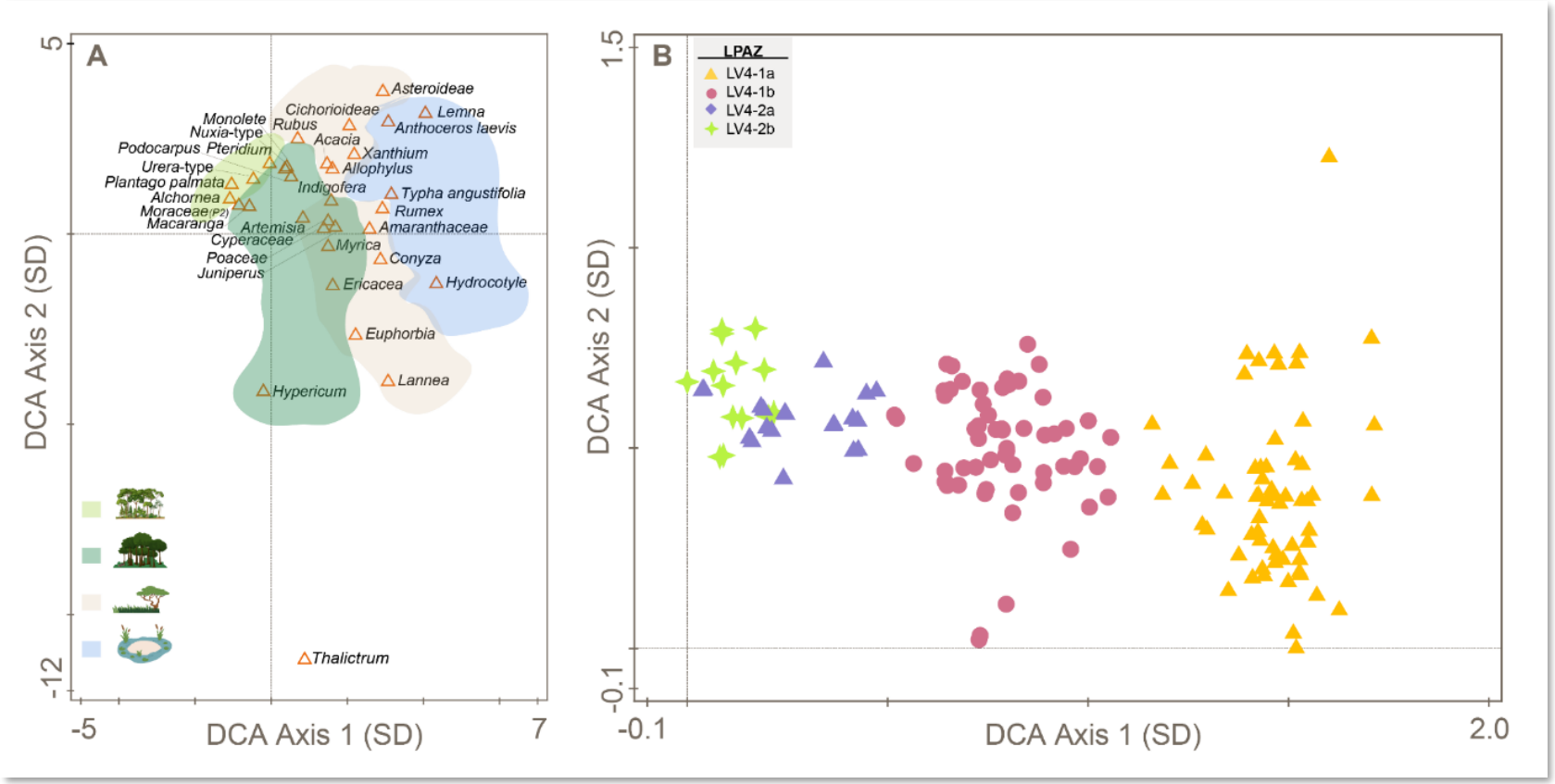

Figure 6. *(A) Detrended Correspondence Analysis (DCA) scatterplots of species, and (B) samples scores. In (A) the scatter of species scores along DCA Axis 1 (21.07 % of variance) indicates a gradient of temperature and moisture, with taxa associated with lower lake levels, dry and cold environments (e.g. Typha, Lemna, Amaranthaceae, Asteroideae) with high scores and those associated with warm, moist, and forested environments (e.g. Moraceae, Macaranga, Alchornea) with low scores: Species scores along axis 2 (4.04 % of variance) suggest a weak gradient between eroding shale habitats (e.g. Thalictrum, Hypericum, Lannea, Euphorbia, low scores) and more stable landscapes (e.g. Asteroideae, Lemna, Acacia-type, high scores). The shaded area represents the main different biomes: Aquatic (light blue), Savanna (light brown), Afromontane (dark green), Rainforest (light green). In (B) the samples are grouped according to the local pollen assemblage zones (LPAZ).*

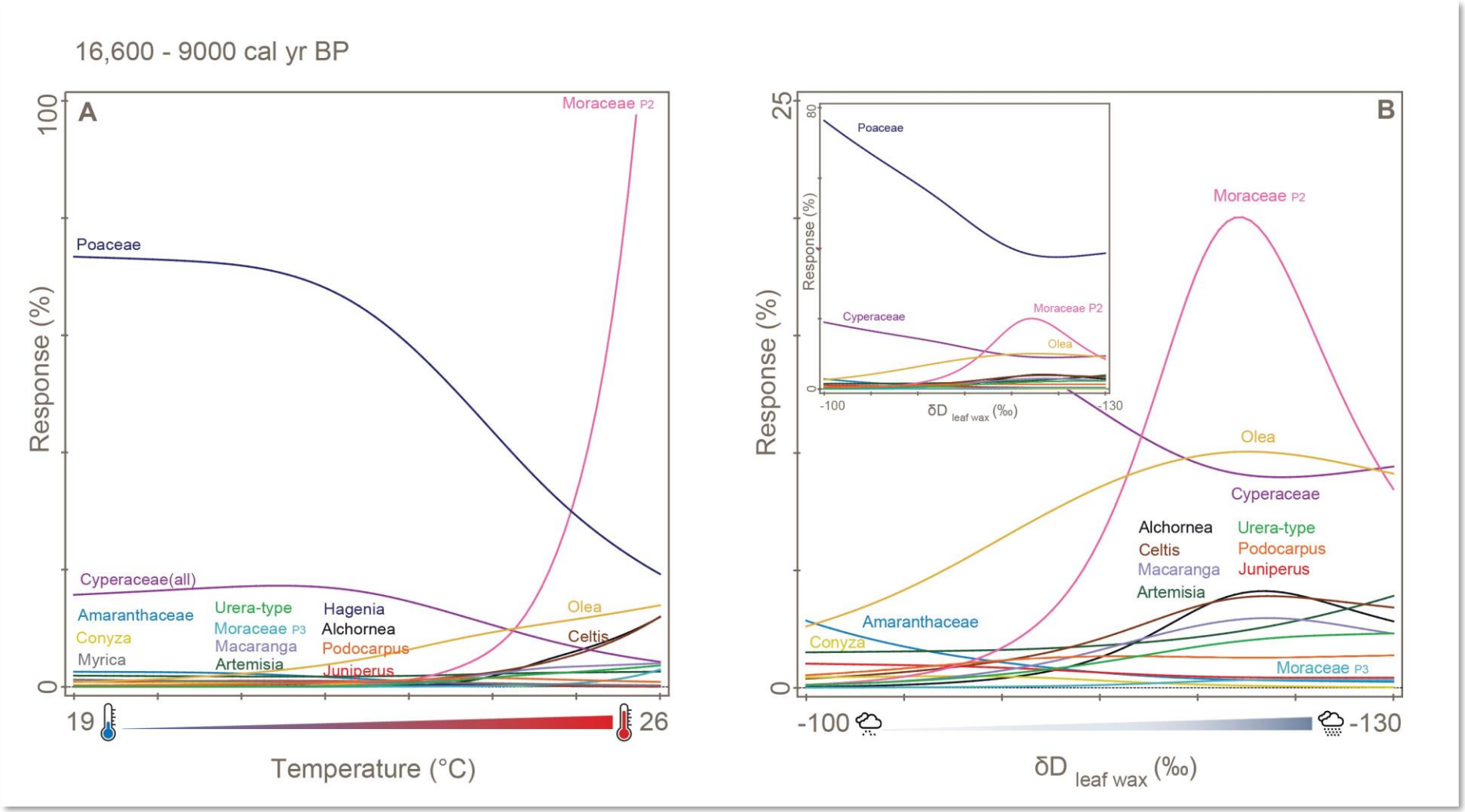

Figure 7. Response curves of the main taxa in the pollen record to: (A) Temperature in °C inferred from TEX_{86} using Kim et al. (2010) calibration, Berke et al. 2012), (B) $\delta D_{leaf\ wax}$ used as a proxy of rainfall amount (Berke et al. 2012), more negative values indicate more rainfall. The smaller image shows a zoom-out of the response curves to illustrate the dominant response of Poaceae. Fitted using General Additive Models (GAM).

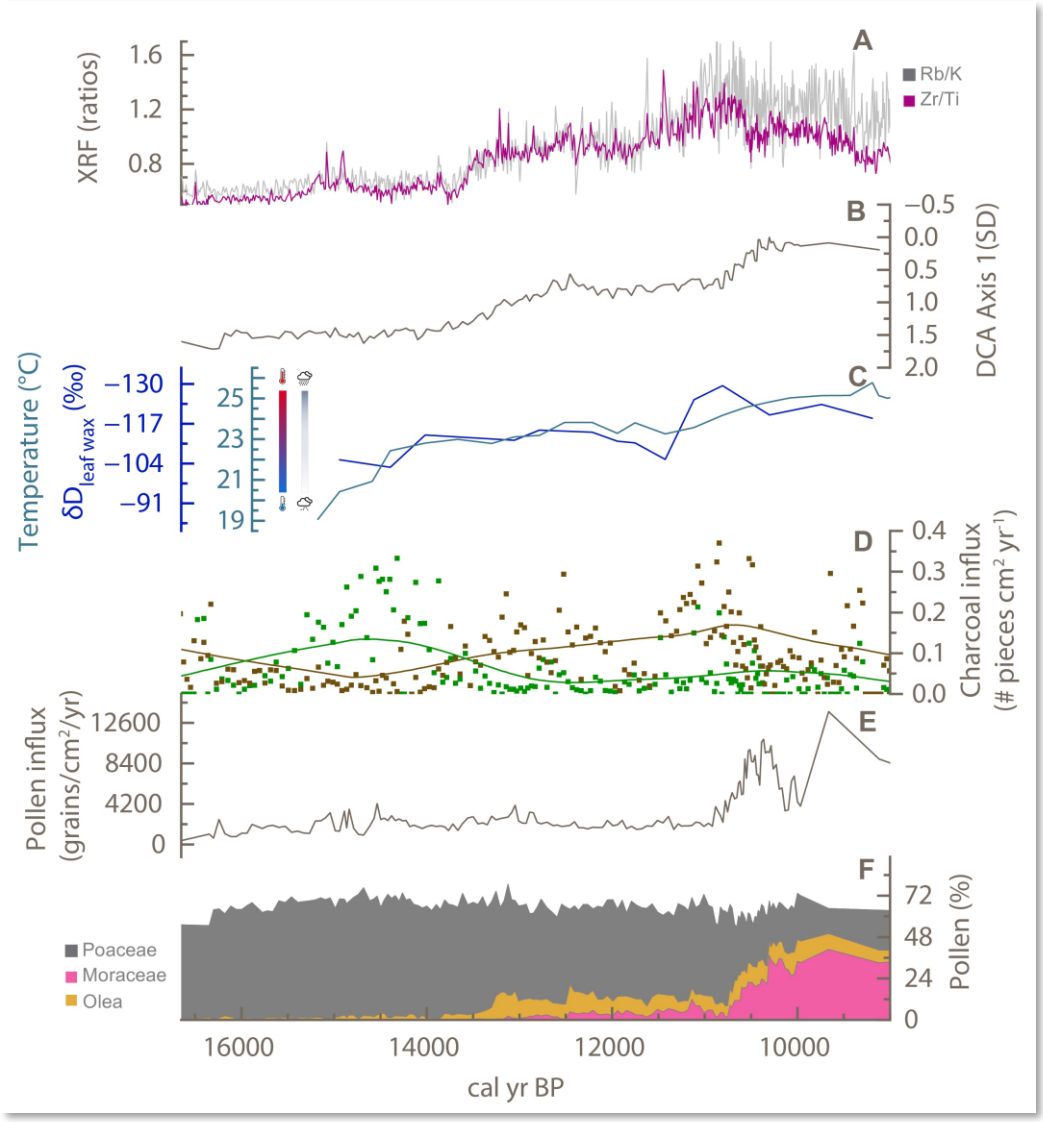

Figure 8. (A) XRF ratio record of Rb/K (Wienhues et al. submitted) indicating chemical weathering, and Zr/Ti as grain size proxy in Lake Victoria. (B) DCA Axis 1of the LV4 pollen record from 16,600 to 9000 cal yr BP. (C) Temperature (light blue) and moisture (dark blue) proxies, temperature in °C inferred from TEX_{86} using the calibration of Kim et al. (2010) according to $\delta D_{leaf\ wax}$ record of Lake Victoria from Berke et al. (2012), more negative values indicate more rainfall. (D) Macro charcoal record, the dots represent the herbs charcoal influx (green) and the woody charcoal influx (brown). The brown (woody) and the green (herbs) continuous line indicates a trend line based on LOWESS smoothing used only for visualization purposes. (E) Total terrestrial pollen influx of Lake Victoria (LV4). (F) Pollen percentages of the most dominant species in each ecosystem type.

3.5 Discussion

3.5.1 Causes of Vegetation Dynamics in the Latest Pleistocene

During the latest Pleistocene at around ca. 19,000 cal yr BP (Hughes et al., 2013; Lang et al., 2023), dry and cool conditions prevailed across East Africa over a range of elevations, from the summit of Mt. Kilimanjaro (Schüler et al., 2012) to intermediate and low altitudes such as at Lake Albert (Berke et al., 2014), Lake Tanganyika (Vincens et al., 1993) and Lake

Victoria (Berke et al., 2012). Later, the southward shift of the Afrotropical rainbelt and reorganization of the monsoon circulation, in combination with a weakening of regional rainfall systems at ca. 17,000 cal yr BP, altered the climate at lower elevation sites causing aridity, which played an important role at several sites in tropical Africa at that time (Stager et al., 2011). In the Lake Victoria area, Afromontane taxa requiring warm-temperate (or subtropical) and rather moist conditions, such as *Podocarpus*, *Olea* and *Myrica* formed isolated stands at the start of our vegetational record at ca. 16,600 cal BP. Likely, at intermediate altitudes, the grassland savanna dominated the landscape (Figs. 3 and 4). Our record starts with the occurrence of Afromontane and savanna vegetation (Fig. S1) until temperatures started to gradually rise by ca. 2°C before 15,500 cal yr BP in eastern Africa (Berke et al., 2012), as also documented in other regions such as the Mediterranean realm (Samartin et al., 2012) and in Europe north of the Alps (Bolland et al., 2020), where warming at around 16,000 cal BP was associated with the end of Heinrich event 1. In our study area, warming probably induced ecosystem changes such as the increased likelihood of grassland-savanna fire events at around 16,000-15,500 (Figs. 3, 4 and 7D). In agreement, Polycyclic Aromatic Hydrocarbons (PAH) show that biomass burning at this time was dominated by angiosperms in the Lake Victoria area (Karp et al., 2023), supporting our evidence of increased burning in herb-dominated savanna ecosystems. It is likely that during this time, *Conyza* benefited from fire spreads because of its resistance to disturbance (Schüler & Hemp, 2016) and could, therefore, spread in the savanna (Figs. 3 and 4). Our findings also indicate the occurrence of tree and/or shrub stands of *Acacia*-type, *Combretum*, *Indigofera* and *Lannea* in the grassland-savanna which was dominated by herbaceous taxa such as Poaceae, Cyperaceae, *Artemisia* and Amaranthaceae.

At Lake Masoko, ca. 700 km south of Lake Victoria, an expansion of semi-deciduous forests took place between 16,000 and 14,000 cal yr BP (Vincens et al., 2007) when precipitation was rather high. It is conceivable that warmer and/or moister conditions caused the minor increase of *Olea* abundances at Lake Victoria around 15,000 cal yr BP (Figs. 3, 4 and 7F). However, in addition to higher temperatures (Berke et al., 2012), precipitation regimes must have varied significantly given that some lakes in eastern Africa started to dry out approximately at 15,000 cal yr BP (Lézine, 2007). Indeed, afforestation was interrupted ca. 200 km north-west of Lake Victoria at Lake Albert and further west in western Africa at Lake

Bosumtwi (Bonnefille & Riollet, 1988) and herb taxa re-expanded in the surroundings of Lake Magadi ca. 250 km south-east of Lake Victoria (Elmoutaki, 1994).

Afromontane *Olea* spread at ca. 13,250 cal. yr BP (Figs. 3, 4 and 7F). While drought-adapted trees and shrubs such as *Acacia*-type, *Combretum*, *Indigofera* and *Lannea* declined, the thicketed clumps such as Syzygium, Scutia, Grewia, *Trema*, Allophylus and Croton expanded in the savanna (Fig. S1). This vegetation shift likely promoted diverse microclimates within the savanna, which helped among others, to retain water and provide habitat for pollinators. The expansion of *Olea* was followed by other Afromontane trees such as *Podocarpus*, *Celtis* and *Macaranga*, the latter preferring swamp forest habitats (Beuning, 1999). Our results also show that the savanna herbs contracted slightly, while rainforest taxa such as Moraceae, *Acalypha* and *Alchornea* benefitted, probably forming gallery forests along streams. Indeed, the lake levels of Lake Victoria rose between 14,000 and 13,600 cal yr BP (Wienhues et al. submitted), suggesting that moisture availability increased. About 300 km south of Lake Victoria, the Miombo flora diversified around Lake Tanganyika, promoting diversity in the savanna with more moisture-loving plants (Vincens, 1991).

The latest Pleistocene increase of Afromontane pollen has led to debates about long-distance transport (e.g. Beuning, 1999; Kendall, 1969; Ssemmanda & Vincens, 2018). At Lake Victoria the increase of Afromontane pollen is recorded at all coring sites, and over long distances (e.g. LV4 in Temoltzin-Loranca et al. 2023 vs. P2 in Kendall, 1969, and V95-2P, in Beuning, 1999). Therefore, it is likely that the expansion of Afromontane vegetation at around 13,250 cal yr BP occurred in the entire Lake Victoria catchment. Moreover, we propose that due to cooler conditions, the Afromontane stands were growing at lower altitudes and closer to the lake shore than today (Temoltzin-Loranca et al. 2023).

Between ca. 12,800-11,700 cal yr BP water tables dropped at several lakes in East Africa, suggesting arid conditions (Roberts et al., 1993). However, hydroclimatic reconstructions indicate that this was not the case at Lake Victoria (Castañeda et al., 2016; Overpeck et al., 1996). Forest cover remained comparable to the preceding period, when arboreal pollen (AP) reached ca. 20-25%, while pollen influx slightly declined (Fig. 7E). At this time, our data point to minor expansions of rainforest taxa (e.g., Moraceae, *Alchornea*), which occurred at the expenses of Afromontane *Olea* but not *Podocarpus* (Figs. 3, 4 and S1). Such a

vegetation response would require a minor warming and/or moisture increase, which is indeed recorded in the Lake Victoria palaeoclimatic proxies (Berke et al., 2012, see Figs. 3 and 4).

Increasing moisture during the latest Pleistocene prompted changes in aquatic plant communities. Kendall (1969) had already noticed an increase in *Nymphaea* at ca. 14,500 cal yr BP, interpreting it as a change of water chemistry, probably in pH, resulting from more diluted conditions. This finding agrees well with the inference of a continuous water table rise at Lake Victoria (Temoltzin-Loranca et al., 2023; Wienhues, et al. submitted). Our new macrophyte pollen record refines this notion and suggests that *Nymphaea caerulea* and *Nymphaea lotus* formed stands rather close to the coring site, together with other macrophytes such as *Lemna* and *Potamogeton* during the period 16,600-13,800 cal yr BP, when lake-levels were lower than today (Wienhues et al. submitted). Macrophyte populations may have grown next to the *Typha* reed belt, which is unambiguously documented by pollen percentages reaching 2-15 % from 16,600-13,800 cal yr BP. After 13,800 cal yr BP aquatics completely disappeared locally and *Typha* declined massively at Lake Victoria, as also documented by Beuning et al. (1999).

In sum, during the period 16,600 - 11,500 cal yr BP, prior to the onset of the Holocene, the Lake Victoria basin was characterized by gradually increasing temperatures and precipitation. The grassy savanna was converted into a woodland savanna, and subtropical or warm-temperate Afromontane species became more prominent at lower elevations together with rare first gallery or rainforest patches. Fires occurred regularly throughout the period, with a change in biomass burnt at around 13,800 cal BP, from a grass-dominated fuel type during the earliest part of the period to a woody-dominated fuel type after this period.

3.5.2 Biome Reorganizations During the Holocene AHP

Increases in temperatures and moisture were likely caused by the strengthening of the East African Monsoon activity, towards the onset of the Holocene (Tierney, et al., 2011). During the Holocene AHP, monsoon activity was higher across East Africa (Dallmeyer et al., 2020; Liu et al., 2017), inducing more mesic conditions. Enhanced trade wind circulation and moisture increase led to two sharp peaks of pollen influx in tropical Africa (Lézine, 1998) as also observed in our record (Fig. 7). At Lake Victoria, increases in temperature and precipitation caused a rapid transformation from savanna to rainforest, while Afromontane vegetation remained

rather stable, probably moving to higher altitudes (Kendall, 1969; Temoltzin-Loranca et al., 2023).

Previous studies in Lake Victoria discussed the timing of the spread of the rainforest. For instance, in V95-2P (Beuning, 1999), an initial phase was recognized in the Late Pleistocene (11,200 ^{14}C yr BP, ca. 13,100 cal yr BP), after which a discontinuity attributed to a hiatus in sedimentation occurred, preventing any more detailed assessment. In this study (LV4, Figs. 2 and 3) we show that, after an initial spread at the earliest Holocene, the main rainforest expansion to > 20% occurred at ca. 10,700 –10,500 cal yr BP (Fig. 5). This finding is supported by three other sedimentary records with independent chronologies: LV1, LV2; (Temoltzin-Loranca et al. 2023), and by the core P2 (Kendall, 1969), where the rainforest expansion is dated at ca. 9500 ^{14}C yr BP, corresponding to 10,900 cal yr BP.

The climatic change was more abrupt during the Early Holocene than during the latest Pleistocene, with precipitation increasing more rapidly than the temperature at ca. 11,500-10,700 cal yr BP. (Figs. 3, 5, and 7). Concurrently, a simultaneous rise in biomass burning accompanied the biome reorganization (Fig. S1). Specifically, at ca. 11,700–11,100 cal yr BP Moraceae increased from ca. 3-5% (at the end of the Younger Dryas), to ca. 5-10% during the Early Holocene. The first Moraceae peak of >10 % occurred at ca. 11,200 cal yr BP, when precipitation peaked (Fig. 5). When Moraceae expanded more massively at ca. 10,700 cal yr BP, the Afromontane vegetation spread as well. This spread of the rainforest and Afromontane plants is congruent with similar dynamics at other sites in the region, displaying expansions of Afromontane (mainly *Olea*), and pioneer forest taxa (*Alchornea*, *Macaranga*; Lézine, 2007). At Lake Victoria, drought adapted *Combretum* shrublands collapsed, giving rise to *Trema* trees/shrubs. Moreover, increased rainfall promoted the establishment of forest taxa which appeared for the first time in the pollen record such as *Tetrorchidium* and *Musanga*. While the first one is well adapted to moist conditions in the understories, the latter is well known for adapting in nutrient-poor or disturbed areas (Akinnifesi et al., 2010; De Caluwé & De Smedt, 2005; Vincens, 1991). Kendall (1969) suspected a misidentification of *Musanga* pollen, causing a spurious peak; however, in our record, we observe the same increase at the same time, so we can infer that its expansion, together with that of *Urera*-type, was real. It is plausible that, as an effect of the forest closing, fire occurrence decreased between 10,500 and 9700 cal yr BP.

Later at ca. 10,300 cal yr BP, when high rainfall stabilized (Figs. 5 and 7, Berke et al. 2012), savanna-herb patches, composed of Poaceae and Amaranthaceae, started to shrink in response to moister environments and Moraceae flourished (Fig. S1). Similarly, and contemporaneously, at higher elevations in Mt. Kilimanjaro (Schüler et al., 2012), warmer and wetter conditions than today were recorded, allowing the expansion of Afromontane and Ericaceous vegetation at the expense of grasslands. Wetter and warmer conditions promoted biomass production, and thus, fuels that intensified burning, this time mainly of woody species (Figs. 3 and 7D). The new high-resolution evidence is in agreement with previous studies (e.g. Temoltzin Loranca et al. 2023; Karp et al., 2023) that emphasized the role of vegetation for fire incidence. Cross correlations (see Supplementary material and Fig. S5) suggest that fire had a significant impact on some plant taxa during the Early Holocene. For instance, *Olea* and *Trema* were reduced, while *Grewia*, *Myrica* and Ericaceae increased in response to burning (Fig. S5). Similar vegetational patterns in response to fire emerged during the latest Pleistocene, with fire-induced reductions of *Trema* and increases of *Grewia* during the period 16,600-12,000 cal yr BP (Fig. S5).

Overall, during the Holocene AHP, temperature and precipitation increased. We propose that the increase of moisture played a major role if compared to the latest Pleistocene, during which temperature changes were probably more important for vegetational reorganizations. Increasing Holocene moisture triggered the transformation of the savanna to the rainforest at lower altitudes and released the expansion of Afromontane vegetation at higher elevations, at or above the altitudinal positions observed today.

3.6 CONCLUSIONS

Our record provides detailed evidence of major shifts in vegetation. We assume that during the latest Pleistocene and the Early Holocene, vegetation was in dynamic equilibrium with climate, as illustrated by the response curves of plant taxa to climatic change (Fig. 8). Specifically, our response analyses show that, over the entire study period (16,600-9000 cal yr BP), warm and/or humid conditions favoured both Afromontane and rainforest communities (Fig. 8). Conversely, cooler or drier periods were associated with savanna grassland vegetation. Even minor changes in temperature and/or precipitation likely induced vegetation shifts, arguing for the high climate sensitivity of tropical and Afromontane vegetation. Fire regime

changed also according to climate and vegetation, acting as a co-driver in the ecosystem dynamics.

Our newly obtained high-resolution record provides insights into the environmental conditions characterized by shifts attributed to natural climatic changes, in which alterations of vegetation composition and structure took place, with moisture fluctuations likely acting as the primary driving force to cause complete biome reorganizations in the area. The high sensitivity of natural ecosystems illustrated here may be used to assess the magnitude and rate of future vegetation responses to warmer and/or moister climate conditions, especially where vegetation conditions are still close to natural. Investigating the subsequent Mid and Late Holocene periods with enough temporal resolution, in combination with the effects of changes in land use, could provide more insights to better assess the human-caused fragmentation of ecosystems.

3.7 SUPPLEMENTARY MATERIAL

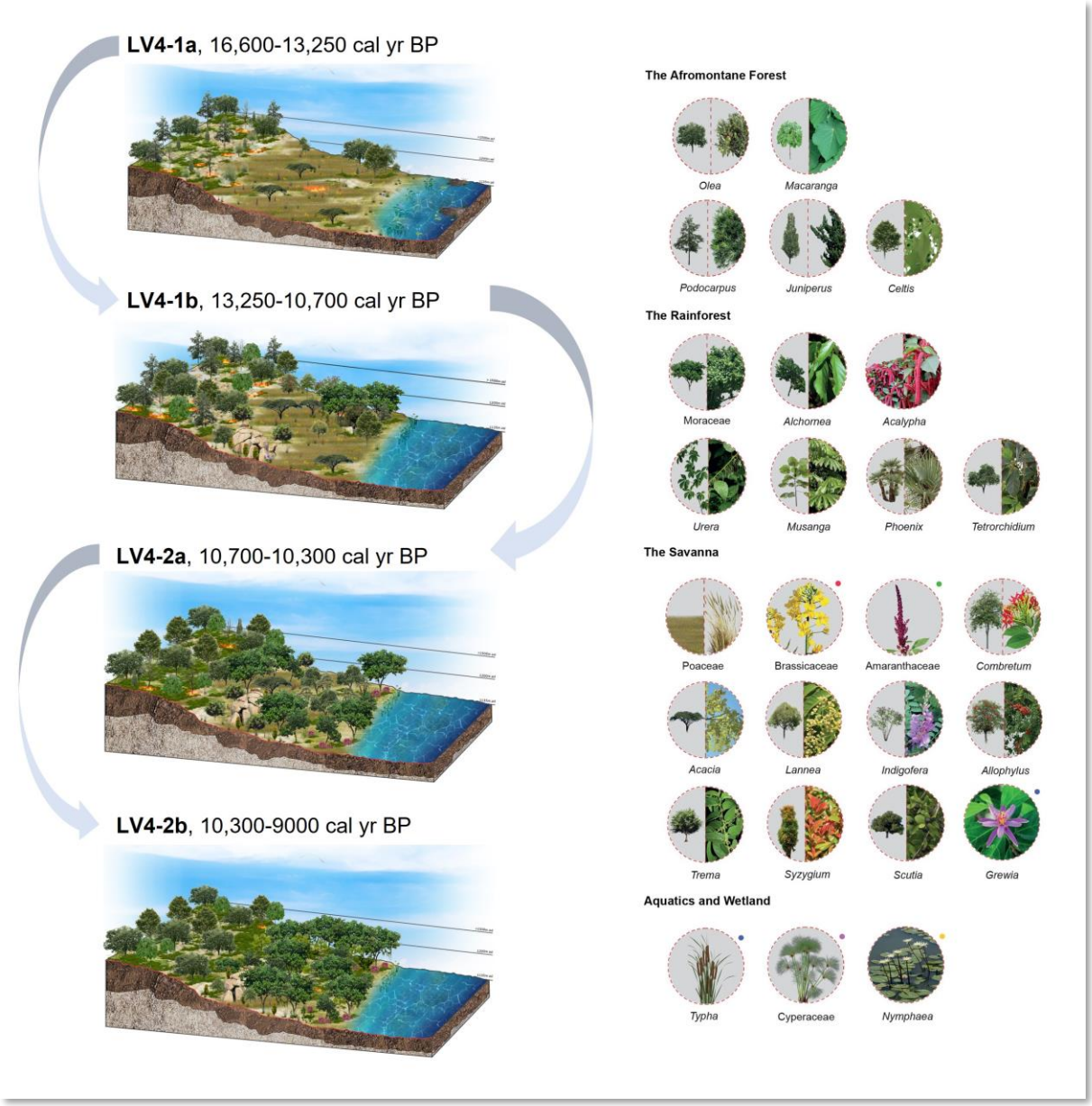

Figure S1. Illustrative palaeoecological reconstruction from 16,600 to 9000 cal yr BP, taking into account the 4 significant Local Pollen Assemblage Zones (LPAZ). The images show some of the most important plant genera/families, which are shown more in detail on the right side.

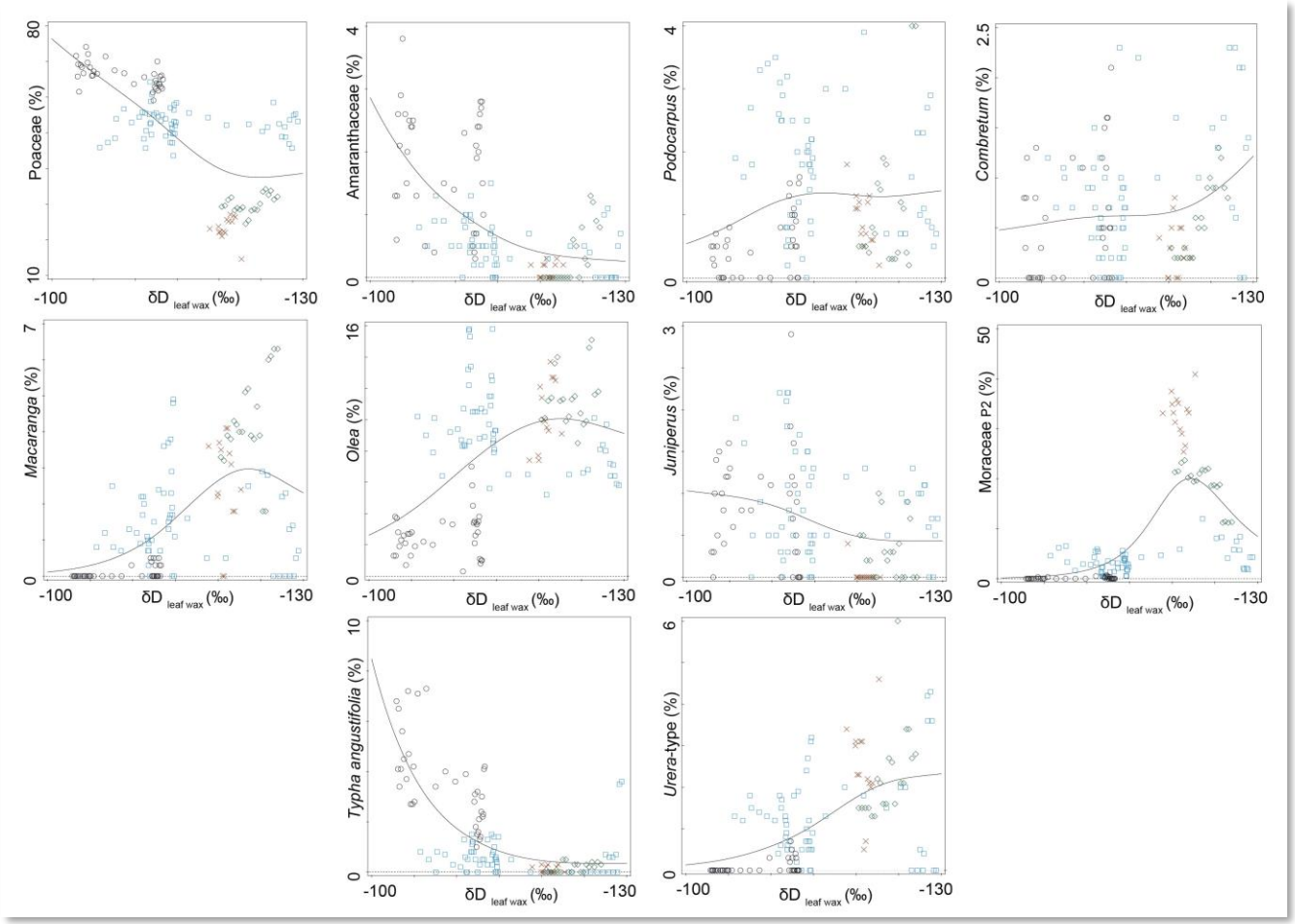

Figure S2. Response curves of selected taxa of the pollen record from Lake Victoria (LV4) to δD $_{leaf\ wax}$ used as a proxy of rainfall amount (Berke et al. 2012), more negative values indicate more rainfall. Fitted using General Additive Models (GAM).

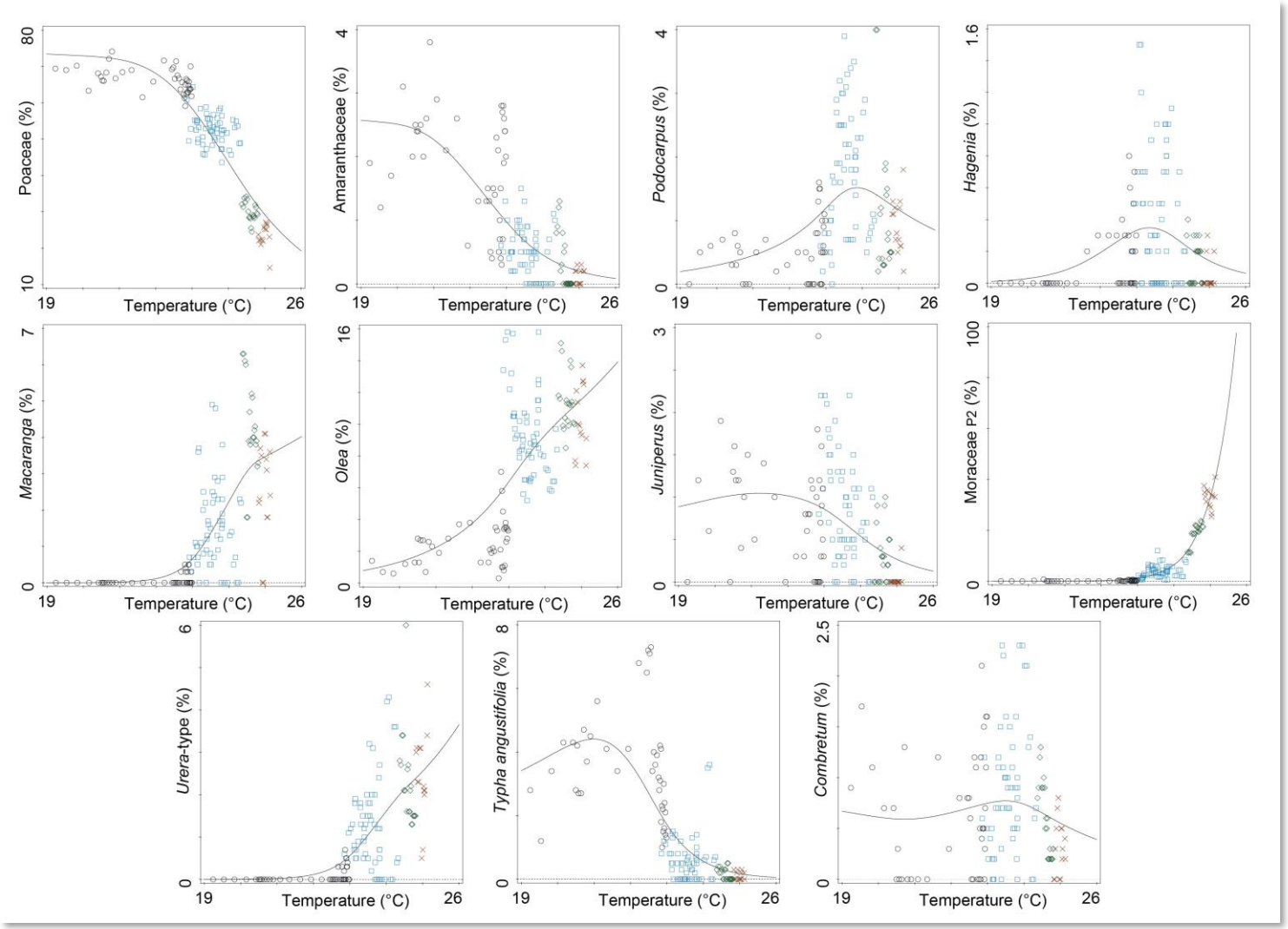

Figure S3. Response curves of selected taxa of the pollen record from Lake Victoria (LV4) to Temperature inferred from TEX_{86} using Kim et al. (2010) calibration, fitted using General Additive Models (GAM).

3.7.1 CROSS-CORRELATION ANALYSES

To analyse lead-lag effects between fire and vegetation, we used cross-correlation analyses using Origin Pro 2023 (OriginLab Corporation, 2023). The time window between 16,600 and 12,000 presents an interval sample age of 53 ± 11 calibrated years, whereas between 12,000 and 9,000, theinterval sample age is 33 ± 13 calibrated years. The charcoal influx was compared with pollen percentages to avoid spurious effects (Colombaroli et al., 2007; Tinner et al., 1999). Results indicated that, from 16,600 to 12,000 cal yr BP (Fig. S4) under drier and colder conditions, charcoal has a significant positive correlation with Grewia and Myrica but a negative correlation with Trema, Podocarpus, Xanthium, Myrica and, especially at lag 0, with Ericaceae. From 12,000 to 9,000 cal yr BP (Fig. S5) under wetter and warmer conditions, charcoal has a significant positive correlation with Lannea, Grewia, Podocarpus, Ericaceae, Xanthium and Myrica but a negative correlation with Trema, Olea, Tetrorchidium, Alchornea and Macaranga.

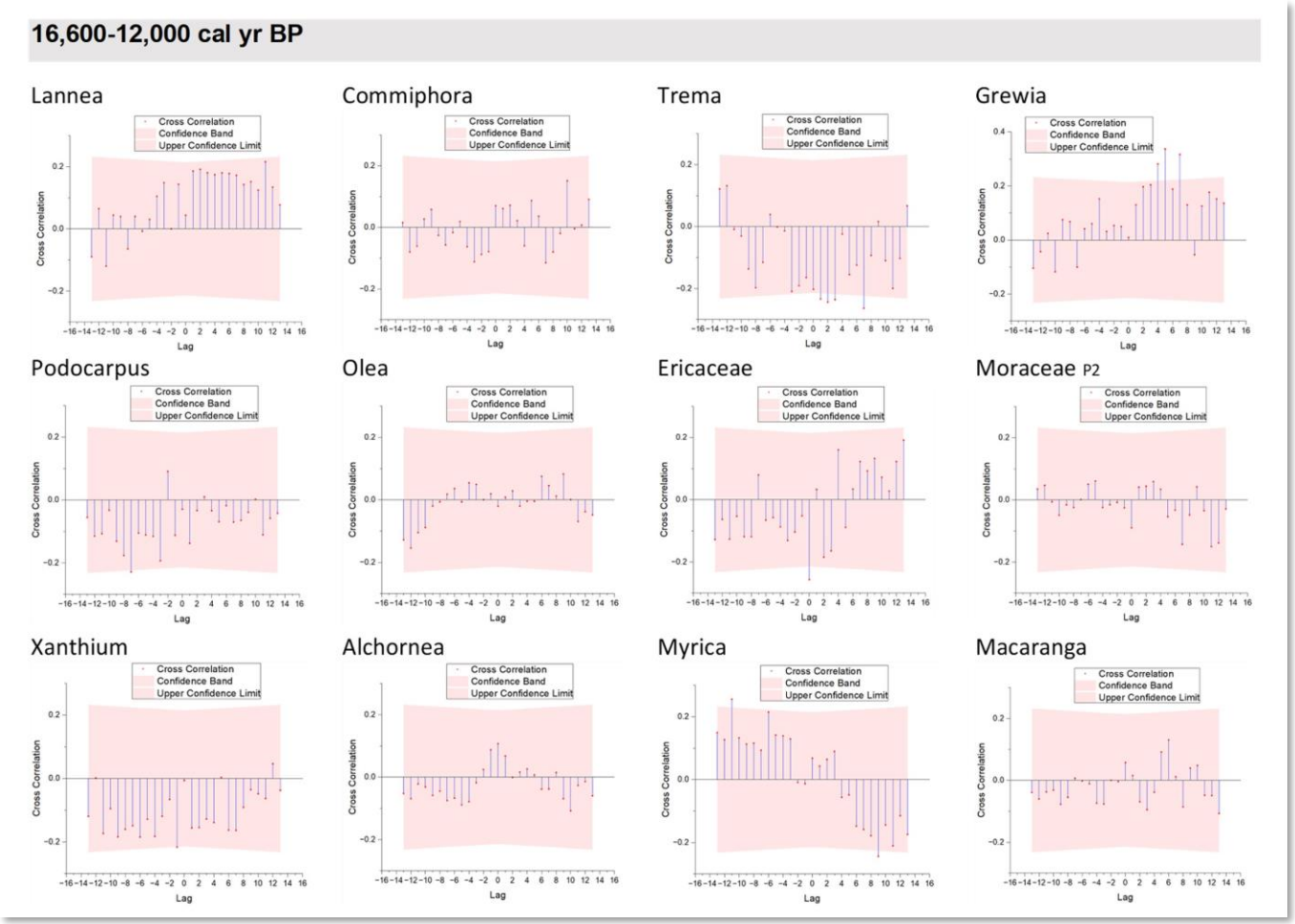

Figure S4. Cross-correlation analysis of macroscopic charcoal influx vs. selected pollen taxa from 16,600 to 12,000 cal yr BP. 1 Lag=56 years. Vertical axes show correlation coefficients; those outside the red area are significant at p=0.05

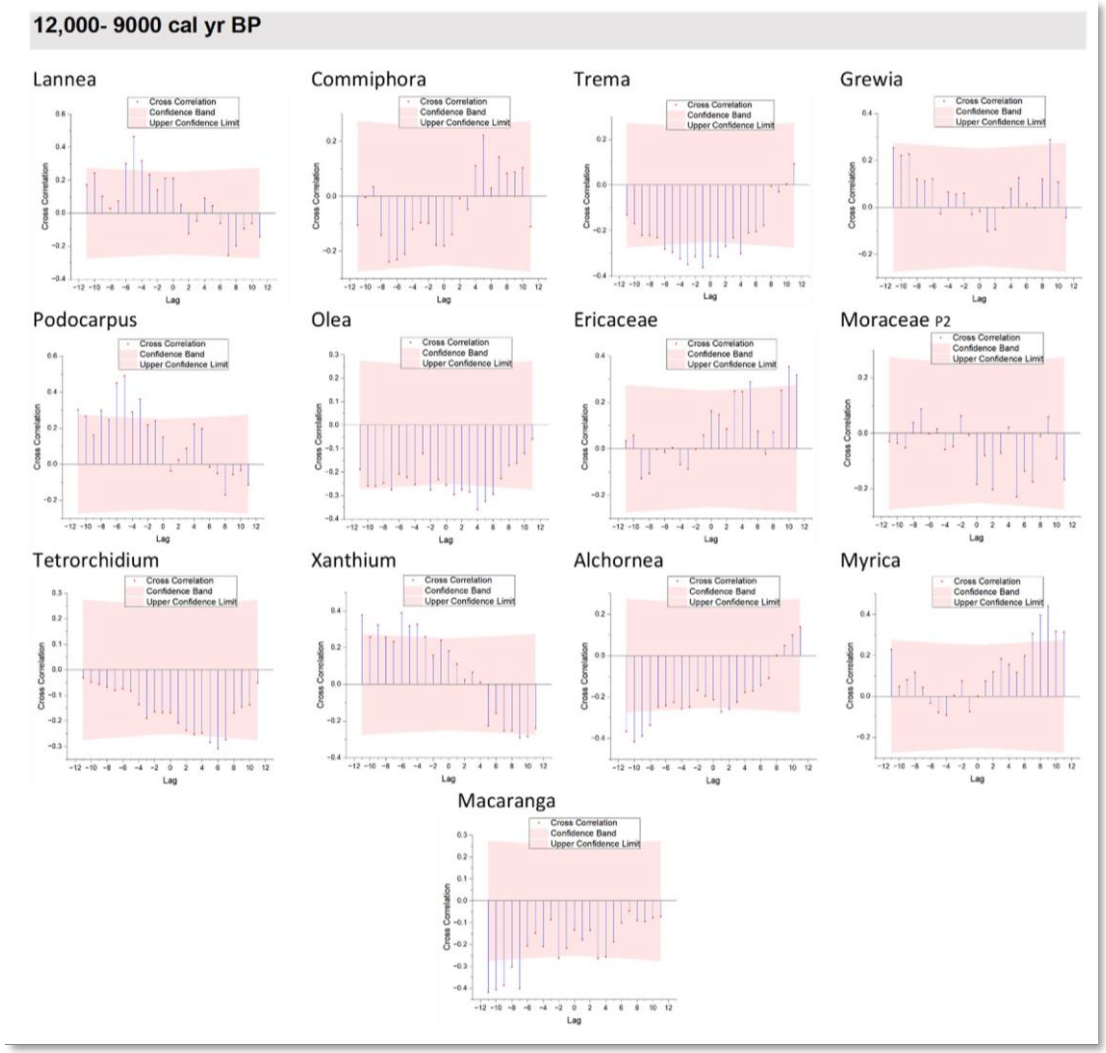

Figure S5. Cross-correlation analysis of macroscopic charcoal influx vs. selected taxa from 12,000 to 9000 cal yr BP. 1 Lag=33 years. Vertical axes show correlation coefficients; those outside the red area are significant at p=0.05

Acknowledgements

The authors Yunuén Temoltzin–Loranca, Giulia Wienhues, and Moritz Muschick were supported by SNSF Sinergia grant number 183566 awarded to Ole Seehausen, Martin Grosjean, Tom Gilbert, and Blake Matthews. The coring expedition was made possible by means of the strategic pool of the Faculty of Natural Sciences of University of Bern awarded to Ole Seehausen, Anna Sapfo Malaspinas, Willy Tinner, Oliver Heiri, Martin Grosjean and Flavio Anselmetti. We gratefully acknowledge the coring leaders Petra Boltshauser-Kaltenrieder, Moritz Muschick, Salome Mwaiko, and Willi Tanner and the coring team members Sandra Brügger and Alexander Bolland. We are deeply indebted to TAFIRI for all the logistic support during the campaigns in Tanzania. This research was supported by TAFIRI and conducted under COSTECH research permit No. 2018-237-NA-2018-57. We thank Josephat Kalugasha from the University of Daar Es Salaam for his careful guidance in the field for identifying the flora. Assistance in Arusha, Kilimanjaro and Mwanza provided by Joshua Mokoz, Elias Stanley and Charles Michael James is greatly appreciated.

References

Akinnifesi, F. K., Ajayi, O. C., Sileshi, G. W., Chakeredza, S., Mng'omba, S., & Kwesiga, F. (2010). Domesticating priority non-timber tree species as a response to food insecurity and climate change in sub-Saharan Africa. Forests, Trees and Livelihoods, 19(2), 107–136.

Allen, K. E., Tapondjou, W. P., Freeman, B., Cooper, J. C., Brown, R. M., & Peterson, A. T. (2021). Modelling potential Pleistocene habitat corridors between Afromontane forest regions. Biodiversity and Conservation, 30(8–9), 2361–2375. https://doi.org/10.1007/s10531-021-02198-4

Bekele, T. (1993). Bekele, T. (1993). Vegetation ecology of remnant Afromontane forests on the central plateau of Shewa, Ethiopia. (Vol. 79). Sv. växtgeografiska sällsk.

Berke, M. A., Johnson, T. C., Werne, J. P., Grice, K., Schouten, S., & Sinninghe Damsté, J. S. (2012). Molecular records of climate variability and vegetation response since the Late Pleistocene in the Lake Victoria basin, East Africa. Quaternary Science Reviews, 55, 59–74. https://doi.org/10.1016/j.quascirev.2012.08.014

Berke, M. A., Johnson, T. C., Werne, J. P., Livingstone, D. A., Grice, K., Schouten, S., & Sinninghe Damsté, J. S. (2014). Characterization of the last deglacial transition in tropical East Africa: Insights from Lake Albert. Palaeogeography, Palaeoclimatology, Palaeoecology, 409, 1–8. https://doi.org/10.1016/J.PALAEO.2014.04.014

Beuning, K. R. M. (1999). A re-evaluation of the Late Glacial and Early Holocene vegetation history of the Lake Victoria region, East Africa. In E. M. van Zinderen Bakker & K. Heine (Eds.), Palaeoecology of Africa and the Surrounding Islands (First, pp. 115–136). Routledge.

Beuning, K. R. M., Kelts, K., Ito, E., & Johnson, T. C. (1997). Paleohydrology of Lake Victoria, East Africa, inferred from18O/16O ratios in sediment cellulose. Geology, 25(12), 1083–1086.

Bolland, A., Rey, F., Gobet, E., Tinner, W., & Heiri, O. (2020). Summer temperature development 18,000–14,000 cal. BP recorded by a new chironomid record from Burgäschisee, Swiss Plateau. Quaternary Science Reviews, 243, 106484. https://doi.org/10.1016/j.quascirev.2020.106484

Bonnefille, R., & Riollet, G. (1988). The Kashiru Pollen Sequence (Burundi) Palaeoclimatic Implications for the Last 40,000 yr B.P. in Tropical Africa. Quaternary Research, 30(1), 19–35. https://doi.org/10.1016/0033-5894(88)90085-3

Castañeda, I. S., Schouten, S., Pätzold, J., Lucassen, F., Kasemann, S., Kuhlmann, H., & Schefuß, E. (2016). Hydroclimate variability in the Nile River Basin during the past 28,000 years. Earth and Planetary Science Letters, 438, 47–56. https://doi.org/10.1016/j.epsl.2015.12.014

Chapman, L. J., Chapman, C. A., Kaufman, L., Witte, F., & Balirwa, J. (2008). Biodiversity conservation in African inland waters: Lessons of the Lake Victoria region. SIL Proceedings, 1922-2010, 30(1), 16–34. https://doi.org/10.1080/03680770.2008.11902077

Colombaroli, D., Marchetto, A., & Tinner, W. (2007). Long-term interactions between Mediterranean climate, vegetation and fire regime at Lago di Massaciuccoli (Tuscany, Italy). Journal of Ecology, 95(4), 755–770. https://doi.org/10.1111/j.1365-2745.2007.01240.x

Colombaroli, D., Ssemmanda, I., Gelorini, V., & Verschuren, D. (2014). Contrasting long-term records of biomass burning in wet and dry savannas of equatorial East Africa. Global Change Biology, 20(9), 2903–2914. https://doi.org/10.1111/GCB.12583

Colombaroli, D., van der Plas, G., Rucina, S., & Verschuren, D. (2018). Determinants of savanna-fire dynamics in the eastern Lake Victoria catchment (western Kenya) during the last 1200 years. Quaternary International, 488, 67–80. https://doi.org/10.1016/J.QUAINT.2016.06.028

Dallmeyer, A., Claussen, M., Lorenz, S. J., & Shanahan, T. (2020). The end of the African humid period as seen by a transient comprehensive Earth system model simulation of the last 8000 years. Climate of the Past, 16(1), 117–140. https://doi.org/10.5194/cp-16-117-2020

Davies, S. J., Lamb, H. F., & Roberts, S. J. (2015). Micro-XRF core scanning in palaeolimnology: recent developments. Micro-XRF Studies of Sediment Cores: Applications of a non-destructive tool for the environmental sciences, 189-226.

De Caluwé, E., & De Smedt, S. (2005). Propagation and transplantation of Musanga cecropioides R. Brown (Moraceae) in DR Congo. Journal of Tropical Ecology, 21(6), 649–652.

De Menocal, P., Ortiz, J., Guilderson, T., Adkins, J., Sarnthein, M., Baker, L., & Yarusinsky, M. (2000). Abrupt onset and termination of the African Humid Period: Quaternary Science Reviews, 19(1–5), 347–361. https://doi.org/10.1016/S0277-3791(99)00081-5

Elmoutaki, S. (1994). Transition glaciaire-interglaciaire et Younger Dryas dans l'hémisphère sud (1°-20° Sud): analyse palynologique à haute résolution de sondages mari et continentaux (lac et marécage).

Gosling, W. D., Miller, C. S., & Livingstone, D. A. (2013). Atlas of the tropical West African pollen flora. Review of Palaeobotany and Palynology, 199, 1–135. https://doi.org/10.1016/J.REVPALBO.2013.01.003

Hamilton, S. E., McGehee, D. D., Nyamweya, C., Ongore, C., Makori, A., Mangeni-Sande, R., Kagoya, E., Kashindye, B. B., Elison, M., Shaban, S. S., Mlaponi, E., Mwainge, V. M., Ocaya, H., Krach, N., Ogari, Z., Mugeni, B., Taabu-Munyaho, A., Kayanda, R., Muhumuza, E., & Natugonza, V. (2022). High-resolution bathymetries and shorelines for the Great Lakes of

the White Nile basin. Scientific Data, 9(1), 642. https://doi.org/10.1038/s41597-022-01742-3

Hastie TJ, & Tibshirani RJ. (1990). Generalized additive models. Chapman & Hall/CRC.

Hedberg, O. (1955). Altitudinal zonation of the vegetation on the East African mountains. Proceedings of the Linnean Society of London, 165(2), 134–136. https://doi.org/10.1111/j.1095-8312.1955.tb00730.x

Hughes, P. D., Gibbard, P. L., & Ehlers, J. (2013). Timing of glaciation during the last glacial cycle: evaluating the concept of a global 'Last Glacial Maximum' (LGM). Earth-Science Reviews, 125, 171–198. https://doi.org/10.1016/j.earscirev.2013.07.003

IPCC. (2022). IPCC, 2022: Climate Change 2022: Impacts, Adaptation, and Vulnerability. Contribution of Working Group II to the Sixth Assessment Report (H.-O. Pörtner, D.C. Roberts, M. Tignor, E.S. Poloczanska, K. Mintenbeck, A. Alegría, M. Craig, S. Langsdorf, S. Löschke, V. Möller, A. Okem, & B. Rama, Eds.). Cambridge University Press.

Jensen, K., Lynch, E. A., Calcote, R., & Hotchkiss, S. C. (2007). Interpretation of charcoal morphotypes in sediments from Ferry Lake, Wisconsin, USA: Do different plant fuel sources produce distinctive charcoal morphotypes? Holocene, 17(7). https://doi.org/10.1177/0959683607082405

Karp, A. T., Uno, K. T., Berke, M. A., Russell, J. M., Scholz, C. A., Marlon, J. R., Faith, J. T., & Staver, A. C. (2023). Nonlinear rainfall effects on savanna fire activity across the African Humid Period. https://doi.org/10.1016/j.quascirev.2023.107994

Kendall, R. L. (1969). An Ecological History of the Lake Victoria Basin. Ecological Monographs, 39(2), 121–176.

Lang, G., Ammann, B., Behre, K.-E., & Tinner, W. (2023). Quaternary Vegetation Dynamics of Europe. Haupt.

Legendre, P., & Birks, H. J. B. (2012). From Classical to Canonical Ordination. https://doi.org/10.1007/978-94-007-2745-8_8

Lejju, J. B. (2012). The influence of climate change and human-induced environmental degradation on Lake Victoria. African Books Collective.

Lepš, J., & Šmilauer, P. (2003). Multivariate analysis of ecological data using CANOCO. Cambridge university press.

Lézine, A.-M. (1998). Pollen Records of Past Climate Changes in West Africa since the Last Glacial Maximum. In A. Isaar & N. Brown (Eds.), Water, Environment and Society in time of Climatic Change (pp. 295–317). Dordrecht. https://doi.org/10.1007/978-94-017-3659-6_14

Lézine, A.-M. (2007). Postglacial pollen records of Africa. In S. C. Elias (Ed.), Encyclopaedia of Quaternary Sciences (Vol. 4, pp. 2682–2698). Elsevier.

Lillesø, J.-P. B., van Breugel, P., Kindt, R., Bingham, M., Demissew, S., Dudley, C., Friis, I., Gachathi, F., Kalema, J., Mbago, F., Minani, V., Moshi, H. N., Mulumba, J., Namaganda, M., Ndangalasi, H. J., Ruffo, C., Jamnadass, R., & Graudal, L. O. V. (2011). Potential Natural Vegetation of Eastern Africa (Ethiopia, Kenya, Malawi, Rwanda, Tanzania, Uganda and Zambia).: Vol. Volume 1: The Atlas. Forest & Landscape, University of Copenhagen.

Liu, X., Rendle-Bühring, R., Kuhlmann, H., & Li, A. (2017). Two phases of the Holocene East African Humid Period: Inferred from a high-resolution geochemical record off Tanzania. Earth and Planetary Science Letters, 460, 123–134. https://doi.org/10.1016/j.epsl.2016.12.016

Luhunga, P. M., & Songoro, A. E. (2020). Analysis of Climate Change and Extreme Climatic Events in the Lake Victoria Region of Tanzania. Frontiers in Climate, 2. https://doi.org/10.3389/fclim.2020.559584

Maher, L. J. (1981). Statistics for microfossil concentration measurements employing samples spiked with marker grains. Review of Palaeobotany and Palynology, 32(2–3), 153–191. https://doi.org/10.1016/0034-6667(81)90002-6

Marchant, R., Mumbi, C., Behera, S., & Yamagata, T. (2007). The Indian Ocean dipole ? the unsung driver of climatic variability in East Africa. African Journal of Ecology, 45(1), 4–16. https://doi.org/10.1111/j.1365-2028.2006.00707.x

Moore, P. D., Webb, J. A., & Collinson M.E. (1991). Pollen Analysis (Second). Blackwell Scientific Publications.

Mucina, L., & Geldenhuys, C. J. (2016). Afrotemperate, subtropical and azonal forests. In L. Mucina & M. C. Rutherford (Eds.), The Vegetation of South Africa, Lesotho and Swaziland (Vol. 19, pp. 585–615). South African National Biodiversity Institute.

Nicholson, S. E., & Kim, J. (1997). The relationship of the El Niño–Southern Oscillation to African Rainfall. International Journal of Climatology, 17, 117–135. https://doi.org/10.1002/(SICI)1097-0088(199702)17:2

Nicholson, S. E., & Yin, X. (2001). Rainfall Conditions in Equatorial East Africa during the Nineteenth Century as Inferred from the Record of Lake Victoria. Climatic Change, 48(2/3), 387–398. https://doi.org/10.1023/A:1010736008362

Nieuwolt, S. (1979). The East African monsoons and their effects on agriculture. GeoJournal, 3, 193-200.

Odada, E. O., & Olago, D. O. (2006). The East African Great Lakes: Limnology, Palaeolimnology and Biodiversity (Vol. 12). Springer Science & Business Media.

Okungu, J. O., Njoka, S., Abuodha, J. O. Z., & Hecky, R. E. (2005). Lake Victoria Environment Report Water Quality and Ecosystem Status: Kenya National Water Quality Synthesis Report.

OriginLab Corporation. (2023). OriginPro (10.0).

Overpeck, J., Anderson, D., Trumbore, S., & Prell, W. (1996). The southwest Indian Monsoon over the last 18 000 years. Climate Dynamics, 12(3), 213–225. https://doi.org/10.1007/BF00211619

Powell, L. L., Vaz Pinto, P., Mills, M. S. L., Baptista, N. L., Costa, K., Dijkstra, K.-D. B., Gomes, A. L., Guedes, P., Júlio, T., Monadjem, A., Palmeirim, A. F., Russo, V., & Melo, M. (2023). The last Afromontane forests in Angola are threatened by fires. Nature Ecology & Evolution, 7(5), 628–629. https://doi.org/10.1038/s41559-023-02025-9

Reille, M. (1992). Pollen et spores d'Europe et d'Afrique du nord. Laboratoire de Botanique Historique et Palynologie.

Roberts, N., Taieb, M., Barker, P., Damnati, B., Icole, M., & Williamson, D. (1993). Timing of the Younger Dryas event in East Africa from lake-level changes. Nature, 366(6451), 146–148. https://doi.org/10.1038/366146a0

Roubik, D. W., & Moreno P., J. E. (1991). Pollen and spores of Barro Colorado Island [Panama].

Samartin, S., Heiri, O., Lotter, A. F., & Tinner, W. (2012). Climate warming and vegetation response after Heinrich event 1 (16 700–16 000 cal yr BP) in Europe south of the Alps. Climate of the Past, 8(6), 1913–1927. https://doi.org/10.5194/cp-8-1913-2012

Sayer, C. A., Máiz-Tomé, L., & Darwall, W. R. T. (2018). Freshwater biodiversity in the Lake Victoria Basin: Guidance for species conservation, site protection, climate resilience and sustainable livelihoods. IUCN, International Union for Conservation of Nature. https://doi.org/10.2305/IUCN.CH.2018.RA.2.en

Schüler, L., & Hemp, A. (2016). Atlas of pollen and spores and their parent taxa of Mt Kilimanjaro and tropical East Africa. Quaternary International, 425, 301–386. https://doi.org/10.1016/J.QUAINT.2016.07.038

Schüler, L., Hemp, A., Zech, W., & Behling, H. (2012). Vegetation, climate and fire-dynamics in East Africa inferred from the Maundi crater pollen record from Mt Kilimanjaro during the last glacial-interglacial cycle. Quaternary Science Reviews, 39, 1–13. https://doi.org/10.1016/j.quascirev.2012.02.003

Shanahan, T. M., McKay, N. P., Hughen, K. A., Overpeck, J. T., Otto-Bliesner, B., Heil, C. W., King, J., Scholz, C. A., & Peck, J. (2015). The time-transgressive termination of the African Humid Period. Nature Geoscience, 8(2), 140–144. https://doi.org/10.1038/ngeo2329

Šmilauer, P., & Lepš, J. (2014). Multivariate analysis of ecological data using CANOCO 5. Cambridge University Press.

Ssemmanda, I., & Vincens, A. (1993). Végétation et climat dans le bassin du lac Albert (Ouganda, Zaïre) depuis 13000 ans BP: Apport de la palynologie. Comptes Rendus de l'Académie Des Sciences. Série 2, Mécanique, Physique, Chimie, Sciences de l'univers, Sciences de La Terre, 4(316), 561–567.

Ssemmanda, I., & Vincens, A. (2002). Vegetation changes and their climatic implications for the Lake Victoria region during the late Holocene. In The East African Great Lakes: Limnology, Palaeolimnology and Biodiversity (pp. 509–523).

Ssemmanda, I., & Vincens, A. (2018). Preliminary pollen record from the deep waters of Lake Victoria (East Africa). In Palaeoecology of Africa and the Surrounding Islands (pp. 137–145). Routledge.

Stager, J. C., Ryves, D. B., Chase, B. M., & Pausata, F. S. R. (2011). Catastrophic drought in the Afro-Asian monsoon region during Heinrich event 1. Science, 331(6022), 1299–1302. https://doi.org/10.1126/science.1198322

Stockmarr, J. (1971). Tablets with spores used in absolute pollen analysis. Pollen Spores, 13, 615–621.

Temoltzin-Loranca, Y., Gobet, E., Vannière, B., van Leeuwen, J. F. N., Wienhues, G., Szidat, S., Courtney-Mustaphi, C., Kishe, M., Muschick, M., Seehausen, O., Grosjean, M., & Tinner, W. (2023). A chronologically reliable record of 17,000 years of biomass burning in the Lake Victoria area. Quaternary Science Reviews, 301. https://doi.org/10.1016/j.quascirev.2022.107915

ter Braak, C. J. F., & Prentice, I. C. (1988). A theory of gradient analysis. In M. Begon, A. H. Fitter, E. D. Ford, & A. Macfadyen (Eds.), Advances in Ecological Research (pp. 271–317). Academic Press.

ter Braak, C. J. F., & Šmilauer, P. (2018). Canoco Reference Manual and User's Guide: Software for Ordination (5.10). Biometris.

Tierney, J. E., Russell, J. M., Sinninghe Damsté, J. S., Huang, Y., & Verschuren, D. (2011). Late Quaternary behavior of the East African monsoon and the importance of the Congo Air Boundary. Quaternary Science Reviews, 30(7–8), 798–807. https://doi.org/10.1016/j.quascirev.2011.01.017

Tinner, W., Hubschmid, P., Wehrli, M., Ammann, B., & Conedera, M. (1999). Long-term forest fire ecology and dynamics in southern Switzerland. Journal of Ecology, 87(2), 273–289. https://doi.org/10.1046/j.1365-2745.1999.00346.x

UN-Habitat. (2008). Promoting biodiversity in and around the Lake Victoria Basin.

Van Zinderen Bakker, E. M., & Coetzee, J. A. (1988). A review of late quaternary pollen studies in East, Central and Southern Africa. Review of Palaeobotany and Palynology, 55(1–3), 155–174. https://doi.org/10.1016/0034-6667(88)90083-8

Verschuren, D., Sinninghe Damsté, J. S., Moernaut, J., Kristen, I., Blaauw, M., Fagot, M., & Haug, G. H. (2009). Half-precessional dynamics of monsoon rainfall near the East African Equator. Nature, 462(7273), 637–641. https://doi.org/10.1038/nature08520

Vincens, A. (1991). Late quaternary vegetation history of the South-Tanganyika basin. Climatic implications in South Central Africa. Palaeogeography, Palaeoclimatology, Palaeoecology, 86(3–4), 207–226. https://doi.org/10.1016/0031-0182(91)90081-2

Vincens, A., Buchet, G., Williamson, D., & Taieb, M. (2005). A 23,000 yr pollen record from Lake Rukwa (8°S, SW Tanzania): New data on vegetation dynamics and climate in Central Eastern Africa. Review of Palaeobotany and Palynology, 137(3–4), 147–162. https://doi.org/10.1016/j.revpalbo.2005.06.001

Vincens, A., Chalié, F., Bonnefille, R., Guiot, J., & Tiercelin, J.-J. (1993). Pollen-Derived Rainfall and Temperature Estimates from Lake Tanganyika and Their Implication for Late Pleistocene Water Levels. Quaternary Research, 40(3), 343–350. https://doi.org/10.1006/qres.1993.1087

Vincens, A., Garcin, Y., & Buchet, G. (2007). Influence of rainfall seasonality on African lowland vegetation during the Late Quaternary: pollen evidence from Lake Masoko, Tanzania. Journal of Biogeography, 34(7), 1274–1288. https://doi.org/10.1111/j.1365-2699.2007.01698.x

Wienhues, G., Temoltzin-Loranca, Y., Vogel, H., Morlock, M., Anselmetti, F., Bernasconi, S., Jaggi, M., Tylmann, W., Kishe, M., King, L., Ngoepe, N., Courtney-Mustaphi, C., Muschick, M., Matthews, B., Mwaiko, S., Seehausen, O., Tinner, W., Grosjean, M. From desiccation to wetlands and outflow: rapid re-filling of Lake Victoria during the Lates Pleistocene 14 – 13 ka. [Manuscript submitted for publication].

Yin, X., & Nicholson, S. E. (1998). The water balance of Lake Victoria. Hydrological Sciences Journal, 43(5), 789–811. https://doi.org/10.1080/02626669809492173

CHAPTER IV: CONCLUDING REMARKS AND OUTLOOK

4.1 CONCLUDING REMARKS

Palaeoecological studies are key for understanding the climate-vegetation interaction and the dynamics that have shaped the ecosystems in our planet, in order to better assess the future natural and anthropogenic impacts. Tropical lakes are especially important for studying environmental changes due to their high sensitivity to climate shifts. However, East Africa, specifically Lake Victoria, has been left behind, with only a few further contributions after Kendall's (1969) seminal study. To improve our understanding of the past, it is crucial to promote palaeo research in areas that have been underrepresented in previous efforts. High resolution and complete data sequences allow us to develop more accurate reconstructions.

Therefore, we devoted **Chapter II** of this PhD-thesis to establish a new chronology based on three novel sediment cores and to elaborate the first continuous fire record in the lake for the last 17,000 years. We present three high reliable age-depth models, ensured by a total of 94 radiocarbon dates which were crosschecked biostratigraphically with major vegetation changes, demonstrating the robust and spatially reproducible chronologies. For vegetation reorganizations such as the expansion of the rainforest, the timing was debated, due to differences in the accuracy of the chronologies previously published, here our new chronology was used to better assess the paramount vegetation and fire regime changes. Taken together, our study reveals that natural forces such as climate change and vegetation responses triggered some shifts in the fire regime. During the latest Pleistocene and early Holocene anthropogenic impact did not play a significant role in biome and fire regime reorganizations.

Some questions arose from the first manuscript included in this thesis, in particular, whether the expansion of the rainforest was triggered by moist conditions alone, or if the latest Pleistocene and Holocene warming was also a contributing factor. Additionally, the cause of the late-glacial expansion of the Afromontane belt was still unclear. Hence, **Chapter III** addresses these and other questions by providing the first high-resolution pollen record for the latest Pleistocene and the early Holocene with a temporal resolution of 40 years. Our findings reveal that moisture increase during the early Holocene played a significant role in the transformation of the savanna to the rainforest at lower altitudes, and an expansion of Afromontane vegetation at higher elevations. Whilst temperature changes were more

important for vegetational reorganizations during the preceding period, specifically the first expansion of Afromontane vegetation in the Lake Victoria area.

4.2 OUTLOOK

Future research may further explore the linkages between climate, fire and vegetation in the Lake Victoria area during the Mid and Late Holocene. One potential avenue is to extend the high-resolution pollen analyses to gain additional insights on how these factors interacted in these specific periods, shedding the light on anthropogenic pressure. Although our coarse-resolution analysis did not reveal a clear human impact pattern, increasing the temporal resolution may change this outcome. As demonstrated in previous research (Verschuren et al., 2002; Marchant et al. 2018; Schmidt, 1997; Kendall, 1969), the lake's catchment has been intensely affected by several anthropogenic influences starting at ca. 2500 cal yr BP, when major deforestation and soil degradation likely impacted the littoral zones of the lake (Hecky et al. 2010). Moreover, it would be interesting to compare the rates of ecosystem changes during the onset of the Holocene, and those in the Mid and Late Holocene. Then, to examine the findings from the different periods in a regional context with similar biome transformations, quantifying common patterns at different (novel) sites with increased temporal and taxonomic resolutions would result in a more thorough understanding of tropical ecosystem dynamics in East Africa.

Given the scarcity of references available for pollen identification in east Africa compared to Europe, future research may focus on developing a more sophisticated pollen key in a non-mountainous area. This would enhance our understanding of past vegetation dynamics. Additionally, making a reference collection of the Lake Victoria basin using modern pollen grains could provide a more robust calibration for identifying pollen types that we were able to identify only at a family level.

Another interesting area for further investigations is the one devoted to potential impacts of future climate change in the Lake Victoria basin. This implies using climate models to project future climate scenarios and to apply process-based vegetation models to assess climate effects on fire regimes and vegetation dynamics. Adding Mid and Late Holocene high-resolution evidence may also be useful to refine conservation measures, such as land use

strategies which might be implemented to reduce the vulnerability of ecosystems in a way that production economy may become sustainable for the society and the environment.

References

Hecky, R. E., Mugidde, R., Ramlal, P. S., Talbot, M. R., & Kling, G. W. (2010). Multiple stressors cause rapid ecosystem change in Lake Victoria. Freshwater Biology, 55, 19-42.

Kendall, R. L. (1969). An Ecological History of the Lake Victoria Basin. *Ecological Monographs*, *39*(2), 121–176.

Marchant, R., Richer, S., Boles, O., Capitani, C., Courtney-Mustaphi, C. J., Lane, P., ... & Wright, D. (2018). Drivers and trajectories of land cover change in East Africa: Human and environmental interactions from 6000 years ago to present. Earth-Science Reviews, 178, 322-378.

Schmidt, P. R. (1997). Archaeological views on a history of landscape change in East Africa. The Journal of African History, 38(3), 393-421.

Verschuren, D., Johnson, T. C., Kling, H. J., Edgington, D. N., Leavitt, P. R., Brown, E. T., ... & Hecky, R. E. (2002). History and timing of human impact on Lake Victoria, East Africa. Proceedings of the Royal Society of London. Series B: Biological Sciences, 269(1488), 289-294.

DISSERTATION ACKNOWLEDGEMENTS

I would like to express my gratitude to my supervisors Willy Tinner and Martin Grosjean for guiding me through the course of this research adventure, for their patient guidance, encouragement, meaningful discussions, and joyful trips and excursions. I am particularly grateful to my advisor Erika Gobet, for her willingness end encouragement to try out new things, also her wise advice on when to stop trying new things for a better time management, fruitful science discussions, and her time for training me in lab methods and pollen determination. I wish to acknowledge Jacqueline van Leeuwen and Pim van der Knaap for their valuable time and help with pollen determination, this was not an easy task but with your support, it was definitely easier. I am grateful to Lisa Schüler for facilitating me the access to the pollen reference collection of Mt. Kilimanjaro and for her support with pollen identification. I would like to cordially thank Hermann Behling for hosting me at the Department of Palynology and Climate Dynamics at the University of Göttingen, for accepting the invitation to be the external examiner and for his time reviewing this thesis. I extend my thanks to Stefan Müller who helped me out in trying out the sorting for pollen grains with the cytometer, even though the lab is used mainly for medical purposes, thanks for giving it a try. I would like to thank all members of the SNF Sinergia Project for the exciting debates and collaboration during these 4 years. I would like to express my very great appreciation to all members of the palaeolimnology and the palaeoecology groups (2019-2023) for all adventures, lunches, dinners, and trips together. I really appreciate the support of Lara Zinkl and Sarah Schär, especially during the COVID outbreak when we continued going to the lab for working in my project with enjoyable days full of music and sieving. Mary Kishe, Josephat Kalugasha Joshua Mokoz, Elias Stanley and Charles Michael James are greatly acknowledged for her support during the trip to Tanzania. I thank the Swiss National Science Foundation (Sinergia grant number 183566) for making this research financially possible. And I extend my gratitude to the “Taller the Ciencia para Jóvenes” (Proyecto PAPIME-PE103409) from the Geosciences division of the National Autonomous University of Mexico where my interest in science was materialized when I was 15 years old. Thanks to my mentor in life and in science Juan Martín Gómez-González, to my mother Águeda A. Loranca-Espinosa and my grandparents for always supporting my career in science. Thanks to my husband Pascal Zumbühl, for listening my complaints, my ideas about research, helping me improving my graphics and learning some palynology with me. And last, but not least,

thanks to my friends Maria Leunda and Miguel Bartolomé, for supporting me in all aspects during this important phase of my life.

DECLARATION OF CONSENT

on the basis of Article 18 of the PromR Phil.-nat. 19

Name/First Name: Temoltzin Loranca, Yunuén

Registration Number: 18-129-809

Study program: PhD in Climate Sciences

Bachelor ☐ Master ☐ Dissertation ☑

Title of the thesis: Late Pleistocene and Holocene Vegetation, Fire and Climate Dynamics in the Lake Victoria Area

Supervisor: Prof. Dr. Willy Tinner and Prof. Dr. Martin Grosjean

I declare herewith that this thesis is my own work and that I have not used any sources other than those stated. I have indicated the adoption of quotations as well as thoughts taken from other authors as such in the thesis. I am aware that the Senate pursuant to Article 36 paragraph 1 litera r of the University Act of September 5th, 1996 and Article 69 of the University Statute of June 7th, 2011 is authorized to revoke the doctoral degree awarded on the basis of this thesis.
For the purposes of evaluation and verification of compliance with the declaration of originality and the regulations governing plagiarism, I hereby grant the University of Bern the right to process my personal data and to perform the acts of use this requires, in particular, to reproduce the written thesis and to store it permanently in a database, and to use said database, or to make said database available, to enable comparison with theses submitted by others.

Bern, 19.06.2023

Place/Date

Yunuen Temoltzin-Loranca

Digitally signed by Yunuen Temoltzin-Loranca
Date: 2023.06.20 10:35:28 +02'00'

Signature